Pharmacological characterization and functional rescue of human melanocortin-4 receptor mutants

by

Hui Huang

A dissertation submitted to the Graduate Faculty of
Auburn University
in partial fulfillment of the
requirements for the Degree of
Doctor of Philosophy

Auburn, Alabama
August 2, 2014

Keywords: G protein-coupled receptor, Melanocortin-4 receptor, Obesity, Pharmacoperone

Copyright 2014 by Hui Huang

Approved by

Ya-Xiong Tao, Chair, Professor of Anatomy, Physiology, and Pharmacology
Benson Akingbemi, Professor of Anatomy, Physiology, and Pharmacology
Ellen Behrend, Professor of Clinical Sciences
Terry Brandebourg, Assistant Professor of Animal Sciences

Abstract

The melanocortin-4 receptor (MC4R) plays an important role in regulating food intake and energy expenditure. Previous studies reported that the transmembrane domain 6 was important in activating several G protein-coupled receptors. To better understand the function of thirty-one residues in the transmembrane domain 6 of the MC4R, we performed alanine-scanning mutagenesis. We identified residues that are important for cell surface expression, ligand binding, cAMP signaling, and residues for maintaining the wild type MC4R in inactive conformation. We also observed constitutive activation of the mitogen-activated protein kinase signaling and biased signaling of the MC4R.

Up to now, approximately 170 mutations in the *MC4R* have been identified from obese patients. Functional studies of these mutants are important in understanding the role of the MC4R in causing obesity and in developing personalized medicine. We performed detailed functional studies on nine MC4R mutants (G55V, R165G, R165W, R165Q, C172R, F202L, M208V, I269N, and A303P) that were identified from Pima Indian heritage and Hispanic heritage. We showed that the majority of these mutants (six) (R165G, R165W, R165Q, C172R, I269N, and A303P) were completely or partially defective in cell surface expression.

The intracellularly retained mutants may retain intrinsic function and become functional when coaxed to the cell surface. We therefore investigated whether small molecule ligands could act as pharmacological chaperones (pharmacoperones) promoting the proper folding of

intracellularly retained MC4R mutants. Three MC4R ligands including two antagonists (ML00253764 and Ipsen 5i) and one agonist (THIQ) and eleven intracellularly retained MC4R mutants (S58C, N62S, I69R, P78L, C84R, G98R, Y157S, W174C, P260Q, F261S, and C271Y) were studied using different cell lines. We showed that the three small molecule ligands could act as pharmacoperones rescuing the cell surface expression and signaling of intracellularly retained MC4R mutants with various efficacies.

In summary, we comprehensively studied the transmembrane domain 6 of the MC4R and nine MC4R mutants identified from obese patients. We also identified three pharmacoperones of the MC4R.

Acknowledgments

First and foremost, I would like to express my sincere appreciation to my mentor Dr. Ya-Xiong Tao for his endless help in my graduate study and continual support of my academic career. This dissertation would not be done without his critical comments, constructive advices, valuable trust, and constant encouragements. I am also deeply grateful to all my committee members, Drs. Benson Akingbemi, Ellen Behrend, and Terry Brandebourg for sharing their wisdom and experience and devoting their valuable time to instruct my study. I warmly thank my university reader, Dr. Douglas White, for his careful review and precious suggestions of my dissertation.

I would like to thank my lab colleagues and alumni, Zhao Yang, Wei Wang, Shan He, Drs. Fan Yang, Xiulei Mo, Zhiqiang Wang, Zhili Huang, Menghong Dai, Hanchuan Dai, and Weina Xu, for their valuable contributions, inspiring discussions, and helpful support. I would like to thank other colleagues and many other friends for their friendship and help. I would like to thank all faculty members in the College of Veterinary Medicine for their valuable teaching and advices and also kind support. Specifically, I would like to thank Dr. Frank Bartol and College of Veterinary Medicine for providing the fellowship to support my graduate study. Without their financial support, I would not have finished my dissertation.

My sincere thanks go to our collaborators for their support and cooperation: Dr. Joan Han, director of the Pediatric Obesity Program at Le Bonheur Children's Hospital and associate

professor of Pediatric Endocrinology at the University of Tennessee Health Science Center, and her students and collaborators; Dr. David Lefer, director of the Cardiovascular Center of Excellence at the Louisiana State University Health Sciences Center and professor of Pharmacology in the School of Medicine at the Louisiana State University Health Sciences Center, and his students and collaborators.

Our studies are supported by grants from the National Institutes of Health R15DK077213, American Diabetes Association 1-12-BS212, Auburn University Intramural Grant Program, and Interdisciplinary Grant of College of Veterinary Medicine.

I am whole-heartedly grateful to my parents, my older brother, and two sisters for their endless love and encouragement. I owe my deepest gratitude to my husband, Jiansheng Huang, for his unconditional love and support. My family is always there to support me.

Table of Contents

List of Tables

List of Figures

List of Abbreviations

ACTH	Adrenocorticotrophic hormone
AgRP	Agouti-related peptide
ARC	Arcuate nucleus
AVPR2	V2 arginine vasopressin receptor
BSA	Bovine serum albumi
BDNF	Brain-derived neurotrophic factor
Bmax	Apparent maximal binding
BMI	Body mass index
CAM	Constitutively active mutant
cAMP	Cyclic AMP
CaSR	Calcium-sensing receptor
CCK	Cholecystokinin
CFTR	Cystic fibrosis transmembrane conductance regulator
CLR	Calcitonin receptor-like receptor
CNS	Central nervous system
DMEM	Dulbecco's modified eagle medium
DMSO	Dimethyl sulphoxide
DRD1	D_1 dopamine receptor

ER	Endoplasmic reticulum
ERK1/2	Extracellular signal-regulated kinases1/2
$GABA_BR$	Type B γ-aminobutyric acid receptor
GLP-1	Glucagon-like peptide-1
GnRHR	Gonadotropin-releasing hormone receptor
GPCR	G protein-coupled receptor
GRK	GPCR kinase
GRP	Gastrin-releasing peptide
HEK	Human embryonic kidney
Hsc70	Heat shock cognate protein 70
ICV	Intracerebroventricular
IRS-2	Insulin receptor substrate 2
JAK	Janus kinase
LHR	Luteinizing hormone receptor
MAP kinase	Mitogen-activated protein kinase
MC2R	Melanocortin-2 receptor
MC3R	Melanocortin-3 receptor
MC4R	Melanocortin-4 receptor
MCH	Melanin-concentrating hormone
mGluR5	Metabotropic glutamate receptor 5
MSH	Melanocyte stimulating hormone
MTII	Melanotan II
MRAP	Melanocortin 2 receptor accessory protein

NDP-MSH	[Nle^{4}, $_{D}$-Phe^{7}]α-MSH
NDI	Nephrogenic diabetes insipidus
NPY	Neuropeptide Y
ObR	Leptin receptor
OR	Olfactory receptor
PBS-IH	PBS for immunohistochemistry
PI3K	Phosphoinositide 3-kinase
PKA	Protein kinase A
PKC	Protein kinase C
POMC	Proopiomelanocortin
PTHR	Parathyroid hormone receptor
PYY	Peptide tyrosine tyrosine
RAMP	Receptor activity modifying protein
REEP1	Receptor expression enhancing protein 1
Rmax	Maximal response
RTP	Receptor-transport protein
S1P1R	Sphingosine-1-phosphate receptor
STAT	Signal transducer and activator of transcription
TM	Transmembrane domain
TMAO	Trimethylamine N-oxide
TSHR	Thyroid-stimulating hormone receptor
WT	Wild type

Chapter 1 Literature review

1.1 Introduction

G protein-coupled receptors (GPCRs), the largest family of membrane proteins, are the most common therapeutic targets (Conn and Ulloa-Aguirre, 2011). Detailed functional studies reveal that most of the inactivating mutations of GPCRs are defective in protein folding and therefore are retained intracellularly by the cellular quality control system (Tao, 2006). The misfolded GPCRs may remain intrinsic function and restore function when coaxed to the cell surface (Conn et al., 2007). Various approaches have been tried to rescue misfolded GPCRs, such as reducing cell culture temperature, using molecular chaperones, chemical chaperones, or pharmacological chaperones (also known as pharmacoperones) (Tao and Conn, 2014). Pharmacoperones are the most promising approach because of high specificity and potency. Up to now, many antagonists, agonists, or allosteric ligands have been identified as pharmacoperones for many GPCRs (Tao and Conn, 2014).

The melanocortin-4 receptor (MC4R) is a member of family A GPCRs. As a downstream mediator of the leptin-melanocortin pathway, the MC4R plays a vital role in regulating energy homeostasis, regulating both food intake and energy expenditure (Huszar et al., 1997). Inactivating mutations in the *MC4R* are the most common cause of monogenic form of obesity (Farooqi et al., 2003). Currently, approximately 166 mutations in the *MC4R* have been identified in humans and, similar to other GPCRs, most of the inactivating mutations result in intracellular

retention of the MC4R (Hinney et al., 2013). Several studies have used heat shock cognate protein 70 (Hsc70), 4-phenyl butyric acid, several antagonists, or endoplasmic reticulum (ER)-targeted α-melanocyte stimulating hormone (MSH) to promote the proper folding of intracellularly retained MC4Rs and showed that most of the intracellularly retained MC4Rs were rescued to the cell surface and restored function (Tao and Conn, 2014).

This chapter provides an overview of obesity and the MC4R. Current studies of pharmacoperones for GPCRs will also be discussed.

1.2 Obesity and melanocortin-4 receptor

1.2.1 Obesity

Obesity is a medical condition in which body fat is excessively accumulated. In adults, it is generally defined by a body mass index (BMI), which is calculated by weight in kilograms divided by the square of height in meters, of 30 kg/m^2 or higher. Obesity is closely associated with the incidence of a number of comorbidities such as cardiovascular diseases, type 2 diabetes, hypertension, stroke, and certain types of cancers. (Guh et al., 2009). It has been estimated that between the year 1986 and 2006, overweight and obesity were related to 5.0% and 15.6% of adult deaths for Black and White men and 26.8% and 21.7% of that for Black and White women, respectively (Masters et al., 2013). In addition, obesity also has serious social and economic consequences.

Obesity has become a global epidemic. The prevalence of adult obesity is 9.8% in the world (Kelly et al., 2008) and 35.7% in the US (Ogden et al., 2012b). The prevalence of obesity in the US, especially that of severe and morbid obesity, continues to be increasing, but the increasing rate began to slow down since 2005 (Sturm and Hattori, 2013). Obesity has also

become a serious problem among children and adolescents; the prevalence was approximately 16.9% in the US in 2009-2010 (Ogden et al., 2012a).

Different approaches have been conducted to treat obese patients, such as lifestyle intervention, pharmacotherapy, and bariatric surgery. Lifestyle intervention generally significantly reduces body fat for most obese patients but it is difficult, especially for those carry genetic defects, to maintain the weight loss (Reinehr et al., 2009). Pharmacotherapy, including the use of orlistat, sibutramine, and rimonabant, modestly reduces body weight and decreases the incidence of obesity related comorbidities, but tend to induce adverse effects such as depression, hypertension, and gastrointestinal side effects (Rucker et al., 2007). The combination of lifestyle intervention and pharmacotherapy has been reported to have better therapeutic effect on the loss of body weight (Wadden et al., 2005). Bariatric surgery is mostly conducted for morbid obesity. It is very effective in reducing obesity related comorbidities and total mortality, but has high surgical risks (DeMaria, 2007; Terranova et al., 2012).

Obesity is a disorder of energy homeostasis that is affected by both environmental and genetic factors. Genetic factors play a vital role in determining individual differences in susceptibility to the obesogenic environment (Ramachandrappa and Farooqi, 2011). Different genes have been identified to be important in regulating energy homeostasis. Leptin is one of the most important ones. The involvement of leptin in regulating energy homeostasis was first observed in mouse in 1994 (Zhang et al., 1994) and in humans in 1997 (Montague et al., 1997). Leptin is a 16-kDa hormone secreted by the adipocytes and functions as the sensor of body fat content. It is transported across the blood brain barrier and activates leptin receptors in the hypothalamus, inhibiting the neuropeptide Y (NPY)/agouti-related peptide (AgRP) neurons and activating the proopiomelanocortin (POMC) neurons, resulting in the inhibition of food intake

and increase of energy expenditure (Tao et al., 2013).

There are different isoforms of leptin receptors (ObRs) resulting from alternative splicing of a single transcript. Depending on the length of their intracellular domains, ObRs are classified into short and long isoforms. The long isoform ObRb is the fully functional one and accounts for all leptin actions (Villanueva and Myers, 2008). The ObR is a member of family interleukin-6 receptors with a single transmembrane domain. Activation of the ObRb by leptin activates the Janus kinase (JAK)/signal transducer and activator of transcription (STAT) pathway (Villanueva and Myers, 2008).

Insulin and glucagon are also well known in regulating glucose and energy homeostasis (Bloemer et al., 2014; Tao and Liang, 2014). In response to increased blood glucose levels, insulin is secreted by the pancreatic β cells and regulates glucose homeostasis in the peripheral tissues. Insulin also directly acts on different neurons in the central nervous system (CNS) to regulate energy homeostasis (Varela and Horvath, 2012; Vogt and Bruning, 2013). For example, insulin acts in the arcuate nucleus (ARC) activating POMC expression and inhibiting AgRP expression and therefore inhibiting food intake upon feeding (Vogt and Bruning, 2013). The phosphoinositide 3-kinase (PI3K) signaling pathway mediated by insulin receptor substrate 2 (IRS-2) is important for CNS action of insulin in regulating energy homeostasis (Vogt and Bruning, 2013). Glucagon is secreted by the pancreatic α cells and is generally known for its protection from hypoglycemia. However, opposite of its antihypoglycemic action, glucagon is also released in stress and functions to reduce food intake and increase energy expenditure (Jones et al., 2012).

Several gastrointestinal peptides have also been found to be important in regulating energy homeostasis. These gastrointestinal peptides include ghrelin (Li et al., 2013), obestatin

(Zhang et al., 2013), cholecystokinin (CCK) (Sayegh, 2013), glucagon-like peptide-1 (GLP-1) (Tao et al., 2013), gastrin-releasing peptide (GRP) (Sayegh, 2013), peptide tyrosine tyrosine (PYY), etc. (Tao et al., 2013). For example, ghrelin is a 28 amino acid peptide secreted by the fundus of the stomach and functions to, unlike many of the other gastrointestinal peptides, stimulate food intake. Ghrelin activates ghrelin receptors in the ARC that activate the NPY/AgRP neurons and inhibit POMC neurons, resulting in orexigenic effect (Li et al., 2013).

Many other hormones and nutrients, such as melanin-concentrating hormone (MCH) (Antal-Zimanyi and Khawaja, 2009), neuropeptide Y (Zhang et al., 2011), adiponectin (Akingbemi, 2013), reproductive hormones (Shi et al., 2013), and free fatty acids (Huang et al., 2014; Mansour, 2014; Mo et al., 2014), are also vital in maintaining energy homeostasis.

1.2.2 Melanocortin-4 receptor

The MC4R was first cloned in humans in 1990s (Gantz et al., 1993; Mountjoy et al., 1994). The human *MC4R* localized on chromosome 18q21.3 is an intronless gene and the encoded protein has 332 amino acid residues (Gantz et al., 1993). The MC4R is extensively expressed in the CNS including the cortex, thalamus, hippocampus, hypothalamus, brain stem, and spinal cord (Mountjoy et al., 1994). The expression of MC4R mRNA has also been detected in several peripheral tissues such as heart, lung, muscle, kidney, and testis during the fetal period (Mountjoy et al., 2003). However, the function of the MC4R in the peripheral tissues is still not fully understood.

The MC4R plays a vital role in regulating energy homeostasis and this has been verified by a number of studies (Tao, 2010). The *Mc4r* knockout mice develop maturity-onset obesity with hyperphagia and hyperinsulinemia (Huszar et al., 1997). There is also a gene dosage effect

since heterozygous knockout mice have intermediate body weight compared with the wild type (WT) and homozygous knockout mice (Huszar et al., 1997). The obese A^y mice that have ubiquitous agouti expression have reduced food intake upon the intracerebroventricular (ICV) injection of melanotan II (MTII) and this inhibition is abolished by co-injection of SHU9119 (Fan et al., 1997). Transgenic mice overexpressing AgRP, the endogenous antagonist of the MC4R, develop obesity (Graham et al., 1997) whereas *Agrp* knockout mice have reduced body weight (Wortley et al., 2005).

The MC4R is also involved in several other physiological functions such as glucose and lipid homeostasis, reproductive and sexual behaviors, cardiovascular function, pain perception, and brain inflammation (Tao, 2010).

The MC4R has two important endogenous agonists, α-MSH and β-MSH, and one important endogenous antagonist, AgRP. Both α-MSH and β-MSH are derived from different posttranslational processing of the POMC. The precursor POMC, which contains 241 amino acid residues, undergoes tissue specific cleavage by prohormone convertases and produces many peptide hormones, such as α-, β-, γ-MSH, adrenocorticotrophic hormone (ACTH), corticotropin-like intermediate peptide, β-lipotropin, and β-endorphin. Mutations in the *POMC* also cause early-onset obesity (Krude et al., 1998). The AgRP contains 132 amino acid residues. It inhibits the basal signaling of the G_s-cyclic AMP (cAMP) pathway (Haskell-Luevano and Monck, 2001; Nijenhuis et al., 2001) but activates the $G_{i/o}$ pathway and extracellular signal-regulated kinases 1/2 (ERK1/2) pathway, and therefore is a biased ligand of the MC4R (Buch et al., 2009; Mo and Tao, 2013).

Based on the structure-activity relationship studies, many agonist and antagonist analogs of the MC4R have been developed. Some analogs have been widely used in MC4R studies such

as agonists [Nle^4, D-Phe^7]α-MSH (NDP-MSH), MTII, THIQ, and antagonists SHU9119, ML00253764, and Ipsen 5i (Tao, 2010). We recently showed that ML00253764 and Ipsen 5i are also partial inverse agonists of the MC4R inhibiting its basal cAMP production (Tao et al., 2010). These synthetic agonists and antagonists compete with endogenous ligands and therefore are orthosteric ligands of the MC4R. Although allosteric ligands have been developed for several other GPCRs (Conn et al., 2009), to our knowledge, no such ligands have been reported for the MC4R.

It has been reported that the MC4R couples to different types of G proteins including G_s (Gantz et al., 1993), G_q (Newman et al., 2006), and $G_{i/o}$ (Buch et al., 2009). The G_s-cAMP-protein kinase A (PKA) signaling pathway is the classical signaling pathway of the MC4R. Activation of the MC4R activates adenylyl cyclase, which produces cAMP and subsequently activates PKA. Activation of the MC4R also activates ERK1/2. However, it is still controversial how ERK1/2 is activated by the MC4R because studies have shown that this process can be mediated by PKA, protein kinase C (PKC), or PI3K in different cell lines (Tao, 2010). Recently, we have found that MC4R mutants have different signaling properties and several MC4R ligands act differently on the G_s-cAMP-PKA and ERK1/2 signaling pathways in human embryonic kidney (HEK) 293T cells, demonstrating the existence of biased signaling (Huang and Tao, 2012; Mo and Tao, 2013; Mo et al., 2012). Further studies need to be conducted to investigate the detailed mechanisms of the biased signaling of the MC4R.

1.3 Pharmacoperones

1.3.1 G protein-coupled receptors and rescue of intracellularly retained G protein-coupled receptors

GPCRs are the most common targets of modern therapeutic drugs with more than 60% of all approved drugs target GPCRs (Conn and Ulloa-Aguirre, 2011). GPCRs are the largest family of integral membrane receptors that sense signals outside the cell and activate inside signal transductions, which eventually stimulate cellular responses. Ligands that activate GPCRs include smell, photons, pheromones, ions, neurotransmitters, lipids, peptides, and glycoproteins that are diverse in size and structure (Bockaert and Pin, 1999; Conn and Ulloa-Aguirre, 2011). Up to now, more than 800 GPCR sequences have been identified in human genomes and approximately 400 of them have endogenous ligands (Bjarnadottir et al., 2006; Fredriksson et al., 2003). In addition to orphan receptors with no known endogenous ligands identified so far and pseudogenes, GPCRs can be classified into three major families, including family A, family B, and family C (Davenport et al., 2013). Family A comprising approximately 276 members is the largest family (Foord et al., 2005; Tao and Conn, 2014).

GPCRs are traditionally believed to be functional only at the cell surface by activating G proteins and subsequent signaling pathways. Ligand-activated GPCRs possess a conformational change and become phosphorylated by GPCR kinases (GRKs). Phosphorylated GPCRs then recruit the binding of β-arrestins, which results in desensitization and further induces internalization of GPCRs. However, during the past decade, it has been realized that β-arrestins not only desensitize GPCR signaling, but also act as scaffolds recruiting the binding of multiple proteins, such as mitogen-activated protein (MAP) kinases, and initiating signaling independent of G proteins (Lefkowitz, 2013; Shenoy and Lefkowitz, 2011). Therefore, β-arrestins have multiple functions in regulating GPCR signaling, including desensitization, internalization, and mediating G protein-independent signaling (Lefkowitz, 2013).

Recently, it has been observed that GPCRs also initiate signaling intracellularly, such as

in the ER, Golgi apparatus, endosome, and nucleus. For example, GPR30, which is uniquely expressed in the ER, is activated by estrogen in the ER with increased intracellular calcium mobilization (Revankar et al., 2005). Some small molecule hydrophobic ligands or ligand analogs may act similarly to estrogen by activating GPCRs intracellularly. These studies will be discussed in the section *1.3.3 Pharmacoperones for G protein-coupled receptors* in detail. However, most of the endogenous ligands of GPCRs are hydrophilic and therefore are not able to penetrate the cell membrane to activate the target receptor (Tao and Conn, 2014). In fact, these ligands activating GPCRs at the cell surface may remain bound to the receptor during internalization or some disassociated ligands may be internalized in the same vesicle with the receptor and therefore activate the receptor intracellularly (Lohse and Calebiro, 2013). A recently published study has provided direct video evidence that G_s interacted with active β_2-adrenoceptor both at the plasma membrane and later at the early endosome membrane (Irannejad et al., 2013). The internalized β_2-adrenoceptor produced a second phase of cAMP signaling and contributed to the overall cAMP signaling within several minutes upon ligand stimulation (Irannejad et al., 2013). Between the two phases of cAMP signaling, β_2-adrenoceptor did not associated with G_s, but associated with β-arrestin, which probably initiated G-protein-independent signaling as previously described (Irannejad et al., 2013). Intracellular signaling has also been observed in several other GPCRs, such as D_1 dopamine receptor (DRD1) (Kotowski et al., 2011), thyroid-stimulating hormone receptor (TSHR) (Calebiro et al., 2009; Calebiro et al., 2010; Nakamura et al., 2013), parathyroid hormone receptor (PTHR) (Feinstein et al., 2011; Ferrandon et al., 2009), metabotropic glutamate receptor 5 (mGluR5) (Jong et al., 2009; Kumar et al., 2012), and sphingosine-1-phosphate receptor (S1P1R) (Mullershausen et al., 2009). Therefore, "receptor signals come in waves" (Lohse and Calebiro, 2013).

The expression of GPCRs including protein folding, post-translational modifications, and targeting to the cell surface is a complex process. Some GPCRs have signal peptides, which recognizes signal recognition particle and inserts the protein into ER membrane. Most of GPCRs (90%) do not have signal peptides and one of their transmembrane domains acts like signal peptides and recognizes signal recognition particle (Nanoff and Freissmuth, 2012). Correctly folded GPCRs then pass the scrutiny of stringent ER quality control system and are transported forward to the cell surface. Some GPCRs cannot be efficiently targeted to the cell surface themselves and require the assistance of membrane associated accessory proteins. For example, type B γ-aminobutyric acid receptor ($GABA_BR$) 1 requires $GABA_BR2$ (White et al., 1998), the mammalian calcitonin receptor-like receptor (CLR) requires receptor activity modifying proteins (RAMPs) (McLatchie et al., 1998), mammalian olfactory receptor (OR) requires receptor-transport proteins (RTPs) and receptor expression enhancing protein 1 (REEP1) (Saito et al., 2004), and melanocortin 2 receptor (MC2R) requires melanocortin 2 receptor accessory proteins (MRAPs) (Metherell et al., 2005).

Mutations in GPCRs may alter the normal function of GPCRs and eventually lead to human diseases. Inactivating mutations in GPCRs cause a number of human diseases, such as obesity, diabetes, hyperparathyroidism, nephrogenic diabetes insipidus (NDI), familial glucocorticoid deficiency, retinitis pigmentosa, congenital hypothyroidism, and hypogonadotropic hypogonadism (Tao and Conn, 2014). The mutation P23H in rhodopsin that leads to autosomal dominant retinitis pigmentosa was the first mutation found in GPCRs that causes human diseases (Sung et al., 1991). Since then, numerous pathogenic mutations of GPCRs have been identified from human patients (Chaudhuri and Paul, 2006).

In 2003, Tao and Segaloff proposed a classification scheme to classify MC4R mutations,

which they suggested should be able to apply to most GPCRs (Tao and Segaloff, 2003). Class I mutations comprising most of the nonsense and frameshift mutations result in defective receptor biosynthesis; Class II mutations result in defective receptor forward trafficking to the cell surface; Class III mutations result in defective ligand binding; Class IV mutations result in defective receptor activation; Class V mutations have no obvious defects (Tao and Segaloff, 2003). Different methods should be applied to correct different types of mutations. To correct Class I nonsense mutations, we can use aminoglycoside antibiotics that decrease the codon-anticodon fidelity and therefore result in reading through of the premature stop codon (Tao, 2006). To rescue Class II mutations, we can use small compounds that stabilize and target misfolded proteins to the cell surface. To rescue Class III and IV mutations, we need to develop novel ligands (Tao, 2006).

Class II mutations are the most common defect of all GPCR inactivating mutations (Tao, 2006). These mutants are misfolded and therefore retained intracellularly, mostly in the ER with a few in the Golgi apparatus, by the cellular quality control system, ubiquitinated, and degraded by the proteasome. Although misfolded proteins cannot be targeted to the cell surface, they may retain intrinsic function and function normally or partially when coaxed to the cell surface.

Various approaches have been employed to rescue intracellularly retained misfolded GPCRs, such as reducing cell culture temperature, treating mutants with molecular chaperones, chemical chaperones, or pharmacoperones. It has been reported that reducing cell culture temperature from 37 ^{o}C to 26 ^{o}C or to 28 ^{o}C significantly increased the cell surface expression and function of luteinizing hormone receptor (LHR) mutants (Jaquette and Segaloff, 1997) or α_2-adrenoceptor mutants (Jeyaraj et al., 2001), respectively.

Molecular chaperones, the endogenous chaperones residing mostly in the ER, have been

found to interact with many GPCRs. Molecular chaperones interact with non-native like proteins, facilitate their folding, decrease their aggregation, and regulate their intracellular trafficking. There are many molecular chaperones in the ER. For example, calnexin and calreticulin interact with glycosylated proteins; heat shock proteins are induced by increased temperature or other stresses; protein disulfide isomerase facilitates the formation of disulfide bonds and protein folding (Tao and Conn, 2014). Some of these molecular chaperones promote the proper folding and cell surface targeting of GPCR mutants (Conn et al., 2007; Tao and Conn, 2014). Recently, one study revealed that overexpression of the cytosolic cognate 70 kDa (Hsc70) increased the cell surface expression of WT and mutant MC4Rs in different cell lines (Meimaridou et al., 2011).

Chemical chaperones are generally uncharged small molecule compounds that non-selectively stabilize misfolded proteins by providing a hydrophobic environment or changing the expression of molecular chaperones (Arakawa et al., 2006; Babcock and Li, 2013). Many small molecule compounds have been identified as chemical chaperones, such as glycerol, dimethyl sulphoxide (DMSO), trimethylamine N-oxide (TMAO), phenyl butyric acids, and amino acid derivatives (Babcock and Li, 2013). For the MC4R, 4-phenyl butyric acid has been reported to increase the cell surface expression and function of intracellularly retained MC4R mutants (Granell et al., 2010). However, chemical chaperones typically require high concentrations, which are toxic, to be effective and are non-specific for many proteins. Therefore, chemical chaperones have limited applications in treating human diseases.

A recent study conducted by Granell et al. designed an ER-targeted α-MSH construct and found that such modified α-MSH interacts with the MC4R in the ER and later at the cell surface (Granell et al., 2013). Interestingly, ER-targeted α-MSH induces constant cAMP signaling of the

MC4R that is not desensitized (Granell et al., 2013). The MC4R stimulated with ER-targeted α-MSH is resistant to the antagonism of the AgRP and resistant to be routed to the lysosome (Granell et al., 2013). ER-targeted α-MSH also stabilizes the conformation and rescues the cell surface expression and constant signaling of one intracellularly retained MC4R mutant, I316S (Granell et al., 2013). This study suggested that the cellular location where ligand-receptor initially interacted might affect the conformation and desensitization properties of the receptor (Granell et al., 2013). This also provided a novel approach to rescue intracellularly retained GPCRs.

1.3.2 Discovery of pharmacoperones

After the discovery of chemical chaperones that nonspecifically stabilized the correct folding of misfolded proteins, Loo and Clarke wondered whether substrates or modulators of a protein could act specifically on rescuing misfolded proteins and they selected P-glycoprotein, which is a human multidrug transporter, for the study (Loo and Clarke, 1997). Many P-glycoprotein mutants have been identified and characterized to be misfolded and retained intracellularly. Loo and Clark found that the cell surface expression and function of mutant proteins were significantly increased in the presence of drug substrates or modulators (Loo and Clarke, 1997). Compared with glycerol that required 24-72 h for function, substrates are functional within 2-4 h (Loo and Clarke, 1997). The substrates or modulators, which now are known as pharmacological chaperones or pharmacoperones, did not rescue the cystic fibrosis transmembrane conductance regulator (CFTR) mutant, ΔF508, and therefore act specifically for P-glycoprotein (Loo and Clarke, 1997).

Ever since the first discovery of pharmacoperones, numerous small compounds have

been developed and characterized as pharmacoperones for misfolded proteins. Pharmacoperones are now known as small hydrophobic compounds that can cross the cell membrane and specifically bind to and stabilize misfolded proteins, allowing them to be targeted to the appropriate cellular compartments. Because pharmacoperones are specific for one or one type of proteins, they are generally developed from substrates and inhibitors for enzymes or antagonists and agonists for receptors (Bernier et al., 2004a; Conn et al., 2007). Pharmacoperones rescue misfolded proteins in most cellular compartments, especially in the mitochondrion, lysosome, and ER where proteins suffer stress (Loo and Clarke, 2007; Ringe and Petsko, 2009).

Studies proposed the potential mechanism by which pharmacoperones stabilize and rescue misfolded proteins: i) stabilizing the native or native like structure of the target protein; ii) acting as a scaffold and facilitating the folding of the non-native like structure (Arakawa et al., 2006). However, our current understanding of the mechanism is still highly speculative and requires further studies.

Up to now, many pharmacoperones have been developed to treatment human protein misfolding diseases, such as pharmacoperones of the p53 to treat cancer (Bykov et al., 2002; Foster et al., 1999), pharmacoperones of the α-galactosidase A to treat Fabry disease (Frustaci et al., 2001; Yam et al., 2006), pharmacoperones of the β-glucosidase to treat Gaucher disease (Khanna et al., 2010; Lieberman et al., 2007), and pharmacoperones of the CFTR to treat cystic fibrosis (Sampson et al., 2011). More importantly, some pharmacoperones have already been successfully conducted in clinical trials (Clarke et al., 2011; Germain et al., 2012; Giugliani et al., 2013).

1.3.3 Pharmacoperones for G protein-coupled receptors

Morello et al. were the first to use small molecule antagonists as pharmacoperones to rescue the cell surface expression and function of mutant GPCRs (Morello et al., 2000). They studied the effects of nonpeptidic V2 arginine vasopressin receptor (AVPR2) antagonists, SR121463A and VPA-985, on eight AVPR2 mutants (Morello et al., 2000). They showed that SR121463A and VPA-985 promot the proper folding and maturation of AVPR2 mutants and consequently significantly increase the cell surface expression and function of the mutants, whereas a cell impermeant AVPR2 antagonist does not have such effects (Morello et al., 2000). Bernier et al. further found that another antagonist, SR49059, did not prevent the constitutive β-arrestin-promoted receptor endocytosis, indicating that the mechanism underlying the functional rescue of AVPR2 mutants upon SR49059 treatment resultes from its pharmacoperone action in the ER, rather than from the inhibition of receptor constitutive endocytosis (Bernier et al., 2004b). These studies demonstrate that cell permeable ligands can act as pharmacoperones stabilizing misfolded receptors and helping them passing the scrutiny of cellular quality control system to be expressed and functional at the cell surface.

Inactivating AVPR2 mutations cause NDI disease and hundreds of AVPR2 mutations have been identified from NDI patients (Pan et al., 1992; Tao, 2006). Bernier et al. administrated SR49059 to five NDI patients each bearing one type of AVPR2 mutations for a short-term treatment (Bernier et al., 2006).In patients, SR49059 significantly decreases 24 hours urine volume and water intake and increases urine osmolalities (Bernier et al., 2006). This successful trial of SR49059 in human NDI patients demonstrates the utility of applying pharmacoperones in treating human diseases in vivo. Unfortunately, the trial of SR49059 was discontinued due to side effects (Los et al., 2010). Another AVPR2 antagonist OPC41061 (Tolvaptan) has been approved in the USA and Europe to treat hyponatraemia and heart failure with little side effects

(Farmakis et al., 2008; Schrier et al., 2006). OPC41061 is a promising candidate as a pharmacoperone to be tested in clinical trials for the treatment of NDI (Los et al., 2010).

Up to now, most of the pharmacoperones identified for GPCRs are antagonists (Tao and Conn, 2014). For example, a number of the gonadotropin-releasing hormone receptor (GnRHR) peptidomimetic antagonists have been developed as potential pharmacoperones and been extensively studied (Conn and Ulloa-Aguirre, 2011; Conn et al., 2007). Pulsatile infusion of one of them (IN3) successfully restores testis function of hypogonadotropic hypogonadal mice that harbored a *GnRHR* mutation (Janovick et al., 2013). These peptidomimetics are selected from four chemical classes, including indoles, quinolones, thienopyrimidinediones, and erythromycin-derived macrolides (Conn and Ulloa-Aguirre, 2011). Conn's laboratory found that the ability of these small compounds to rescue GnRHR mutants are proportional to their affinity for the WT GnRHR (Conn and Ulloa-Aguirre, 2011). Although low affinity antagonists are not able to bind to and stabilize misfolded receptors efficiently, antagonists with too high affinities are also not ideal candidates. When expressed at the cell surface, antagonists as pharmacoperones need to be disassociated from the receptor to allow the binding of endogenous agonists and antagonists with too high affinities are difficult to be replaced. Therefore, antagonists with appropriate affinities with the receptor are better candidates.

Agonists have also been identified as pharmacoperones for several GPCRs. For example, 24 h treatment of one A_1 adenosine receptor agonist (CPA) increase the cell surface expression of the mutants, whereas it does not decrease that of the WT receptor (Málaga-Diéguez et al., 2010). However, there are also studies reporting that small molecule agonists activate misfolded GPCRs intracellularly without increasing their cell surface expression. For example, three small molecule AVPR2 agonists activated AVPR2 misfolded mutants intracellularly without changing

their maturation and expression levels (Los et al., 2010; Robben et al., 2009). In addition, activation of AVPR2 mutants intracellularly dose not induce receptor degradation as observed at the plasma membrane (Los et al., 2010; Robben et al., 2009). For the calcium-sensing receptor (CaSR), studies reported that one allosteric modulator (NPS R-568) rescues the cell surface expression and signaling of many intracellularly retained CaSR mutants (Huang and Breitwieser, 2007; White et al., 2009). However, another study reported a different observation that NPS R-568 corrects the signaling of two intracellularly retained CaSR mutants without altering their cell surface expression levels (Nakamura et al., 2013). These studies indicate that agonists can act as pharmacoperones correcting the cell surface expression and thereby signaling of GPCRs and also can act as agonists activating GPCRs intracellularly. However, despite these important studies discussed herein, our knowledge about how small molecule agonists activating GPCR mutants intracellularly and how the cell deactivates this signaling is still limited. Further studies need to be carried out to answer these questions.

As discussed above, an allosteric modulator of the CaSR rescues the signaling of intracellularly retained CaSR mutants. Recently, an allosteric agonist has been identified to increase the cell surface expression and function of two LHR mutants (Newton et al., 2011). Allosteric ligands are better candidates of pharmacoperones because they do not compete with the endogenous agonists and therefore do not interfere with the activation of the mutant receptor when expressed at the cell surface. These compounds have major advances in the development of novel drugs (Conn et al., 2009). When we talk about candidates for the development of pharmacoperones, there are several criteria to consider: 1) To be sufficiently lipophilic to penetrate cell membranes; 2) To be specific for the target protein; 3) To bind the target protein with sufficient affinity and dissociate with the targets quickly to allow the binding of endogenous

ligands; 4) To be stable enough to stabilize the target protein; 5) To be potently effective for most of the mutant proteins (Conn et al., 2007).

Pharmacoperones not only rescue intracellularly retained GPCRs but may also improve the maturation of WT GPCRs. Many WT GPCRs are not expressed efficiently at the cell surface (Conn et al., 2007; Tao and Conn, 2014). It is reported that almost 30% of newly synthesized proteins in various cell types never acquire their correct native structures (Schubert et al., 2000). For example, the δ opioid receptor is an opioid receptor that has enkephalins as their endogenous ligands (Broom et al., 2002; Torregrossa et al., 2006). Studies found that only 40% of the newly synthesized δ opioid receptor was targeted to the cell surface, suggesting that the expression of WT δ opioid receptor is inefficient (Petaja-Repo et al., 2000). Opioid agonists and one antagonist (naltrexone) can selectively facilitate the folding and maturation of WT δ opioid receptor and target the WT receptor to the cell surface (Petäjä-Repo et al., 2002). Similar observations have also been reported in several other GPCRs, such as the GnRHR (Conn et al., 2007) and the MC4R (Tao, 2010). The maturation efficacy of WT receptor can be enhanced by pharmacoperones, suggesting that pharmacoperones can be potentially applied to regulate tissue responsiveness in normal individuals. In the case of the δ opioid receptor, pharmacoperones are important in the development of anti-nociceptive drugs.

Besides rescuing the mutant receptor itself, pharmacoperones may also eliminate the dominant negative effect of some mutants on the WT receptor (Conn and Ulloa-Aguirre, 2011). Dimerization and/or oligomerization have become well recognized for GPCR functions. Studies have found that for many GPCRs, some dysfunctional mutants also inhibit the function of the WT receptor through hetero-dimerization and/or oligomerization (dominant negative effect), which makes the disease more serious in heterozygous individuals (Tao, 2006). For example,

D90N MC4R, which has normal cell surface expression and ligand binding, but is loss of signaling, dose-dependently inhibits the signaling of WT MC4R (Biebermann et al., 2003). Many dominant negative mutants are misfolded and therefore retain the WT receptor intracellularly (Tao, 2006). Pharmacoperones may rescue the misfolded mutants or interfere with the dimerization and degradation of the WT-mutant aggregates (Conn and Ulloa-Aguirre, 2011). For example, several GnRHR mutants displayed dominant negative effects on other GnRHR mutants and that addition of a pharmacoperone (IN3) increased the ligand binding and signaling of these pairs of mutants coexpressed in COS-7 cells (Leanos-Miranda et al., 2005). Therefore, pharmacoperones have a more promising potential in treating human diseases caused by misfolded dominant negative mutants.

Pharmacoperones have also been identified for several other GPCRs that will not be discussed herein in detail.

1.3.4 Pharmacoperones for melanocortin-4 receptor

We were the first to identify a small molecule antagonist of the MC4R, ML00253764, as a pharmacoperone rescuing the cell surface expression and function of two MC4R mutants, C84R and W174C (Fan and Tao, 2009). ML00253764 also increases the cell surface expression of WT MC4R, indicating that it can potentially be used to treat obese patients without *MC4R* mutations (Fan and Tao, 2009). Then, we further confirmed the pharmacoperone effect of ML00253764 rescuing the cell surface expression of six other MC4R mutants, including S58C, N62S, P78L, G98R, C271Y, and F261S using confocal microscopy method (Tao, 2010).

Afterwards, Rene et al. tested five small molecule antagonists of the MC4R and found that DCPMP is the most potent pharmacoperone rescuing the cell surface expression and

function of most of the ten mutants studied, including S58C, E61K, N62S, I69T, I125K, T162I, R165Q, R165W, C271Y, and P299H (Rene et al., 2010). They also observed that the compounds studied have different rescuing efficacies for different mutants (Rene et al., 2010). Another group reported four novel antagonists of the MC4R rescuing the cell surface targeting and/or function of three MC4R mutants that were partially retained intracellularly, including V50M, S58C, and I137T (Ward et al., 2012). However, in this study, they have not provided the chemical structures of the four antagonists or their binding properties with the MC4R (Ward et al., 2012).

Chapter 2 Pharmacological study of the transmembrane domain 6 of human melanocortin-4 receptor

2.1 Introduction

The global epidemic of obesity, with a prevalence of 9.8% in the adults worldwide (Kelly et al., 2008) and 33.8% in the adults in the USA (Flegal et al., 2010), has become one of the most significant burdens to public health. Obesity is a major independent risk factor for cardiovascular diseases, and is often associated with type 2 diabetes mellitus, as well as other comorbidities (Guh et al., 2009). Though intervention of dietary control and physical activity can successfully contribute to the prevention of weight gain in some groups, it is difficult to reach long-term weight loss maintenance, especially for those carrying genetic defects (Kraschnewski et al., 2010; Lemmens et al., 2008; Reinehr et al., 2009).

Multiple genes have been identified to be associated with obesity, and mutations in the melanocortin-4 receptor (*MC4R*) have been characterized as the most frequent cause of monogenic obesity in humans, with a prevalence varied from 0 to 6% in different ethnic backgrounds (reviewed in Ref. (Tao, 2010)). Therefore, the MC4R has emerged as a premier target for obesity treatment. Adopting a codominant inheritance model (O'Rahilly et al., 2003), *MC4R* pathogenic mutations exhibit a varied degree of penetrance, interacting with environment (Stutzmann et al., 2008).

The MC4R, which is crucial for regulating both food intake and energy expenditure

(Huszar et al., 1997), is a G protein-coupled receptor (GPCR) primarily expressed in the central nervous system. Although the classical G protein for MC4R is the G_s, recent studies suggested that MC4R couples to all three major classes of G proteins (reviewed in Ref. (Breit et al., 2011)). The G_s-cyclic AMP (cAMP)-PKA and ERK1/2 signaling pathways are of particular interest, because they are identified to be related to the MC4R function of energy homeostasis *in vivo* (Czyzyk et al., 2008; Sutton et al., 2005).

Up to now, more than 150 naturally occurring mutations or common alleles of the *MC4R* have been identified (reviewed in Ref. (Tao, 2009)). They are scattered throughout the receptor. During the past few years, several studies have demonstrated the functional importance of transmembrane domain 6 (TM6) in the MC4R (Chen et al., 2007a; Chen et al., 2007b; Chen et al., 2009). At least 10 naturally occurring mutations or variants have been identified in TM6 and functionally characterized. Some of the mutants (such as L250Q, P260Q, F261S, and I269N) are retained in the endoplasmic reticulum (Fan and Tao, 2009; Proneth et al., 2006; Tan et al., 2009; Wang and Tao, 2011; Xiang et al., 2006), and L250Q (Proneth et al., 2006; Xiang et al., 2006) and I251L (Xiang et al., 2006) are constitutively active. Most of these mutations are associated with obesity, whereas I251L confers strong protection from obesity (Mirshahi et al., 2011; Stutzmann et al., 2007).

Despite these important studies, no systematic investigation of the whole TM6 has been reported. To gain a better understanding of the structure-function relationship of the MC4R, we sought to determine the function of each residue in TM6 of the receptor using alanine scanning mutagenesis. We generated 31 mutants and used the 2 endogenous ligands, α-melanocyte stimulating hormone (MSH) and β-MSH, for ligand binding and signaling studies. We also studied the basal activities of the constitutively active mutants in the ERK1/2 signaling pathway.

2.2 Materials and methods

2.2.1 Materials

[^{125}I]-[Nle^{4},D-Phe^{7}]-α-MSH (NDP-MSH) was purchased from the American Radiolabeled Chemicals (St. Louis, MO), α-MSH from Pi Proteomics (Huntsville, AL), and β-MSH from CHI Scientific (Maynard, MA). ML00253764 and Ipsen 5i were synthesized by Enzo Life Sciences, Inc. (Plymouth Meeting, PA). Radiolabeled cAMP was iodinated with chloramine T method. The c-myc-tagged WT human (h) MC4R at the N-terminus was described previously (Tao and Segaloff, 2003).

2.2.2 Site-directed mutagenesis

Mutant receptors were generated by QuikChange^{TM} site-directed mutagenesis kit (Stratagene, La Jolla, CA) using the WT receptor as the template, and sequenced by the DNA Sequencing Facility of University of Chicago Cancer Research Center (Chicago, IL) to confirm the presence of desired mutations and the absence of errors in the coding sequences.

2.2.3 Cell culture and transfection

HEK293 and 293T cells were purchased from American Type Culture Collection (Manassas, VA), and were cultured in Dulbecco's modified Eagle's medium with 10% newborn calf serum. The HEK293T cells were plated into 6-well clusters coated with 0.1% gelatin, transfected with the WT or mutant constructs at 50% confluence using calcium phosphate precipitation method (Tao et al., 2010), and were used for ligand binding and signaling studies approximately 48 h later. For western blot, HEK293T were seeded into gelatin-coated 100 mm

dishes and were transfected using the same method. The transfected HEK293 cells were selected by G418 for imaging the cell surface expression levels of the WT or mutant receptors by confocal microscopy.

2.2.4 Ligand binding assay

HEK293T cells were transfected as described above. On the day of experiment, cells were washed twice with warm Waymouth's MB752/1 media (Sigma-Aldrich, St. Louis, MO) containing 1 mg/ml bovine serum albumin (Waymouth/BSA). Then cells were incubated with 1ml Waymouth/BSA containing 50 µl 100,000 cpm of ^{125}I-NDP-MSH, and with or without different concentrations of α- or β-MSH giving a final concentration ranging from 10^{-10} M to 10^{-5} M for 1 h at 37^{o}C. Cells were then washed twice with cold Hank's Balanced Salt Solution to terminate the reactions, lysed by 100 µl 0.5 M NaOH, collected by cotton swabs, and counted in a gamma counter.

2.2.5 Cyclic AMP assay

HEK293T cells were transfected as described above. On the day of experiment, cells were washed twice with warm Waymouth/BSA and then incubated with 1 ml fresh Waymouth/BSA containing 0.5 mM isobutylmethylxanthine (Sigma-Aldrich) for 15 min at 37 ^{o}C. Then cells were treated with or without different concentrations of α- or β-MSH giving a final concentration ranging from 10^{-11} M to 10^{-5} M. After incubation at 37 ^{o}C for 1 h, cells were lysed by 0.5 M percholoric acid containing 180 µg/ml theophylline and neutralized by 0.72 M KOH/0.6 M $KHCO_3$. Cyclic AMP levels were measured using radioimmunoassay (Tao et al., 2010).

2.2.6 Confocal microscopy assay

The method for immunohistochemistry has been described before (Tao and Segaloff, 2003). Briefly, HEK293 cells stably expressing c-myc tagged WT or mutant MC4Rs were established as described above. Cells were seeded into lysine-coated 8-well chamber slides (Biocoat cellware from Falcon, BD Systems, Franklin Lakes, NJ) and incubated at 37 ^{o}C for approximately 24 h. Cells were fixed with 4% paraformaldehyde in filtered PBS for immunohistochemistry (PBS-IH) for 30 min and incubated with 5% BSA in PBS-IH for 1 h to block non-specific binding. Cells were then incubated with the primary antibody, 9E10 monoclonal anti-myc antibody (Developmental Studies Hybridoma Bank at the University of Iowa, Iowa City, IA) (1:100 dilution in PBS-IH with 0.5% BSA) for 1 h, and this was followed by incubation with the secondary antibody, Alexa Fluor 488-conjugated goat anti-mouse IgG (Invitrogen) (1:1000 dilution in PBS-IH 0.5% BSA) for 1 h. The slide was then covered by a coverslip using Vectashield Mounting Media (Vector Laboratories, Burlingame, CA). Fluorescent images were taken using a Bio-Rad confocal microscope.

2.2.7 Protein preparation and western blot

HEK293T cells were seeded and transfected as described above. Approximately 24 h after transfection, cells were starved in Waymouth/BSA at 37 ^{o}C overnight, and then were treated with or without different concentrations of NDP-MSH giving a final concentration ranging from 10^{-9} M to 10^{-6} M in 5 ml Waymouth/BSA for 5 min at 37 ^{o}C. Cells were placed directly on ice and washed twice with cold 0G (150 M NaCl, 20 mM Hepes, pH 7.4), and then were scraped into lysis buffer in 0G (containing 0.5% NP-40, 2 mM EDTA, 1 mMNa_3VO_4, and

1 mM NaF). Total protein concentrations were determined by Bradford protein assay, and 30 μg protein samples were separated by 10% SDS-PAGE using the Tris-glycine buffer system and blotted onto pre-wetted PVDF membranes in wet conditions. The membranes were blocked in 10% non-fat dry milk (containing 0.2% Tween-20) for at least 3 h at room temperature with agitation, and then immunoblotted with the primary antibodies, rabbit p-ERK1/2 antibody (Cell Signaling, Billerica, MA) 1:1000 and mouse β-tubulin antibody (Developmental Studies Hybridoma Bank at the University of Iowa) 1:40,000 diluted in TBST/5% BSA overnight at 4 ^{o}C. This was followed by the incubation of the HRP-conjugated secondary antibodies, anti-rabbit antibody (Jackson ImmunoResearch, West Grove, Pennsylvania) 1:1000 and anti-mouse antibody (Jackson ImmunoResearch) 1:40,000 diluted in 10% non-fat dry milk for at least 1 h at room temperature. Specific bands were detected with ECL reagent (Thermo Scientific, Rockford, IL), and were analyzed and quantified by ImageJ software (NIH, Bethesda, MD).

2.2.8 Data analysis

The competitive binding curves and cAMP dose-response curves were fitted to a one-site model using GraphPad Prism 4.0 software (San Diego, CA). Concentrations that result in 50% inhibition (IC_{50}) and apparent maximal binding (Bmax) were calculated from competitive binding data. Concentrations that result in 50% maximal responses (EC_{50}) and maximal responses (Rmax) were calculated from cAMP assays. The significance of differences in p-ERK1/2 levels, and binding and signaling parameters between WT and mutant MC4Rs were analyzed by Student's t-test using Prism 4.0.

2.3 Results

The two endogenous agonists of MC4R, α-MSH (Fan et al., 1997) and β-MSH (Abbott et

al., 2000), have been shown to be capable of controlling feeding and energy balance through activation of MC4R. Here, we first studied the binding and signaling properties of all thirty-one MC4R mutants using α- or β-MSH as the ligand.

2.3.1 Pharmacology of the WT and mutant MC4Rs at α-MSH

Competitive binding assays were performed using ^{125}I-NDP-MSH as the radioligand, and different concentrations of α-MSH, from 10^{-10} M to 10^{-5} M, were used to displace radioligand in HEK293T cells transiently transfected with WT or mutant MC4Rs. IC_{50} values were calculated and analyzed for the WT and mutant MC4Rs. Our data showed that H264A had no detectable binding; L265A and Y268A had decreased affinities, whereas M241A, A244G, T246A, L250A, C257A, P260A, I266A, and F267A had increased affinities for α-MSH (Figure 2.2A and Table 2.1).

To measure the signaling capacities of the mutant receptors, HEK293T cells transiently transfected with WT or mutant MC4Rs were stimulated with increasing concentrations of α-MSH. Intracellular cAMP levels were measured after 1 h stimulation. Maximal response (Rmax) and EC_{50} values were calculated from the dose-response curves. Our data showed that H264A only responded to 10^{-5} M α-MSH. Six mutants (L247A, W258A, P260A, F261A, L265A, and Y268A) had increased EC_{50} values compared to the WT MC4R (Figure 2.2B). One mutant (A259G) had decreased EC_{50}. Four mutants (G243A, T246A, L250A, and F254A) had decreased Rmax, whereas five mutants (P260A, F261A, L265A, I266A, and I269A) had increased maximal responses compared to the WT MC4R. The other mutants had similar EC_{50} and Rmax as the WT MC4R (Figure 2.2B and Table 2.1).

2.3.2 Pharmacology of the WT and mutant MC4Rs at β-MSH

When ligand binding and signaling experiments were performed using β-MSH as the ligand, similar data were obtained, with some moderate differences. In binding experiments, L265A and Y268A had significantly increased IC_{50}s, whereas T246A, L250A and P260A had decreased IC_{50}s (Figure 2.3A and Table 2.1). In signaling experiments, H264A was only responsive to 10^{-5} M β-MSH stimulation. Twelve mutants (T246A, L247A, L250A, I251A, G252A, F254A, W258A, P260A, F261A, F262A, L265A, and Y268A) had increased EC_{50}s compared to the WT MC4R, and two mutants (V253A and A259G) had decreased EC_{50}s (Figure 2.3B and Table 2.1). Three mutants (I245A, F254A, and A259G) had decreased Rmax (Figure 2.3B and Table 2.1).

Bmax values were also calculated from these binding assays. As described above, H264A had no measureable binding. In addition, twelve mutants (G243A, A244G, L250A, I251A, F254A, V255A, C257A, P260A, F261A, L265A, I266A, and I269A) had decreased Bmax (Figure 2.4).

2.3.3 Cell surface expression of several mutant MC4Rs

Retention of mutant receptors in the endoplasmic reticulum (ER) by the quality control system is the major defect of inactivating *MC4R* mutations (reviewed in Ref. (Tao, 2005)). For the six mutants (L250A, C257A, P260A, F261A, H264A, and L265A) that caused dramatic decrease in Bmax, by more than 50% of WT, F261A and H264A were previously reported to be targeted to the plasma membrane normally (Chen et al., 2007b; Chen et al., 2009), and L250A was described to be expressed at the cell surface at 57% of WT (Proneth et al., 2006). C257A showed increased affinity for ligand binding and normal signaling properties, therefore it was not

studied here.

We selected the two mutants (P260A and L265A) not studied before and one mutant (H264A) lacking ligand binding to investigate their expression at the plasma membrane. HEK293 cells stably expressing c-myc tagged WT or mutant MC4Rs were used and imaged by the confocal microscope at the nonpermeabilized status. Immunostaining of H264A and L265A was at least as strong as the WT MC4R, demonstrating that the two mutants were indeed successfully transported to the plasma membrane. The immunostaining of P260A was weaker than that of the WT (Figure 2.5).

2.3.4 Constitutive activity of WT and mutant MC4Rs in the G_s-cAMP-PKA pathway

The MC4R was previously described to be constitutively active (Nijenhuis et al., 2001), and the extracellular N-terminus of the receptor, which could be positioned similar to the endogenous agonists (Pogozheva et al., 2005), acted as a tethered intramolecular ligand (Srinivasan et al., 2004). Impairment in the fine-tuning of constitutive activity, the basal signaling in the absence of any ligand, was reported to affect the long-term energy balance (Srinivasan et al., 2004). Herein, the constitutive activities of the thirty-one mutants were measured and analyzed. The basal cAMP level of the WT receptor was 32.60 ± 4.39 pmol/10^6 cells. We found nine mutants (K242A, G243A, T246A, L247A, I251A, G252A, W258A, P260A and H264A) had significantly lower basal cAMP levels compared with that of the WT receptor. Eight mutants (N240A, M241A, A244G, L250A, A259G, I266A, F267A and I269A) displayed a modest elevation of basal activities, and hence were identified to be constitutively active mutants (CAMs) (Figure 2.6A).

Both Ipsen 5i (K_i, 2nM) (Poitout et al., 2007) and ML00253764 (K_i 0.16 μM) (Vos et al.,

2004) were synthesized and identified as selective antagonists of MC4R, and subsequently were characterized to exert partial inverse agonistic actions at MC4R (Tao, 2010; Tao et al., 2010). We studied the inverse agonistic properties of these two small molecules at the eight constitutively active mutants described above. HEK293T cells transiently transfected with WT or mutant MC4Rs were incubated in the presence or absence of 10^{-6} M Ipsen 5i or 10^{-5} M ML00253764, and cAMP levels were measured. The basal activities of the WT and all the mutants were significantly decreased by the treatment of either Ipsen 5i or ML00253764. The maximal inhibition of L250A was 41% for Ipsen 5i and 60% for ML00253764. Of the WT and other mutants, the maximal inhibition ranged from 65% to 85% for Ipsen 5i, and from 80% to 88% for ML00253764 (Figure 2.6B).

2.3.5 Constitutive activity of WT and mutant MC4Rs in the ERK1/2 pathway

MC4R activation results in phosphorylation of ERK1/2 (reviewed in Ref. (Tao, 2010)). We showed seven mutants generated in this study were constitutively active in cAMP pathway. We investigated whether these seven mutant MC4Rs were also constitutively active in the ERK1/2 signaling pathway. The phosphorylation levels of ERK1/2 (pERK1/2) were measured through western blots. Data from the experiments showed that five of these mutants (M241A, L250A, I266A, F267A, and I269A) were also constitutively active in the MAP kinase pathway with significantly enhanced basal ERK1/2 phosphorylation. Two mutants (A244G and A259G) displayed similar basal pERK1/2 levels as the WT MC4R (Figure 2.7).

2.3.6 Signaling property of H264A MC4R in the ERK1/2 pathway

H264A, undetectable in competitive binding assays, was only responsive to 10^{-5} M α- or

β-MSH stimulation with increased cAMP production. One previous study reported the EC_{50} of H264A was 0.14 μM for NDP-MSH (Chen et al., 2007b). To investigate whether it also affects ERK1/2 signaling pathway, we studied the phosphorylation levels of ERK1/2 in the absence or presence of different concentrations of NDP-MSH giving a final concentration ranging from 10^{-9} M to10^{-6} M. H264A was only responsive to 10^{-6} M NDP-MSH stimulation. Compared with the WT, H264A was significantly defective in both basal and stimulated ERK1/2 phosphorylation (Figure 2.8).

2.4 Discussion

In rhodopsin-like GPCRs, transmembrane domain 6 has been demonstrated to be able to directly contact the ligand (Chien et al., 2010; Hanson et al., 2012; Jaakola et al., 2008; Xu et al., 2011), alter receptor conformations through intramolecular interactions (Palczewski et al., 2000; Park et al., 2008), and interact with cognate G proteins (Abell and Segaloff, 1997; Murakami and Kouyama, 2008; Scheerer et al., 2008). In the β_2-adrenoceptor, TM6 has been shown to cause the largest changes between agonist- and inverse agonist-bound conformations (Rasmussen et al., 2007), and also been suggested to be involved in regulating the high basal activity of this receptor (Rasmussen et al., 2007; Rosenbaum et al., 2007). For the current study, we performed detailed pharmacological study of thirty-one alanine mutants of each residue in the TM6 of MC4R.

Two residues (L250 and P260) were important for cell surface expression of MC4R. Alanine mutations of the two residues (L250A and P260A) severely impaired normal plasma targeting of the receptor. At these positions, two naturally occurring mutations, L250Q (Proneth et al., 2006; Xiang et al., 2006) and P260Q (Wang and Tao, 2011), were also reported to cause

intracellular retention of MC4R, characterized by decreased cell surface expression, but normal total expression levels. Further studies on the interactions between these mutants and molecular chaperones might help to understand the forward trafficking mechanism of MC4R.

Five residues (F254, F261, H264, L265, and Y268) were indispensable for α- and β-MSH binding. F254$^{6.44}$A, which signaled normally with NDP-MSH stimulation (Chen et al., 2007b), had impaired interactions with α- and β-MSHs. The corresponding residue of Phe$^{6.44}$ in other GPCRs was reported to be important for the rotation of TM6, which led to an outward shift of the cytoplasmic end of this transmembrane domain (Lebon et al., 2011; Rasmussen et al., 2011), and this movement opened the binding site for the carboxyl terminus of Gα (Scheerer et al., 2008). Previously, F261A and H264A were reported to severely impair the ligand binding and signaling processes of NDP-MSH (Chen et al., 2007b; Haskell-Luevano et al., 2001; Yang et al., 2000), though another study reported that F261A has no effect on NDP-MSH binding affinity, but restored the signaling efficacy of modified NDP-MSH (Fleck et al., 2007). The residues important for the binding and signaling of α- and β-MSH are mostly located in the upper region of the transmembrane domain. They probably could directly participate in the hydrophobic binding pocket (F261, H264, L265, and Y268) respectively, interacting with the pharmacophore His^{6}-Phe^{7}-Arg^{8}-Trp^{9} of α- and β-MSH.

Six residues (T246, L247, I251, G252, W258, and F262) were crucial for normal receptor signaling upon α- and β-MSH stimulation. Alanine mutations of these residues led to severely decreased signaling potencies and reduced basal signaling activities (except F262A). These residues, primarily located at the cytoplasmic half of the transmembrane domain, probably maintain the active conformation of the receptor. Serine mutation of G252 (G252S) caused significantly decreased signaling potency with α-MSH and ACTH (1-24), but not β-MSH (Xiang

et al., 2007). However, alanine mutation of G252 (G252A) acted differently; it exhibited impaired signaling properties for both α- and β-MSH. W258A was previously reported to cause a 3-fold increase in Ki and >10-fold increase in EC_{50} with NDP-MSH stimulation by some studies (Chen et al., 2007b; Chen et al., 2009), and was described not to affect interactions with NDP-MSH by another study (Pogozheva et al., 2005). This mutant showed normal ligand binding, but severe defect in signaling to α- and β-MSH in our study. The homologous residues of $Trp^{6.48}$ was described to directly contact with the ligand in A_{2A} adenosine receptor (Jaakola et al., 2008) and rhodopsin (Cherezov et al., 2007) but not in β_2-adrenoceptor (Cherezov et al., 2007; Rasmussen et al., 2007).

Although no binding could be detected for H264A, with the more sensitive signaling assays, we showed that it responded to high concentrations of ligand stimulation with increased cAMP levels (10^{-5} M α- or β-MSH stimulation) and ERK1/2 phosphorylation (10^{-6} M NDP-MSH stimulation). Basal signaling in both pathways was also decreased compared to the WT receptor. No apparent biased signaling (see below) was observed.

The basal activities of the MC4R have been suggested to be of physiological and pathophysiological significance. Defects in basal signaling have been suggested to be a potential cause of genetic obesity caused by *MC4R* mutations (Srinivasan et al., 2004). We also showed that some naturally occurring *MC4R* mutations decrease basal signaling activity (Fan and Tao, 2009; Tao and Segaloff, 2005; Wang and Tao, 2011). Unlike the related MC3R that has no basal activity (Tao, 2007), the WT MC4R has modest basal activity that can be decreased by Agouti-related protein (Nijenhuis et al., 2001; Tao et al., 2010). In this study, we showed that of the thirty-one mutations generated, nine mutants had significantly decreased basal activities (Figure 2.6). Eight mutants (N240A, M241A, A244G, L250A, A259G, I266A, F267A and I269A) had

increased basal cAMP levels and the basal activities of these mutants could be partially inhibited by the treatment of either Ipsen 5i or ML00253764 (Figure 2.6), two MC4R inverse agonists (Nicholson et al., 2006; Tao et al., 2010), suggesting that these mutants are constitutively active mutants (CAM). They are numbered as 6.30, 6.31, 6.34, 6.40, 6.49, 6.56, 6.57, and 6.59 according to the numbering scheme of Ballesteros and Weinstein (Ballesteros and Weinstein, 1995). Previous studies with the glycoprotein hormone receptors showed that mutations at some of these loci (such as 6.30, 6.34, and 6.40) were found to cause constitutive activation that cause human diseases (reviewed in (Tao, 2008)). However, other loci found to cause constitutive activation in the glycoprotein hormone receptors, including the hotspot 6.44 and surrounding residues 6.37, 6.38, 6.41, 6.42, 6.43, and 6.45 (see (Tao, 2008) for original references), did not cause constitutive activation in MC4R. These results suggested that although TM6 is a domain that is important for constraining the WT in inactive conformation in many GPCRs through interhelical interactions with TM5 and TM7 (Schneider et al., 2010; Tao et al., 2002), there are important differences in the local environment that contributed to the differences in constitutive activities.

It has been suggested that in family A GPCRs, an acidic residue at position 6.30 and R3.50 of the DRY motif in TM3 form a salt bridge constraining the WT receptor in inactive conformation. Mutations of 6.30 cause constitutive activation in rhodopsin (Ramon et al., 2007), β_2-adrenoceptor (Ballesteros et al., 2001), and lutropin receptor (Angelova et al., 2002). The salt bridge was indeed observed in the crystal structure of rhodopsin (Palczewski et al., 2000). However, the ionic lock is not observed in the crystal structures of the turkey β_1-adrenoceptor (Warne et al., 2008), the human β_2-adrenoceptor (Cherezov et al., 2007; Rosenbaum et al., 2007), human A_{2A} adenosine receptor (Jaakola et al., 2008), and human κ-opioid receptor (Wu et al.,

2012). Mutagenesis data also suggested that this ionic lock is not important in other GPCRs (Schneider et al., 2010). N240 in MC4R cannot form a salt bridge with R3.50, although its mutation led to constitutive activation.

MC4R also activates ERK1/2 signaling pathway. We asked whether the mutants that had increased basal cAMP levels also constitutively activated the ERK1/2 pathway. Transfected cells were starved overnight in serum-free media and levels of phosphorylated ERK1/2 were measured by western blots. We showed herein that five of these mutants (M241A, L250A, I266A, F267A, and I269A) were also constitutively active in the MAP kinase pathway with significantly enhanced basal ERK1/2 phosphorylation. To the best of our knowledge, this is the first study to show that mutations in the MC4R could constitutively activate the ERK1/2 pathway. We showed that two mutants (A244G and A259G) had increased basal cAMP levels but had normal basal pERK1/2 levels. The results suggested that these mutants preferentially stabilize certain active conformations of the receptor. Mutations displaying biased signaling have already been identified in MC4R and several other GPCRs, such as MC4R-D90N (Buch et al., 2009), MC1R-E92K (Benned-Jensen et al., 2011), and M_2 muscarinic acetylcholine receptor-Y104A and Y177A (Gregory et al., 2010). Phosphorylation of ERK1/2 induced by MC4R had been described to be mediated by PKA (Sutton et al., 2005), PKC (Chai et al., 2006), or PI3K (Vongs et al., 2004) depending on the cell lines used, and also may be initiated independently by β-arrestins as suggested in other GPCRs (reviewed in Ref. (Reiter et al., 2012; Violin and Lefkowitz, 2007)). More studies are needed to elucidate the biased signaling mechanisms of MC4R.

In summary, of the thirty-one residues in the TM6 of MC4R, we have identified residues that were important for cell surface expression, ligand binding, cAMP production, and

maintaining the WT receptor in active conformation. We also reported the constitutive activation of ERK1/2 pathway. These data provided comprehensive information on the structure-function relationship of the TM6 of MC4R, and will be useful for rationally designing MC4R agonists and antagonists for treatment of energy balance disorders.

Table 2.1 The ligand binding and signaling properties of WT and mutant MC4Rs in response to α- or β-MSH stimulation.

hMC4R	α-MSH Binding	α-MSH-stimulated cAMP		β-MSH Binding	β-MSH-stimulated cAMP	
Construct	IC_{50} (nM)	EC_{50} (nM)	Rmax (% WT)	IC_{50} (nM)	EC_{50} (nM)	Rmax (% WT)
WT	1120.36 ± 157.69	4.29 ± 0.79	100	858.18 ± 216.64	2.34 ± 0.17	100
N240A	415.00 ± 68.27	3.18 ± 1.14	89.22 ± 15.27	240.49 ± 79.69	2.82 ± 1.45	102.60 ± 23.91
M241A	202.70 ± 14.63[a]	1.54 ± 0.44	131.42 ± 22.37	126.41 ± 30.19	1.30 ± 0.29	74.76 ± 13.74
K242A	614.50 ± 235.71	35.05 ± 10.77	112.32 ± 23.61	387.53 ± 122.68	10.88 ± 4.00	74.39 ± 17.02
G243A	730.80 ± 268.06	12.55 ± 4.26	65.83 ± 5.91[b]	216.57 ± 53.71	4.043 ± 0.99	106.61 ± 29.00
A244G	183.10 ± 45.30[a]	4.23 ± 1.44	87.11 ± 13.98	115.03 ± 9.56	1.48 ± 0.47	136.98 ± 24.91
I245A	828.10 ± 190.35	2.62 ± 0.94	133.69 ± 25.68	192.70 ± 34.30	3.24 ± 1.15	65.33 ± 3.51[b]
T246A	23.23 ± 2.39[a]	6.09 ± 1.66	68.52 ± 3.22[b]	31.11 ± 3.46[b]	38.05 ± 12.9[a]	128.87 ± 43.23
L247A	1337.97 ± 463.56	37.82 ± 3.23[b]	76.84 ± 10.34	723.97 ± 149.75	30.18 ± 4.82[b]	143.71 ± 41.51
T248A	2502.67 ± 382.82	1.86 ± 0.39	98.35 ± 16.20	642.17 ± 83.42	2.65 ± 0.72	79.52 ± 11.07
I249A	423.63 ± 67.09	3.36 ± 1.24	118.89 ± 34.01	280.73 ± 19.34	4.34 ± 0.93	95.39 ± 27.75
L250A	23.85 ± 15.89[a]	4.13 ± 1.57	43.67 ± 6.72[a]	50.57 ± 6.54[a]	9.51 ± 2.2[a]	94.73 ± 5.54
I251A	1147.97 ± 450.20	22.08 ± 7.02	78.00 ± 11.17	834.33 ± 217.62	31.76 ± 9.12[a]	115.50 ± 9.44
G252A	1717.98 ± 512.41	5.64 ± 1.06	91.99 ± 25.52	867.10 ± 251.24	14.82 ± 2.18[b]	117.70 ± 5.97[a]
V253A	889.45 ± 308.28	2.23 ± 0.30	89.49 ± 14.29	981.70 ± 231.31	0.77 ± 0.28[a]	86.58 ± 12.45
F254A	277.57 ± 109.98	5.36 ± 1.61	54.82 ± 11.67[a]	173.77 ± 20.73	6.18 ± 1.01[a]	69.12 ± 8.28[a]
V255A	501.77 ± 79.09	2.28 ± 0.68	74.86 ± 11.6	1010.53 ± 192.72	1.71 ± 0.55	81.47 ± 7.56
V256A	1043.67 ± 314.14	4.52 ± 1.77	90.5 ± 11.95	1532.90 ± 503.43	1.71 ± 0.31	80.25 ± 13.46
C257A	198.33 ± 58.36[a]	3.98 ± 0.94	98.12 ± 31.62	364.03 ± 74.94	1.99 ± 0.24	101.55 ± 20.04
W258A	1638.00 ± 532.63	36.78 ± 11.84[a]	132.24 ± 14.59	1461.13 ± 404.94	29.94 ± 4.11[b]	95.60 ± 10.70
A259G	886.73 ± 226.82	1.29 ± 0.48[a]	139.67 ± 23.16	1233.60 ± 280.59	0.75 ± 0.36[a]	64.93 ± 13.20[a]
P260A	90.28 ± 6.48[a]	47.24 ± 16.79[a]	157.82 ± 22.42[a]	95.51 ± 28.85[a]	41.06 ± 5.97[b]	134.20 ± 21.77
F261A	1154.50 ± 324.91	39.41 ± 14.57[a]	186.61 ± 15.41[b]	829.20 ± 196.47	37.36 ± 7.06[b]	174.82 ± 34.61
F262A	2201.67 ± 298.8	11.80 ± 3.61	179.57 ± 59.19	1624.25 ± 429.92	13.88 ± 1.73[b]	121.68 ± 22.23
L263A	854.47 ± 61.23	4.09 ± 1.36	237.90 ± 63.41	768.05 ± 295.29	2.83 ± 0.60	100.97 ± 2.77
H264A	N/A[c]	N/A[d]	N/A[d]	N/A[c]	N/A[d]	N/A[d]
L265A	4893.67 ± 922.79[b]	196.76 ± 58.24[b]	204.86 ± 23.85[a]	3255.33 ± 682.79[b]	164.80 ± 31.35[b]	98.06 ± 12.54
I266A	200.47 ± 33.83[a]	2.42 ± 1.08	164.88 ± 15.52[a]	246.51 ± 94.79	1.60 ± 0.10	96.29 ± 27.55
F267A	415.27 ± 40.69[a]	4.09 ± 1.26	148.20 ± 22.56	378.08 ± 127.62	1.88 ± 0.31	94.54 ± 4.13
Y268A	2823.00 ± 605.36[a]	31.12 ± 12.24[a]	110.29 ± 13.04	4440.00 ± 1010.88[b]	46.53 ± 8.68[b]	86.18 ± 13.16
I269A	212.43 ± 43.15	4.32 ± 0.63	139.46 ± 14.59[a]	244.15 ± 60.04	5.61 ± 1.49	168.04 ± 25.97
S270A	665.87 ± 134.75	4.95 ± 1.77	124.34 ± 16.30	799.63 ± 166.75	1.77 ± 0.27	125.15 ± 32.30

[a] Significantly different from WT MC4R, $p<0.05$.

[b] Significantly different from WT MC4R, $p<0.01$.

[c] Not detected.

[d] Only responsive to 10^{-5} M α- or β-MSH stimulation.

Values are mean ± S.E.M. of at least three independent experiments. The Rmax of WT MC4R

was 2744.11 ± 373.20 pmol/10^6 cells with α-MSH stimulation, and was 2848.15 ± 377.85 pmol/10^6cells with β stimulation.

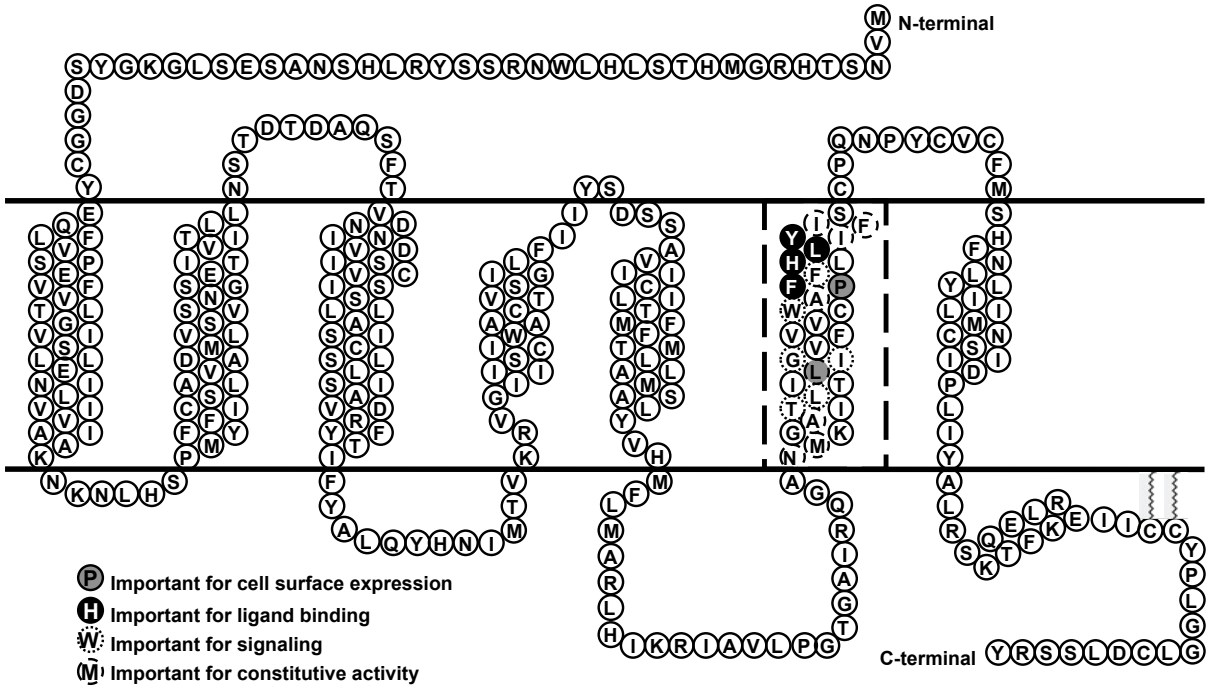

Figure 2.1 Schematic representation of the thirty-one residues in TM6 of MC4R.

The phenotypes of mutations at several loci that changed cell surface expression, ligand binding, signaling, and constitutive activity are highlighted.

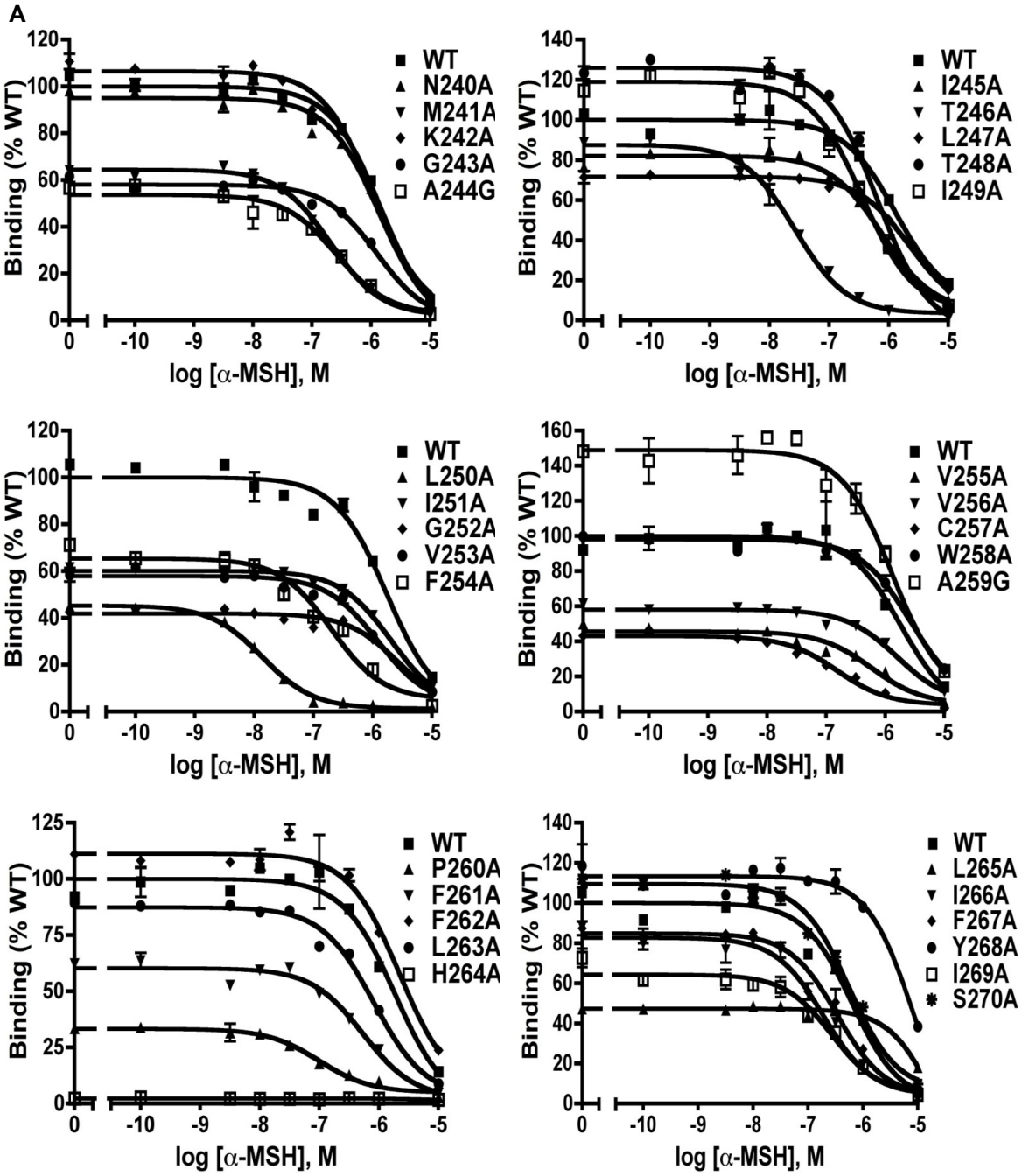
A
Binding (% WT)
log [α-MSH], M
WT
N240A
M241A
K242A
G243A
A244G
WT
I245A
T246A
L247A
T248A
I249A
WT
L250A
I251A
G252A
V253A
F254A
WT
V255A
V256A
C257A
W258A
A259G
WT
P260A
F261A
F262A
L263A
H264A
WT
L265A
I266A
F267A
Y268A
I269A
S270A

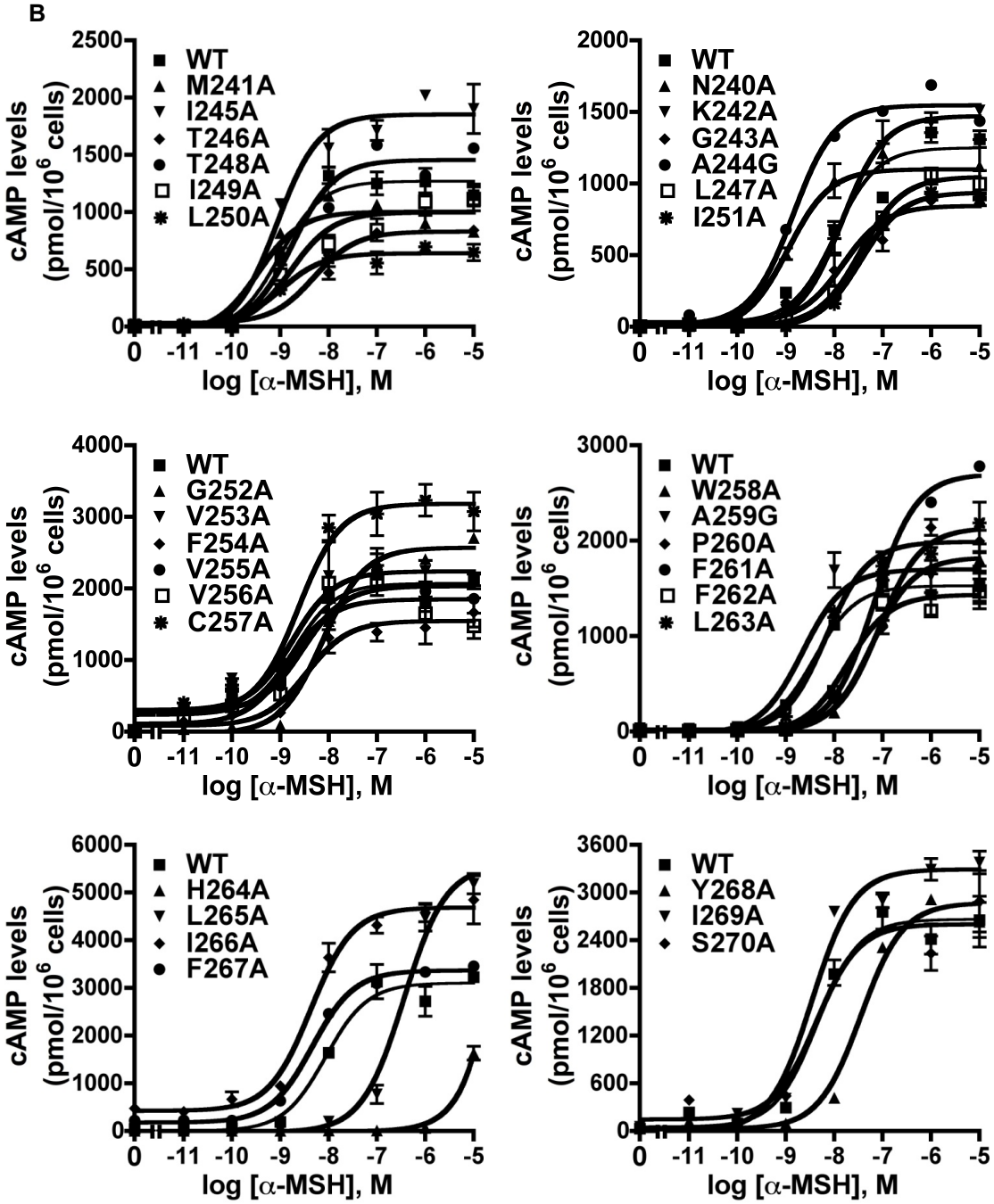

Figure 2.2 The ligand binding (A) and signaling (B) properties of WT and mutant MC4Rs with α-MSH as the ligand.

HEK293T cells were transiently transfected with WT or mutant constructs, and 48 h later were

used for binding and signaling studies. (A) Intact cell surface binding was measured by competitive inhibition of ^{125}I-NDP-MSH with serial concentrations of α-MSH. Data are depicted as % of WT maximal binding. (B) Intracellular cAMP samples were collected with or without stimulation with different concentrations ofα-MSH, and cAMP concentrations were determined by radioimmunoassay. Data points are mean ± S.E.M. of duplicate (A) or triplicate (B) measurements within one experiment. Results are representative of at least three independent experiments.

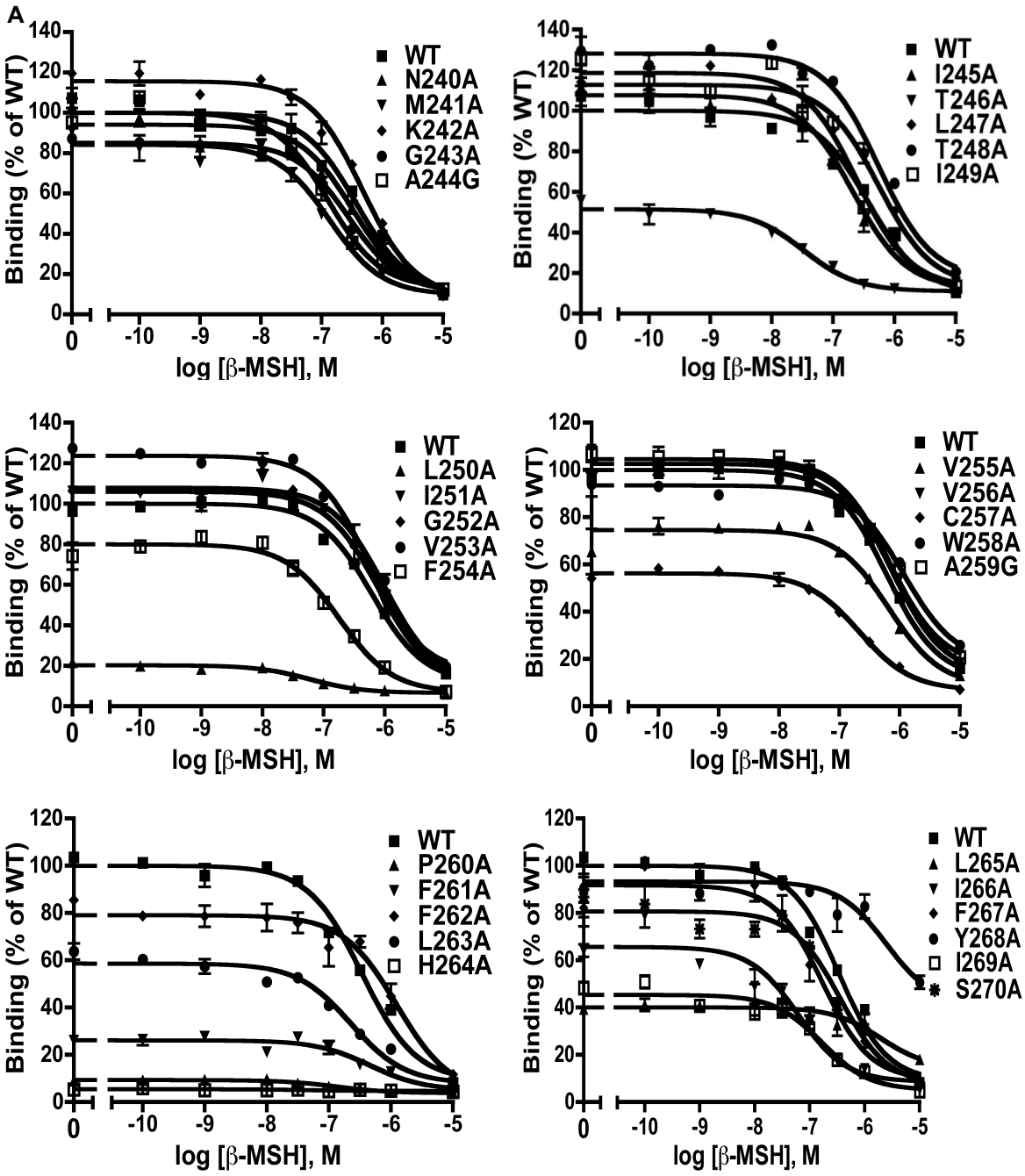
A
Binding (% of WT)
log [β-MSH], M
WT
N240A
M241A
K242A
G243A
A244G
WT
I245A
T246A
L247A
T248A
I249A
WT
L250A
I251A
G252A
V253A
F254A
WT
V255A
V256A
C257A
W258A
A259G
WT
P260A
F261A
F262A
L263A
H264A
WT
L265A
I266A
F267A
Y268A
I269A
S270A

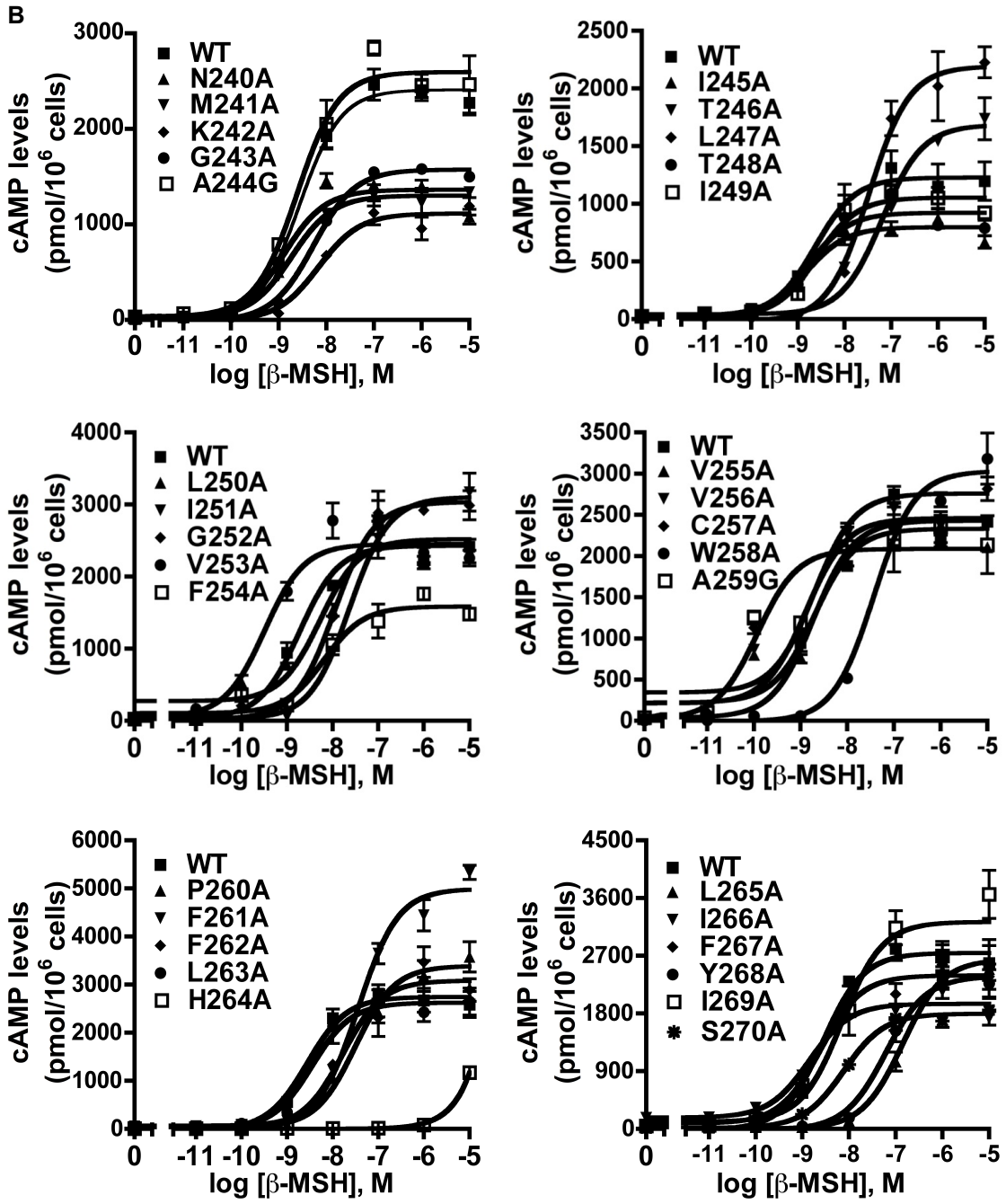

Figure 2.3 The ligand binding (A) and signaling (B) properties of WT and mutant MC4Rs with β-MSH as the ligand.

HEK293T cells were transiently transfected with WT or mutant constructs and 48 h later were used for binding and signaling studies. (A) Intact cell surface binding were measured by

competitive inhibition of ^{125}I-NDP-MSH with serial concentrations of β-MSH. Data are depicted as % of WT maximal binding. (B) Intracellular cAMP samples were collected with or without stimulation with different concentrations of β-MSH, and cAMP concentrations were determined by radioimmunoassay. Data points are mean ± S.E.M. of duplicate (A) or triplicate (B) measurements within one experiment. Results are representative of at least three independent experiments.

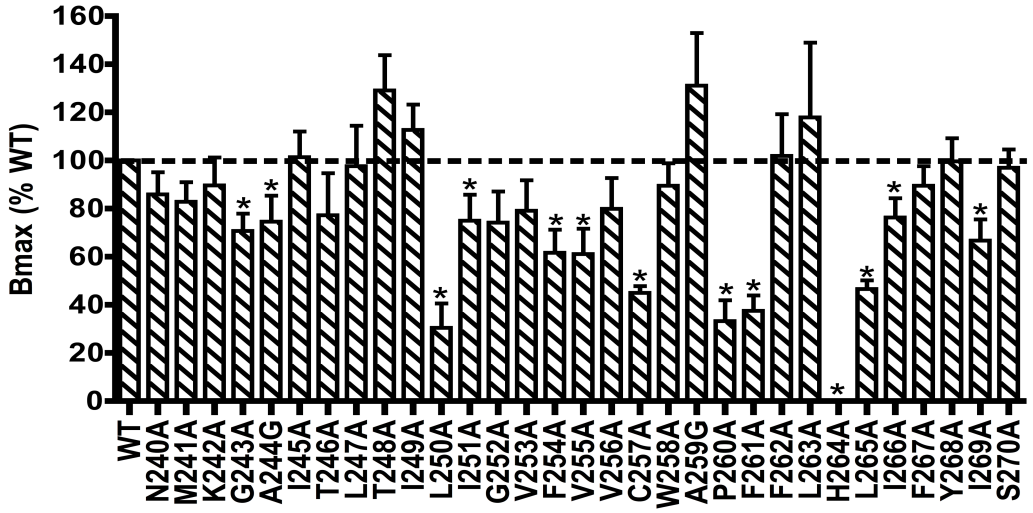

Figure 2.4 Total specific binding of WT and mutant MC4Rs (% WT).

Data are mean ± S.E.M. of at least six independent experiments. * Significantly different from WT MC4R, $p<0.05$.

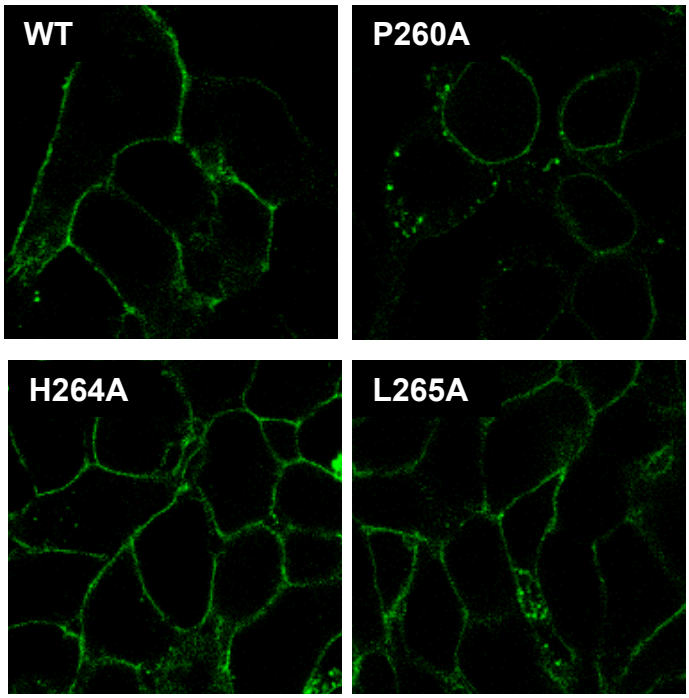

Figure 2.5 Confocal imaging of WT and mutant MC4Rs.

The intact HEK293 cells stably expressing WT or mutant receptors were stained with fluorescein-conjugated anti-myc monoclonal antibody and cell surface fluorescence were detected by confocal microscopy.

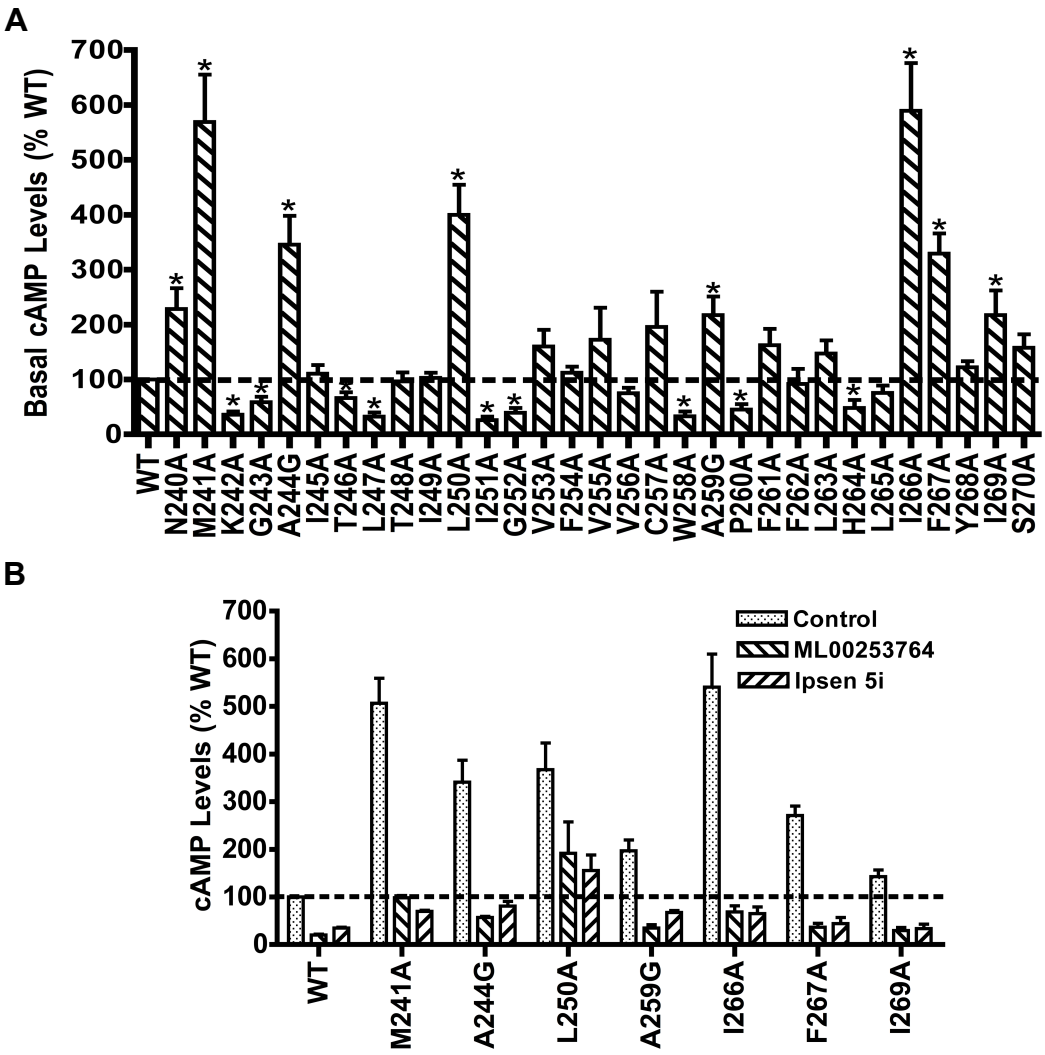

Figure 2.6 Basal activities of WT and mutant MC4Rs.

(A) HEK293T cells were transiently transfected with WT or mutant receptors, and intracellular cAMP levels were measured without any stimulation of the ligand. Data, expressed as % WT basal activity, are shown as mean ± S.E.M. of at least six independent experiments. The cAMP levels of WT MC4R were 32.60 ± 4.39 pmol/10^6 cells. * Significantly higher or lower than WT MC4R, $p<0.05$. (B**)** Partial inverse agonism of Ipsen 5i and ML00253764. HEK293T cells were transiently transfected with WT or mutant receptors, and 48 h later were treated with 10^{-6} M Ipsen 5i or 10^{-5} M ML00253764. Cyclic AMP levels were measured with radioimmunoassay.

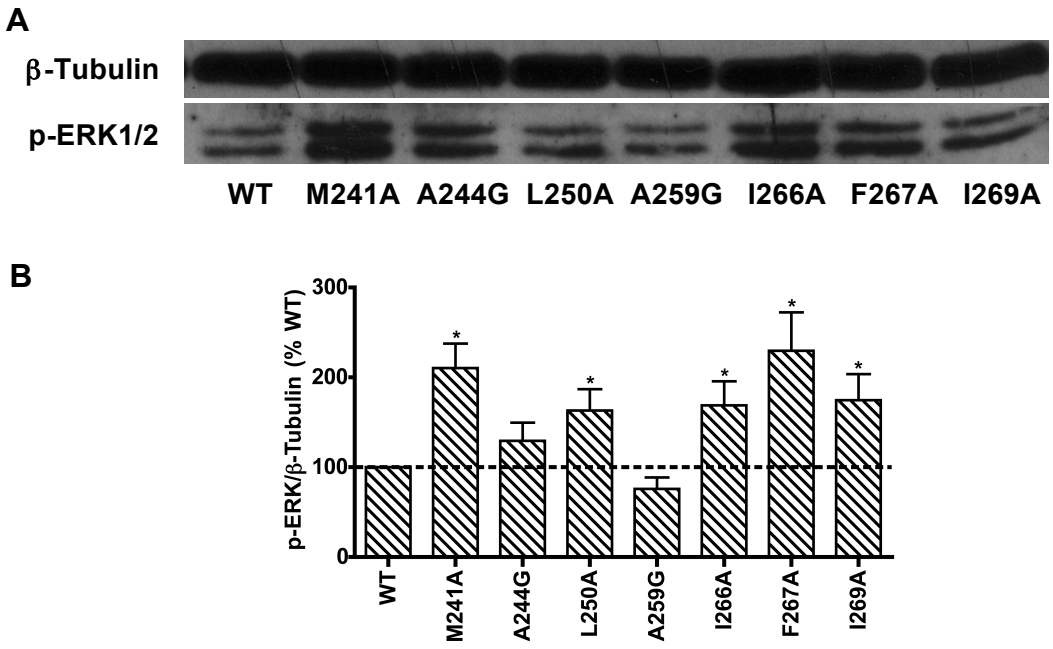

Figure 2.7 Constitutive activation of MAP kinase pathway.

(A) HEK293T cells were transiently transfected with pcDNA 3.1, WT, or mutant MC4Rs, and 24 h later, cells were starved overnight and then harvested. Western blot analysis was performed using antibody against p-ERK1/2 and β-tubulin as a control. (B) Values are mean ± S.E.M. of at least three independent experiments. * Significantly different from WT MC4R, $p<0.05$.

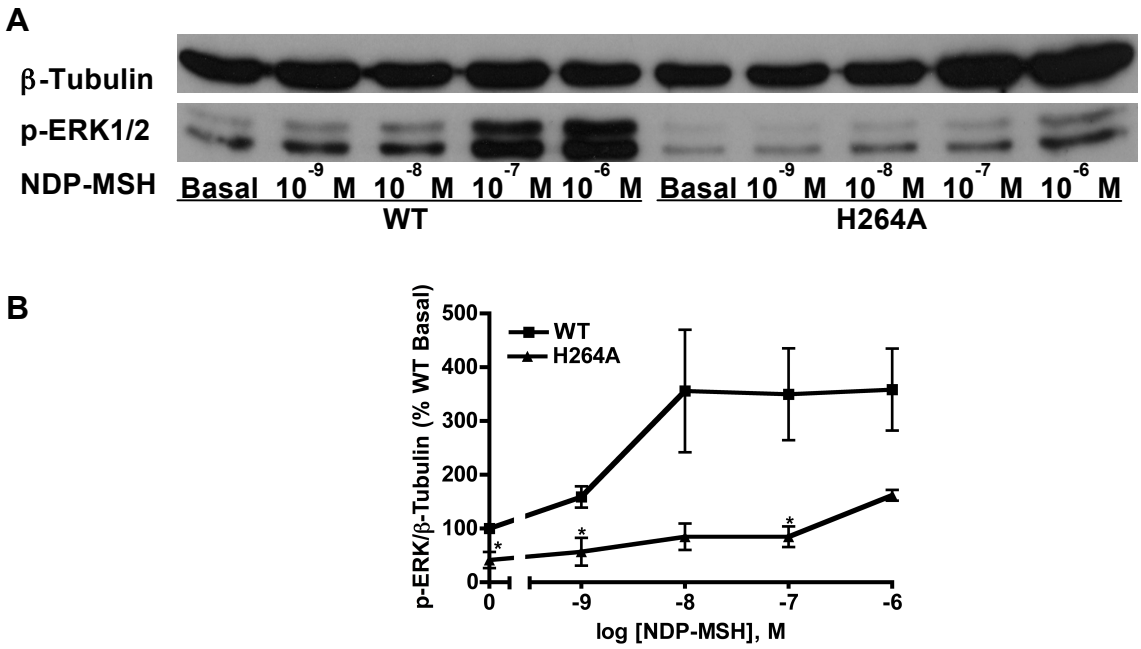

Figure 2.8 MAP kinase signaling of MC4R H264A.

(A), HEK293T cells were transiently transfected with WT or H264A MC4R, and 24 h later, cells were starved overnight and stimulated with different concentrations of NDP-MSH ranging from 10^{-9} M to10^{-6} M for 5 min. Cell lysates were harvested. Western blot analysis was performed using antibody against p-ERK1/2 and β-tubulin as a control. (B), values are mean ± S.E.M. of three independent experiments. * Significantly different from WT MC4R treated with the same concentration of NDP-MSH, $p<0.05$.

Chapter 3 Functional characterization of nine naturally occurring human melanocortin-4 receptor mutations

3.1 Introduction

The melanocortin-4 receptor (MC4R) is a G protein-coupled receptor (GPCR) that is extensively expressed in the central nervous system. The MC4R acts downstream of leptin signaling and plays a key role in regulating food intake and energy expenditure. Mice lacking the *Mc4r* are extremely obese, hyperphagic, hyperinsulinaemic, and hyperglycemic (Huszar et al., 1997). Heterozygous mice lacking the *Mc4r* are also seriously obese although less obese than homozygous mice (Huszar et al., 1997). Studies show that food intake and energy expenditure are differently regulated by the MC4R; the MC4R expressed in the paraventricular nucleus and/or the amygdala regulates food intake (Balthasar et al., 2005) whereas the MC4R expressed in cholinergic neurons regulates energy expenditure (Rossi et al., 2011).

Inactivating mutations in the *MC4R* are the most common monogenic cause of severe obesity in humans (Farooqi et al., 2000). Up to now, approximately 170 mutations in the *MC4R* have been identified from humans (Hinney et al., 2013). Extensive functional studies have been performed on these mutations. Studies reveal that mutations in the *MC4R* differently alter MC4R functions; some mutations such as N62S and I69R are loss of function and lead to obesity whereas some mutations such as V103I and I251L are gain of function and confer protection against obesity (Tao, 2010).

In the present study, we performed detailed functional studies on nine *MC4R* mutations, including G55V, R165G, R165W, R165Q, C172R, F202L, M208V, I269N, and A303P, identified from Pima Indian heritage and Hispanic heritage (Hohenadel et al., 2014). Two mutations, C172R and M208V, have not been studied previously whereas the other seven mutations have been characterized or partially characterized in prior studies. This study is part of the project investigating the relationship between the brain-derived neurotrophic factor (BDNF) concentrations and the MC4R functional status. Therefore, confirmatory functional characterizations were performed for all the nine mutations herein.

3.2 Materials and methods

3.2.1 Materials

[Nle^4,D-Phe^7]-α-MSH (NDP-MSH) was purchased from Peptides International (Louisville, KY) and α-MSH was purchased from Pi Proteomics (Huntsville, AL). ^{125}I-NDP-MSH and ^{125}I-cyclic AMP (cAMP) were prepared using a chloramine T method (Tao et al., 2010). Cell culture media, newborn calf serum and antibiotics and cell culture plates and flasks were purchased from Invitrogen (Carlsbad, CA) and (Corning, NY), respectively.

3.2.2 Site-directed mutagenesis

The wild type (WT) human MC4R was previously generated and tagged with a c-myc epitope at the N-terminus (Tao and Segaloff, 2003). Using the WT plasmid as template, mutant receptors were generated using QuikChange site-directed mutagenesis kit (Stratagene, La Jolla, CA). DNA sequencing was then performed by the University of Chicago Cancer Research Center DNA Sequencing Facility (Chicago, IL) to confirm that the intended mutations were

correctly introduced.

3.2.3 Cell culture and transfection

Human embryonic kidney (HEK) 293 and 293T cells were purchased from American Type Culture Collection (Manassas, VA). Cells were cultured in Dulbecco's Modified Eagle Medium (DMEM) supplied with 10% newborn calf serum. HEK293T cells were plated into six-well plates and transfected with the WT or mutant receptors using calcium phosphate precipitation method. Appropriately 48 h after transfection, HEK293T cells were used for ligand binding and signaling studies. Stably transfected HEK293 cells were selected using 0.2 mg/ml G418 and were used for flow cytometry and confocal microscopy studies.

3.2.4 Flow cytometry assay

HEK293 stable cells were seeded into six-well plates and were used for flow cytometry study appropriately 48 h later. On the day of experiment, cells were placed on ice and washed once with cold PBS for immunohistochemistry (PBS-IH) (137 mM NaCl, 2.7 mM KCl, 1.4 mM KH_2PO_4, and 4.3 mM Na_2HPO_4). Cells were then detached and incubated with the monoclonal anti-myc (9E10) antibody (Developmental Studies Hybridoma Bank at the University of Iowa, Iowa City, IA) diluted 1:40 in PBS-IH containing 0.5% BSA for 1 h at room temperature. Cells were washed once and incubated with the Alexa Fluor 488-conjugated goat anti-mouse antibody (Invitrogen) diluted 1:2000 in PBS-IH containing 0.5% BSA for 1 h at room temperature. Fluorescence signals were collected using a C6 Accuri Cytometer (Accuri Cytometers, Inc., Ann Arbor, MI). Fluorescence from cells stably expressing the empty vector was measured as the background staining.

3.2.5 Confocal microscopy assay

HEK293 stable cells were plated into lysine-coated slides (Biocoat cellware from Falcon, BD Systems, Franklin Lakes, NJ) and were used for confocal microscopy study appropriately 48 h later. Briefly, cells were washed three times with PBS-IH and were fixed with 4% paraformaldehyde in PBS-IH for 15 min. Cells were then washed three times and blocked with 5% BSA in PBS-IH for 1 h. Cells were then incubated with the antibodies. The antibodies used and antibody dilutions were the same as described for flow cytometry study. After the incubation of the secondary antibody, cells were washed five times with PBS-IH containing 0.5% BSA. The slide was covered with a glass coverslip using Vectashield Mounting Media (Vector Laboratories, Burlingame, CA). Cells were imaged using a Nikon A1 confocal microscope.

3.2.6 Ligand binding assay

The method for ligand binding assay has been previously described in detail (Tao and Segaloff, 2003). Briefly, on the day of experiment, transfected HEK293T cells were washed twice with warm Waymouth media containing 1 mg/ml BSA (Waymoth/BSA). Then cells were incubated with 100000 cpm of ^{125}I-NDP-MSH and different concentrations of NDP-MSH (from 10^{-11} to 10^{-6} M) or α-MSH (from 10^{-10} to 10^{-5} M) for 1 h at 37 ^{o}C. Cells were then washed twice with ice-cold Hank's Balanced Salt Solution containing 1 mg/ml BSA and lysed with 0.5 M NaOH. Cell lysates were collected and counted in a gamma counter.

3.2.7 cAMP signaling assay

The method for cAMP signaling assay has been previously described in detail (Tao and

Segaloff, 2003). Briefly, on the day of experiment, HEK293T cells were washed twice with warm Waymouth/BSA and were pre-incubated with 0.5 mM isobutylmethylxanthine (Sigma-Aldrich) in Waymouth/BSA for 15 min at 37 ^{o}C. Then different concentrations of NDP-MSH (from 10^{-12} to 10^{-6} M) or α-MSH (from 10^{-11} to 10^{-5} M) were added and cells were incubated for 1 h. Cells were lysed with 0.5 M perchloric acid containing 180 μg/ml theophylline and the solution was neutralized with 0.72 M KOH/0.6 M $KHCO_3$. The intracellular cAMP concentrations were determined by radioimmunoassay.

3.2.8 Statistical analysis

The significance of differences in cell surface expression, ligand binding and signaling parameters between WT and mutant MC4Rs were analyzed using Student's t-test by Prism 4.0 Software.

3.3 Results

3.3.1 Cell surface expression of mutant MC4Rs

To study the cell surface expression of mutant MC4Rs, HEK293 cells stably expressing WT or mutant receptors were used for flow cytometry and confocal microscopy studies. The mutant F202L was not studied because we failed to generate its stable cells. We first performed flow cytometry studies to quantitate the cell surface expression levels of mutant receptors. As shown in Figure 3.1, six mutants including R165G, R165Q, R165W, C172R, I269N, and A303P had either absent or significantly decreased cell surface expression compared with the WT MC4R. The cell surface expression of two mutants, G55V and M208V, were the same as that of WT MC4R.

We then performed confocal microscopy studies to image the cell surface expression of mutant MC4Rs. As shown in Figure 3.2, the results were consistent with that obtained from flow cytometry studies. Six mutants, including R165G, R165Q, R165W, C172R, I269N, and A303P, were expressed poorly on the cell surface whereas two mutants, G55V and M208V, were expressed well at the cell surface.

3.3.2 Pharmacology of mutant MC4Rs at NDP-MSH

NDP-MSH, a potent agonist of MC4R, is the most commonly used agonist in MC4R studies. Therefore, we first studied the ligand binding and signaling properties of the mutants using NDP-MSH as the ligand. HEK293T cells transiently expressing the WT or mutant MC4Rs were incubated with radiolabeled NDP-MSH and different concentrations of unlabeled NDP-MSH. Our results showed that the WT MC4R bound to NDP-MSH with an IC_{50} of 33.93 nM. Five mutants, including R165G, R165Q, R165W, I269N, and A303P that had reduced cell surface expression, had significantly decreased IC_{50}s and therefore increased affinities with NDP-MSH (Table 3.1 and Figure 3.3A). C172R had no measurable binding.

To study the signaling properties of mutant receptors, cells were stimulated with different concentrations of NDP-MSH and intracellular cAMP accumulations were measured. WT MC4R dose-dependently responded to NDP-MSH stimulation with an EC_{50} of 1.60 nM (Table 3.1). Compared with the WT MC4R, three mutants, G55V, C172R, and M208V, had increased EC_{50}s and three other mutants, R165Q, R165W, and A303P, had decreased EC_{50}s (Table 3.1 and Figure 3.3B). R165Q had increased maximal response to NDP-MSH stimulation whereas C172R had decreased maximal response (Table 3.1 and Figure 3.3B).

3.3.3 Pharmacology of mutant MC4Rs at α-MSH

The agonist α-MSH is an important endogenous ligand of MC4R. We then studied the ligand binding and signaling properties of the nine mutants using α-MSH as the ligand. Our results showed that the WT MC4R bound to α-MSH with an IC_{50} of 606.28 nM (Table 3.1 and Figure 3.4A). A303P had significantly reduced IC_{50} compared with the WT receptor. Two mutants, G55V and C172R, had no measurable IC_{50}s because of low affinity (G55V) or low maximal binding (C172R) (Table 3.1 and Figure 3.4A).

Maximal binding of radiolabeled NDP-MSH had been calculated for each mutant in the absence of any unlabeled ligands. As shown in Table 3.1, eight mutants, including G55V, R165G, R165Q, R165W, C172R, M208V, I269N, and A303P, had significantly reduced maximal binding compared with the WT MC4R. F202L had similar maximal binding to the WT receptor.

The WT MC4R dose-dependently responded to α-MSH stimulation with an EC_{50} of 10.81 nM (Table 3.1 and Figure 3.4B). Three mutants, G55V, C172R, and M208V, had significantly increased EC_{50}s compared with the WT receptor. Two mutants, G55V and C172R, had decreased maximal response to α-MSH stimulation whereas other two mutants, R165Q and I269N, had increased maximal response (Table 3.1 and Figure 3.4B).

The basal signaling of MC4R is important in regulating energy homeostasis and therefore we also measured the basal cAMP production of the nine mutants in the absence of any ligands. As shown in Figure 3.5, three mutants, G55V, C172R, and M208V, had significantly decreased basal signaling. We also identified one constitutively active mutant, A303P, which had significantly increased basal signaling to more than six fold of that of the WT MC4R. Other mutants had normal levels of basal signaling.

3.4 Discussion

In the present study, we performed detailed functional studies on nine MC4R mutations identified from children or adults (Hohenadel et al., 2014). We studied the cell surface expression and pharmacology of the nine mutants using two ligands, NDP-MSH and α-MSH. Our results were summarized in Table 3.2 and were consistent with prior studies in determining the defects of the mutants that were previously studied (Tan et al., 2009; Tao and Segaloff, 2005; Thearle et al., 2012; Xiang et al., 2007; Xiang et al., 2010).

For the nine mutants studied, six mutants (R165G, R165Q, R165W, C172R, I269N, and A303P) had reduced cell surface expression (Class II); two mutants (G55V and M208V) had ligand binding (Class III); one mutant F202L had normal function (Class V). These mutants were classified according to the classification scheme proposed by Tao and Segaloff, which states that Class I mutants have diminished proteins, Class II mutants are retained intracellularly, Class III mutants are defective in ligand binding, Class IV mutants are defective in signaling, and Class V mutants have no obvious defect (Tao and Segaloff, 2003). Our result showed that 75% (6/8) of inactivating MC4R mutants studied herein were retained intracellularly. This observation was consistent with previous reports that the most common defect of mutant MC4R and many other GPCRs was intracellular retention (Tao, 2006).

Although R165G, R165Q, R165W, C172R, I269N, and A303P were very poorly expressed at the cell surface, they still fully or partially responded to NDP- or α-MSH stimulation (Table 3.1). This is probably due to the existence of spare receptors. Spare receptors have been observed in in vitro expression systems, even in stably transfected cells (Tao and Segaloff, 2005). Glycine, glutamine, or tryptophan mutation of arginine at the position 165

resulted in intracellular retention of the receptor (Figure 3.1 and 3.2), indicating that the positively charged side chain of R165 (4.41) was required to pass the scrutiny of the cellular quality control system.

G55V and M208V had normal cell surface expression but had reduced maximal binding and increased EC_{50}s (Table 3.1 and 3.2), suggesting they were defective in ligand binding and signaling. G55V was also previously characterized to be defective in cAMP production upon the stimulation of α-MSH (Tan et al., 2009). This is the first time to report that M208 (5.46) was important for MC4R activation. At the position 5.46 it is serine in adrenoceptors. In the two recently published crystal structures of β_1- and β_2- adrenoceptors, it has been observed that S5.46 directly interacted with the ligands and this interaction was important for the conformational changes of the receptor from the inactive to the active status (Rasmussen et al., 2011; Warne et al., 2011).

Basal signaling of MC4R has been reported to be also important in regulating energy homeostasis (Srinivasan et al., 2004). We showed that three mutants, G55V, C172R, and M208V, had reduced basal signaling and one mutant, A303P, had dramatically increased basal signaling (Figure 3.5). We identified that A303P was a constitutively active mutant. Inconsistent with their potential roles in protecting obesity, many constitutively active mutants have been identified from obese patients. These mutants could be pathogenic probably because of their low cell surface expression, constitutive desensitization, or induction of phosphodiesterase (Persani et al., 2000; Shinozaki et al., 2003; Wang and Tao, 2011). However, the detailed mechanism is still unclear.

In summary, of the nine mutants we studied herein, six mutants reduced cell surface expression, two mutants were defective in ligand binding and signaling, and one mutant had

normal function. These data help us to gain a better understanding of the functional consequences of each mutation and their implication in human obesity.

Table 3.1 The ligand binding and signaling properties of WT and mutant MC4Rs in response to NDP-MSH or α-MSH stimulation.

hMC4R Construct	Bmax (% WT)	NDP-MSH Binding	NDP-MSH-stimulated cAMP		α-MSH Binding	α-MSH-stimulated cAMP	
		IC_{50} (nM)	EC_{50} (nM)	Rmax (% WT)	IC_{50} (nM)	EC_{50} (nM)	Rmax (% WT)
WT	100	33.93 ± 4.19	1.60 ± 0.27	100	606.28 ± 139.34	10.81 ± 5.04	100
G55V	55.40 ± 9.63[b]	47.63 ± 16.26	5.41 ± 1.17[a]	97.08 ± 6.46	N/D	612.34 ± 210.05[a]	84.87 ± 4.82[a]
R165G	37.18 ± 3.07[c]	3.24 ± 0.40[b]	1.34 ± 0.22	135.46 ± 13.02	271.20 ± 65.53	5.18 ± 1.32	112.50 ± 4.51
R165Q	34.75 ± 4.44[c]	2.78 ± 0.35[b]	0.91 ± 0.08[a]	142.68 ± 6.64[a]	365.83 ± 86.87	4.46 ± 0.50	134.40 ± 5.28[a]
R165W	43.48 ± 5.06[c]	6.82 ± 0.97[b]	1.04 ± 0.13[a]	105.98 ± 11.05	358.55 ± 117.90	4.74 ± 0.50	110.10 ± 5.48
C172R	N/D	N/D	9.60 ± 2.22[a]	32.86 ± 6.69[b]	N/D	1627.96 ± 430.15[b]	39.21 ± 7.91[b]
F202L	99.24 ± 9.32	26.74 ± 5.92	2.15 ± 0.50	125.99 ± 8.55	492.63 ± 83.57	2.79 ± 0.58	92.67 ± 12.58
M208V	74.16 ± 6.18[b]	70.38 ± 15.20	17.77 ± 5.14[a]	113.88 ± 13.65	913.47 ± 224.19	270.75 ± 122.34[a]	139.40 ± 22.24
I269N	42.86 ± 3.08[c]	10.73 ± 1.39[a]	0.63 ± 0.23	131.12 ± 9.65	561.20 ± 42.92	40.42 ± 23.73	121.30 ± 6.83[a]
A303P	22.42 ± 4.55[c]	2.29 ± 0.34[b]	0.57 ± 0.13[b]	98.49 ± 9.23	54.98 ± 14.23[a]	1.00 ± 0.06	108.30 ± 2.97

[a] Significantly different from WT MC4R, $p<0.05$.

[b] Significantly different from WT MC4R, $p<0.01$.

[c] Significantly different from WT MC4R, $p<0.001$.

N/D Not detected.

Bmax are mean ± S.E.M. of at least six independent experiments and other parameters are mean ± S.E.M. of at least three independent experiments. The Rmax of WT MC4R was 3544.33 ± 471.12 pmol/10^6 cells with NDP-MSH stimulation, and was 3117.01 ± 472.62 pmol/10^6 cells with α-MSH stimulation.

Table 3.2 Summary of the functional properties of the nine mutants studied herein.

MC4R Construct	Surface expression	Binding	cAMP Signaling		Class
			Basal	Stimulated	
G55V	+	↓	↓	↓	III
R165G	↓	↓	+	+	II
R165Q	↓	↓	+	↑	II
R165W	↓	↓	+	+	II
C172R	↓	↓	↓	↓	II
F202L	/	+	+	+	V
M208V	+	↓	↓	↓	III
I269N	↓	↓	+	+	II
A303P	↓	↓	↑	+	II

"+": Denotes that the activity had no significant change.
"↑": Denotes increased activity.
"↓": Denotes decreased activity.
"/": Denotes not studied.

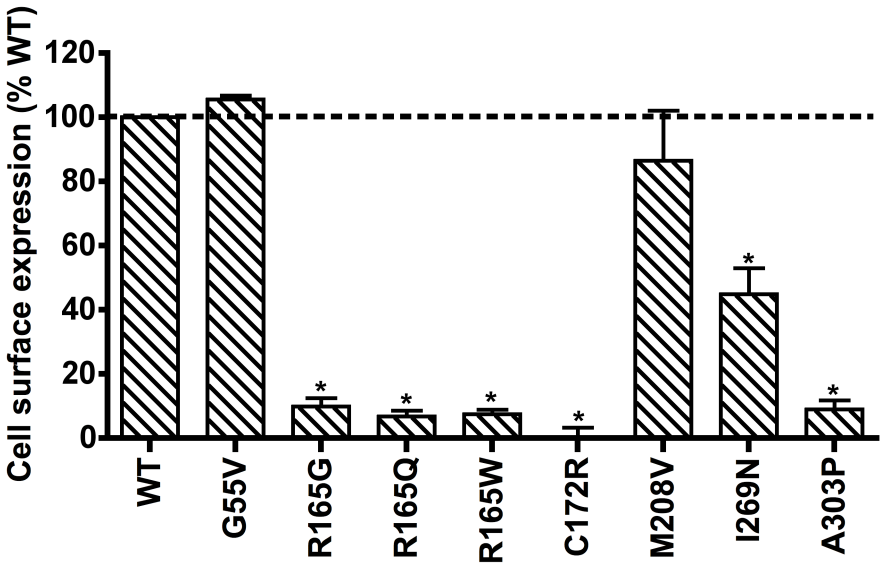

Figure 3.1 The cell surface expression of WT and mutant MC4Rs as quantitated by flow cytometry.

The results were shown as %WT cell surface expression levels after correction of the nonspecific staining in HEK293 cells stably expressing the empty vector. Data were mean ± S.E.M. of at least three independent experiments. * Significantly different from WT MC4R, $p<0.05$.

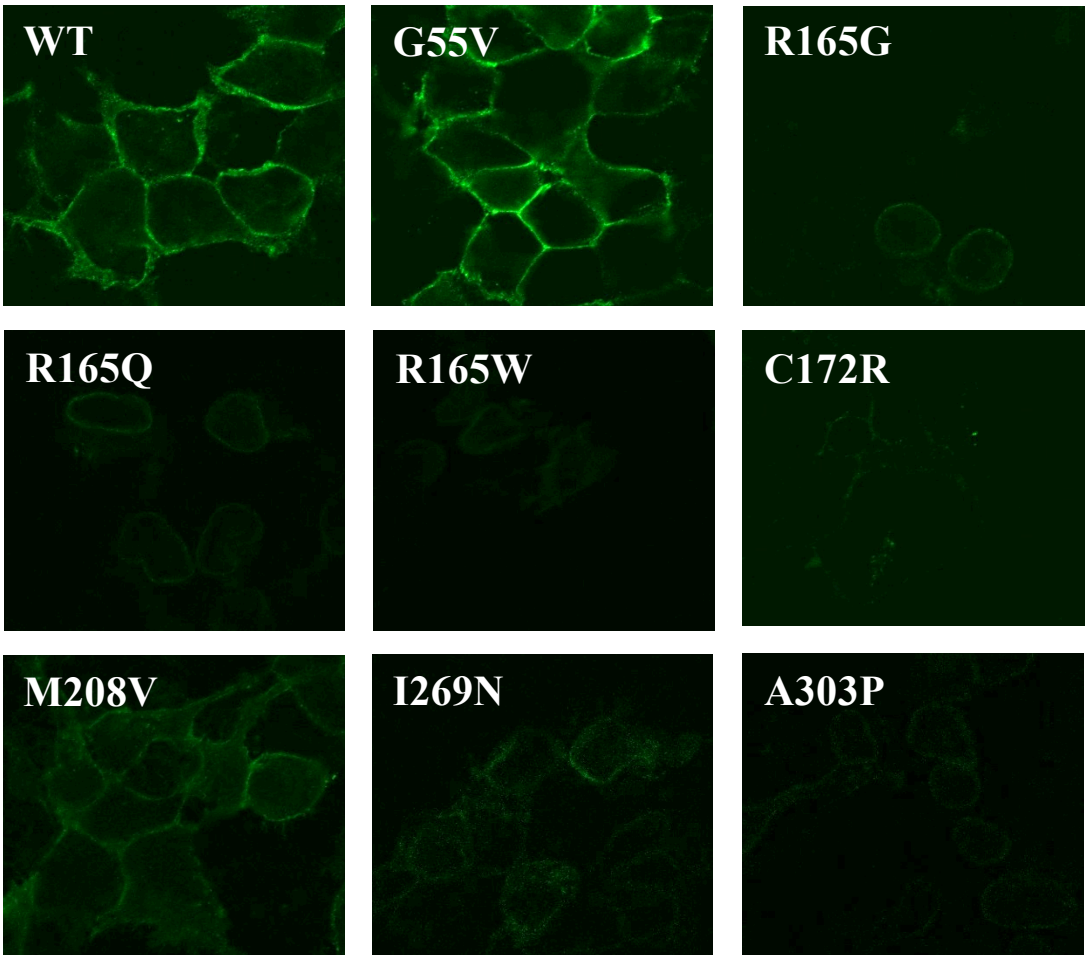

Figure 3.2 Cell surface expression of WT and mutant MC4Rs as visualized by confocal microscopy.

The HEK293 cells stably expressing WT or mutant MC4Rs were stained with Alexa fluor-conjugated anti-myc monoclonal antibody. Cell surface fluorescence was detected by confocal microscopy. Results are representative of at least three independent experiments.

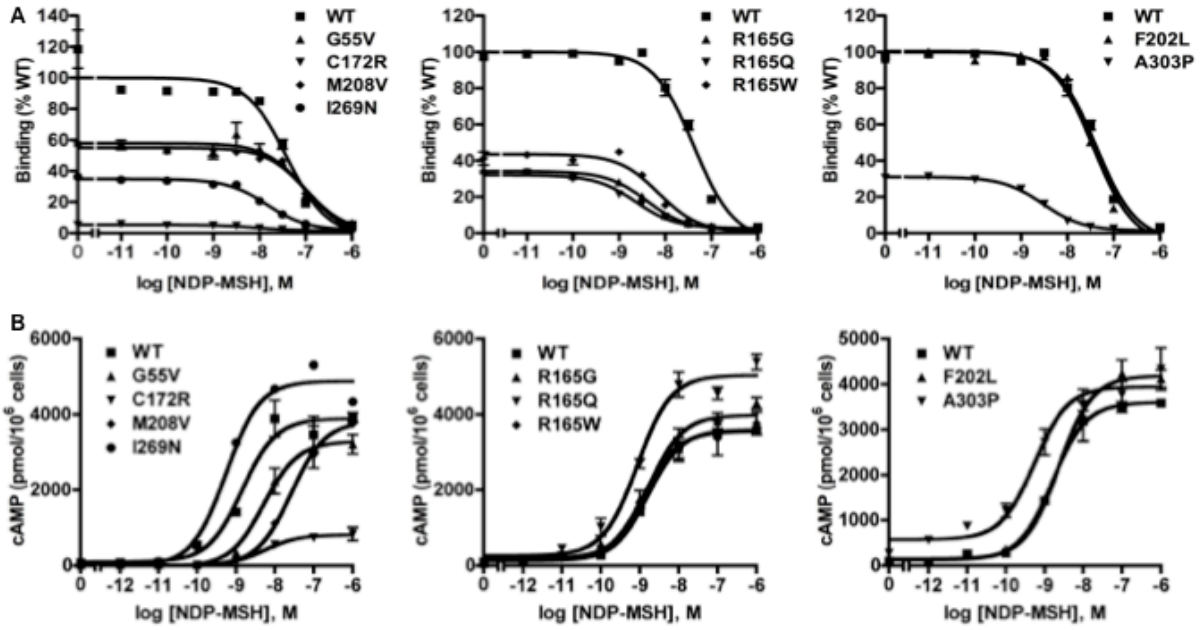

Figure 3.3 Ligand binding (A) and signaling (B) properties of WT and mutant MC4Rs with NDP-MSH as the ligand.

HEK293T cells transiently expressing WT or mutant MC4Rs were used for ligand binding and signaling studies. (A) Intact cell surface binding was measured by competitive inhibition of ^{125}I-NDP-MSH with different concentrations of NDP-MSH. Data are shown as %WT maximal binding. (B) Intracellular cAMP concentrations in response to the stimulation of different concentrations of NDP-MSH were measured by radioimmunoassay. Data are shown as mean ± S.E.M. of duplicate (A) triplicate (B) measurements within one experiment. Results are representative of at least three independent experiments.

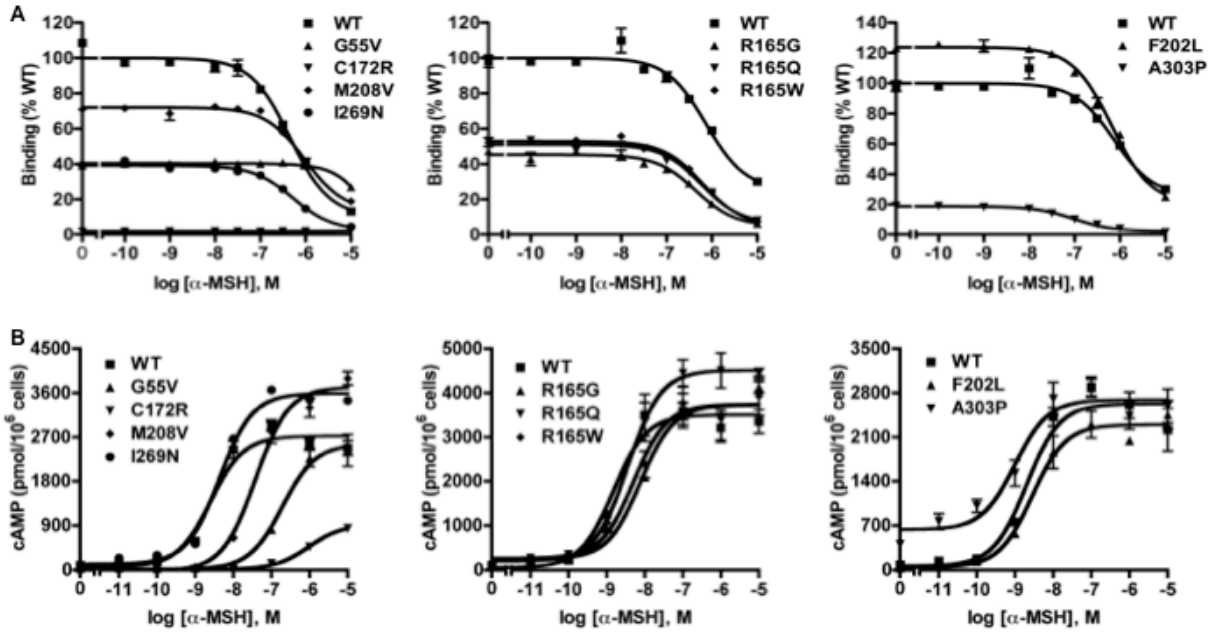

Figure 3.4 Ligand binding (A) and signaling (B) properties of WT and mutant MC4Rs with α-MSH as the ligand.

HEK293T cells transiently expressing WT or mutant MC4Rs were used for ligand binding and signaling studies. (A) Intact cell surface binding was measured by competitive inhibition of ^{125}I-NDP-MSH with different concentrations of α-MSH. Data are shown as %WT maximal binding. (B) Intracellular cAMP concentrations in response to the stimulation of different concentrations of α-MSH were measured by radioimmunoassay. Results are shown as mean ± S.E.M. of duplicate (A) triplicate (B) measurements within one experiment. Results are representative of at least three independent experiments.

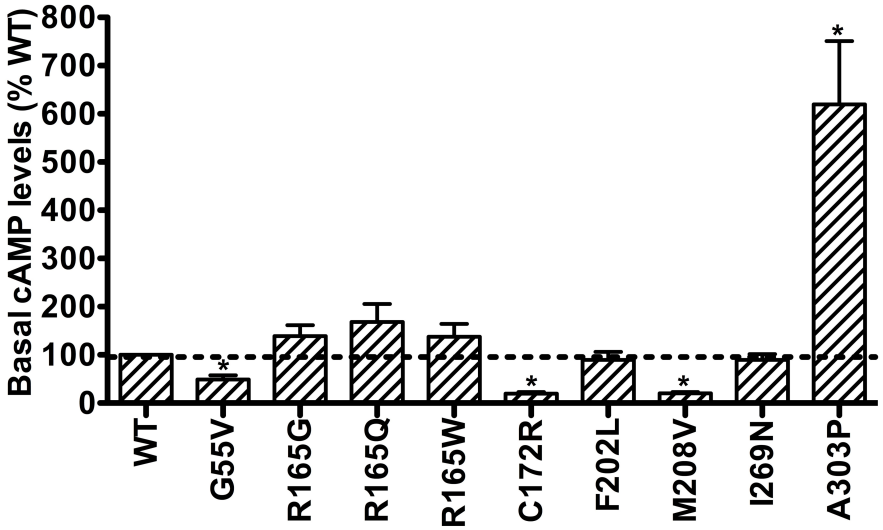

Figure 3.5 Basal signaling of WT and mutant MC4Rs.

Intracellular cAMP accumulations were measured in HEK293T cells transiently expressing WT or mutant MC4Rs in the absence of any ligands. Results are shown as mean ± S.E.M. of at least six independent experiments. The cAMP accumulation of WT MC4R was 74.56 ± 6.49 pmol/10^6 cells.

Chapter 4 Functional rescue of naturally occurring human melanocortin-4 receptor mutations by ML00253764

4.1 Introduction

Obesity is an epidemic with significant health consequences. It increases the incidence of multiple comorbidities such as type 2 diabetes mellitus, hypertension, cardiovascular diseases, and some types of cancers (Guh et al., 2009). In the United States, more than one third of adults are obese and the prevalence, especially that of severe obesity, continues to be increasing (Sturm and Hattori, 2013).

The neural melanocortin-4 receptor (MC4R) is a member of Family A G protein-coupled receptors (GPCRs). As a downstream mediator of leptin action in the hypothalamus, the MC4R plays a vital role in regulating food intake and energy expenditure (Balthasar et al., 2005; Huszar et al., 1997). Mutations in the *MC4R* gene are the most common monogenic form of obesity, with the prevalence as high as 6% in some ethnic population (Farooqi et al., 2003). Therefore the MC4R has been considered as a premier target for obesity treatment.

Up to now, approximately 170 *MC4R* mutations have been identified from obese patients (Hinney et al., 2013). Detailed functional studies revealed that most of the inactivating MC4R mutants are retained intracellularly and that mutants with defects in ligand binding and signaling are rare (Tao, 2009; Tao, 2010). Since some of the intracellularly retained MC4R mutants can potentially be functional when coaxed to the cell surface, various approaches have been used to

rescue the cell surface expression of these mutants, including chemical chaperone 4-phenyl butyric acid (Granell et al., 2010) and molecular chaperone Hsc70 (heat shock cognate protein 70) (Meimaridou et al., 2011). However, these approaches are not clinically feasible because of their non-specific actions and/or high concentrations required.

Pharmacological chaperones, also known as pharmacoperones, are the most promising therapeutic approach because of their high selectivity and efficacy (Conn et al., 2007; Tao and Conn, 2014). Morello et al. used nonpeptidic antagonists of V2 arginine vasopressin receptor (AVPR2) to restore the expression of mutant AVPR2s (Morello et al., 2000). Since then, a number of ligands including antagonists, agonists, and allosteric agonists have been identified as pharmacoperones for several other GPCRs, including δ opioid receptor (Petäjä-Repo et al., 2002), opsin (Noorwez et al., 2003), gonadotropin releasing hormone receptor (GnRHR) (Conn and Ulloa-Aguirre, 2011), luteinizing hormone receptor (Newton et al., 2011), and follicle-stimulating hormone receptor (Janovick et al., 2009) (reviewed in (Tao and Conn, 2014)). Most importantly, pharmacoperone therapies have been successfully conducted in humans with nephrogenic diabetes insipidus harboring *AVPR2* mutations (Bernier et al., 2006) and in mouse models with hypogonadotropic hypogonadism harboring *GNRHR* mutations (Janovick et al., 2013), demonstrating the therapeutic feasibility of pharmacoperones *in vivo*.

We identified the first MC4R pharmacoperone, ML00253764, which rescued the expression and function of two MC4R mutants, C84R and W174C (Fan and Tao, 2009), and partially corrected the expression of six additional mutants, including S58C, N62S, P78L, G98R, C271Y, and F261S (Tao, 2010). However, the pharmacoperone action of ML00253764 on MC4R was not fully elucidated. In the current study, we systematically investigated the effect of ML00253764 on both the cell surface expression and function of eleven MC4R mutants

including mutants described above and three other mutants (I69R, Y157S, and P260Q) using both HEK293 cell line previously used and the more physiologically relevant neuronal cell lines.

4.2 Materials and methods

4.2.1 Materials

[Nle^4,D-Phe^7]- α-MSH (NDP-MSH) was purchased from Peptides International (Louisville, KY). ML00253764 (2-{2-[2-(5-Bromo-2-methoxyphenyl)-ethyl]-3-fluorophenyl}-4,5-dihydro-1H-imidazole) was custom synthesized by Enzo Life Science (Plymouth Meeting, PA). Cell culture media, newborn calf serum, fetal bovine serum, and reagents were purchased from Invitrogen (Carlsbad, CA). Tissue culture plastic wares were obtained from Corning (Corning, NY). [^{125}I]-cyclic AMP (cAMP) was iodinated using chloramine T method (Tao et al., 2010).

4.2.2 Plasmids

The N-terminal c-myc-tagged wild type (WT) human MC4R at the N-terminus was previously described (Tao and Segaloff, 2003). The N-terminal 3×HA-tagged WT human MC3R was obtained from Missouri S&T cDNA Resource Center (http://www.cDNA.org/; Rolla, MO). Mutant MC4Rs and I335S MC3R were previously constructed from the corresponding WT receptors using QuikChange^{TM} site-directed mutagenesis kit (Stratagene, La Jolla, CA) (Donohoue et al., 2003; Fan and Tao, 2009; Tao, 2007; Tao and Segaloff, 2003; Tao and Segaloff, 2005; Wang and Tao, 2011) and sequenced by the DNA Sequencing Facility of University of Chicago Cancer Research Center (Chicago, IL).

4.2.3 Cell culture and transfection

Human embryonic kidney (HEK) 293, Neuro2a, and N1E-115 cells were purchased from American Type Culture Collection (Manassas, VA). HEK293 cells were cultured in Dulbecco's modified Eagle's medium supplemented with 10% newborn calf serum, 10 mM Hepes, 0.25 μg/ml amphotericin B, 50 μg/ml gentamicin, 100 units/ml penicillin, and 100 μg/ml streptomycin at 37 ^{o}C in a humidified atmosphere with 5% CO_2. Neuro2a and N1E-115 cells were cultured in Dulbecco's modified Eagle's medium supplemented with 10% fetal bovine serum. HEK293 cells were seeded into 100 mm dishes, transfected with 5 μg plasmid per dish using calcium phosphate precipitation method and selected using 0.2 mg/ml G418 (Tao and Segaloff, 2003). Neuro2a and N1E-115 cells plated into 6-well plates were transfected with 1 μg plasmid per well using jetPRIME transfection reagent (Polyplus-transfection, New York, NY). Approximately one day after seeding (HEK293 stable cells) or transfection (Neuro2a and N1E-115 cells), cells were incubated with indicated concentrations of ML00253764 or 0.1% dimethyl sulfoxide (DMSO) for 24 h at 37 ^{o}C before confocal microscopy, flow cytometry, or cAMP studies were performed. All 6-well plates and cell culture dishes were coated with 0.1% gelatin before cell seeding unless indicated otherwise.

4.2.4 Confocal microscopy

HEK293 cells stably expressing WT or mutant MC4Rs were seeded into poly-D-lysine-coated 8-well slides (Biocoat cellware from Falcon, BD Systems, Franklin Lakes, NJ) for 24 h and then treated with 0.1% DMSO or 10^{-5} M ML00253764 for 24 h at 37 ^{o}C as described above. On the day of experiment, cells were washed three times with phosphate buffered saline for immunohistochemistry (PBS-IH), followed by fixation with 4% paraformaldehyde for 15 min at

room temperature. Cells were then washed three times with PBS-IH and blocked with 5% bovine serum albumin (BSA) in PBS-IH for 1 h at room temperature. Cells were incubated with monoclonal antibody 9E10 (Developmental Studies Hybridoma Bank, The University of Iowa, Iowa City, IA; 1:40 dilution in PBS-IH with 0.5% BSA) for 1 h at room temperature and washed three times with PBS-IH (10 min each wash). Cells were then incubated with Alexa Fluor 488-labeled goat anti-mouse IgG (Invitrogen, 1:2000 dilution in PBS-IH with 0.5% BSA) for 1 h at room temperature and washed five times with PBS-IH (10 min each wash). Slides were then covered with coverslips using Vectashield mounting media (Vector Laboratories, Burlingame, CA) and dried overnight at 4 ^{o}C. Cells were visualized using a Nikon A1 confocal microscope.

4.2.5 Flow cytometry

Approximately one day after seeding (HEK293 stable cells) or transfection (Neuro2A cells), cells were incubated with 0.1% DMSO or 10^{-5} M ML00253764 for 24 h at 37 ^{o}C as described above. On the day of experiment, cells in 6-well plates were immediately plated on ice and washed once with ice-cold PBS-IH. Cells were detached and then precipitated by centrifugation at 500 × g for 5 min. Following centrifugation, cells were incubated with 9E10 (1:40 dilution in PBS-IH containing 0.5% BSA) to detect the MC4R or anti-HA.11 antibody (Covance, Princeton, NJ) (1:100 dilution in PBS-IH containing 0.5% BSA) to detect the MC3R for 1 h at room temperature. Following one wash with PBS-IH, cells were then incubated with Alexa Fluor 488-labeled goat anti-mouse IgG (1:2000 dilution in PBS-IH containing 0.5% BSA) for 1 h at room temperature. Cells were washed once with PBS-IH and fluorescence signals were measured using a C6 Accuri Cytometer (Accuri Cytometers, Ann Arbor, MI). Fluorescence of cells transfected with the empty vector was used for background staining. The expression levels

of the mutant MC4Rs were calculated as percentage of WT MC4R using the following formula: (mutant - pcDNA3.1) / (WT - pcDNA3.1) × 100% (Wang et al., 2008).

4.2.6 cAMP assay

Approximately one day after seeding (HEK293 stable cells) or transfection (Neuro2A and N1E-115 cells), cells in 6-well plates were incubated with 0.1% DMSO or different concentrations of ML00253764 for 24 h at 37 ^{o}C as described above. On the day of experiment, cells were washed twice with warm Waymouth's MB752/1 media (Sigma-Aldrich, St. Louis, MO) containing 1 mg/ml BSA (Waymouth/BSA). Cells were incubated with fresh Waymouth/BSA containing 0.5 mM isobutylmethylxanthine (Sigma-Aldrich) for 15 min and then incubated with or without 10^{-6} M NDP-MSH for 1h at 37 ^{o}C. Following incubation, cells were lysed with 0.5 M percholoric acid containing 180 μg/ml theophylline (Sigma-Aldrich) and the solution was neutralized with 0.72 M KOH/0.6 M $KHCO_3$. Intracellular cAMP concentrations were measured using radioimmunoassay (RIA) as previously described (Tao et al., 2010). The cAMP production of the mutant MC4Rs was calculated as percentage of WT MC4R using the following formula: mutant / WT × 100% for HEK293 cells or (mutant - pcDNA3.1) / (WT - pcDNA3.1) × 100% for neuronal cells.

4.2.7 Data analysis

All data analysis was performed using GraphPad Prism 4.0 software (San Diego, CA). The differences of cell surface expression levels and cAMP levels between DMSO and ML00253764 treated cells were analyzed using Student's t-test.

4.3 Results

4.3.1 ML00253764 treatment increased cell surface expression of some mutant MC4Rs but not others

To investigate the pharmacoperone action of ML00253764 on MC4R, we studied eleven MC4R mutants (S58C, N62S, I69R, P78L, C84R, G98R, Y157S, W174C, P260Q, F261S, and C271Y) that were previously characterized to be totally or partially retained intracellularly (Fan and Tao, 2009; Tao and Segaloff, 2003; Tao and Segaloff, 2005; Wang and Tao, 2011) (Figure 4.1).

We previously reported the cell surface expression of eight of these eleven mutants with ML00253764 treatment using confocal microscopy (Fan and Tao, 2009; Tao, 2010). In this study, we imaged the cell surface expression of the other three mutants (I69R, Y157S, and P260Q). WT and mutant MC4Rs were stably expressed in HEK293 cells and were treated with or without 10^{-5} M ML00253764 for 24 h. As shown in Figure 4.2, compared with that of the WT MC4R, the immunostaining of I69R, Y157S, and P260Q in nonpermeabilized cells was very weak, suggesting that they were poorly expressed at the cell surface, confirming our previous observations. With ML00253764 treatment, the immunostaining of WT and Y157S was significantly enhanced although the immunostaining of I69R and P260Q was not obviously different from that of the untreated cells.

To quantitate the expression levels of MC4Rs, we performed flow cytometry studies. HEK293 cells stably expressing WT or mutant MC4Rs were treated with or without 10^{-5} M ML00253764 for 24 h. As shown in Figure 4.3, with ML00253764 treatment, the cell surface expression level of the WT MC4R was increased by about 70%. The cell surface expression levels of seven mutants (S58C, N62S, C84R, G98R, Y157S, W174C, and C271Y) were also

significantly increased after ML00253764 treatment. Consistent with the confocal microscopy results, ML00253764 had no significant effect on four mutants (I69R, P78L, P260Q, and F261S) (Figure 4.2 and Ref. (Tao, 2010)).

The MC4R is predominately expressed in the central nervous system. Therefore, we also studied the pharmacoperone action of ML00253764 using a neuronal cell line, Neuro2a, which is widely used in neuroscience research. We performed flow cytometry using Neuro2a cells transiently expressing WT or mutant MC4Rs (Figure 4.4). Herein ten mutants (not including S58C) were studied. Three mutants (N62S, C84R, and W174C) had significantly increased cell surface expression levels with the ML00253764 treatment. One mutant (G98R) had slightly increased cell surface expression level that did not reach statistical significance. Two mutants (Y157S and C271Y) that were rescued in HEK293 cells did not have increased cell surface expression in Neuro2a cells. The four mutants that were not rescued in HEK293 cells (I69R, P78L, P260Q, and F261S) were also not rescued in neuronal cells (Figure 4.4).

4.3.2 ML00253764 treatment increased signaling capacities of some mutant MC4Rs

The MC4R is primarily coupled to G_s, increasing cAMP production after receptor activation. Therefore, to study whether the rescued receptors were functional, we measured the intracellular cAMP accumulations. HEK293 cells stably expressing WT or mutant MC4Rs were treated with or without different concentrations of ML00253764, ranging from 10^{-11} to 10^{-5} M, for 24 h and then were stimulated with 10^{-6} M NDP-MSH for 1 h. The intracellular cAMP accumulation of WT MC4R was decreased by 16% whereas that of six mutants (N62S, P78L, C84R, Y157S, W174C, and C271Y) had been significantly increased with the treatment of 10^{-5} M ML00253764 (Figure 4.5 A and B). However, lower concentrations of ML00253764 ($\leq 10^{-6}$

M) had no obvious effect (Figure 4.5A).

We further confirmed the results using two neuronal cell lines, Neuro2a and N1E-115. Due to high basal signaling of the neuronal cells, data were corrected with that of cells transfected with the empty vector. Treatment of 10^{-5} M ML00253764 restored cAMP production in four mutants (N62S, C84R, W174C, and C271Y) in Neuro2a cells (Figure 4.6) and three mutants (N62S, C84R, and W174C) in N1E-115 cells (Figure 4.7).

4.3.3 ML00253764 did not correct MC4R mutants with other defects or intracellularly retained MC3R mutant

To investigate whether ML00253764 could correct defects in mutants of the other Classes, we further studied four other mutant MC4Rs that are all expressed normally at the cell surface, including Δ88-92 with defect in ligand binding (Class III) (Donohoue et al., 2003), D90N with defect in signaling (Class IV) (Biebermann et al., 2003), I102S with reduced signaling (Class IV) (Tao and Segaloff, 2005), and N274S with normal signaling (Tao and Segaloff, 2003). As shown in Figure 4.6 using Neuro2a cells and in Figure 4.7 using N1E-115 cells, signaling efficacies of these four mutants in the two neuronal cells treated with vehicle were consistent with previous reports in HEK293 or COS-7 cells. ML00253764 treatment did not significantly affect the signaling of these four mutants (Figure 4.6 and Figure 4.7).

To investigate whether ML00253764 was a pharmacoperone specific for MC4R, we studied one MC3R mutant that is retained intracellularly, I335S (Mencarelli et al., 2008; Tao, 2007). As shown in Figure 4.8, ML00253764 did not affect the cell surface expression or cAMP production of I335S MC3R.

4.4 Discussion

ML00253764, with a molecular weight of 377.26, is a MC4R small molecule antagonist (Vos et al., 2004) and partial inverse agonist (Huang and Tao, 2012; Mo and Tao, 2013; Nicholson et al., 2006; Tao et al., 2010). It can cross the blood brain barrier and act on MC4R *in vivo* after intraperitoneal injection (Nicholson et al., 2006; Vos et al., 2004). We previously reported that it acts as a pharmacoperone, correcting the trafficking and signaling of several mutants in HEK293 cells (Fan and Tao, 2009; Tao, 2010). In the present study, we systematically investigated the pharmacoperone action of ML00253764 on both the cell surface expression and function of eleven Class II MC4R mutants, including N62S, I69R, P78L, C84R, G98R, Y157S, W174C, P260Q, F261S, and C271Y, and four MC4R mutants with other defects, including Δ88-92, D90N, I102S, and N274S, in both HEK293 and neuronal cell lines.

Consistent with our previous reports (Fan and Tao, 2009; Tao and Segaloff, 2003; Tao and Segaloff, 2005; Wang and Tao, 2011), the eleven mutants were poorly expressed at the cell surface (Figures 4.2 – 4.4) with no or only some residual signaling (Figures 4.5 – 4.7), except that S58C and F261S had substantial signaling capacities, about 50% of or similar to that of the WT MC4R.

ML00253764 significantly increased cell surface expression levels at seven of the eleven mutants (S58C, N62S, C84R, G98R, Y157S, W174C, and C271Y) studied herein and five of them (N62S, C84R, Y157S, W174C, and C271Y) were responsive to NDP-MSH stimulation in HEK293 cells (Table 4.1). N62S signaling was restored to a similar level as that of the untreated WT MC4R and the signaling of the other four mutants was proportional to or greater than the increases in cell surface expression, suggesting that the primary defect of these mutations was misfolding resulting in detection by the cell's quality control system and intracellular retention

but not ligand binding and signaling.

Signaling efficacies of the five mutants were not increased with the treatment of ML00253764 at lower concentrations ($\leq 10^{-6}$ M) (Figure 4.5). Only 10^{-5} M ML00253764 successfully rescued the function of mutant receptors, which is similar to another MC4R pharmacoperone, *N*-((2*R*)-3(2,4-dichlorophenyl)-1-(4-(2-((1-methoxypropan-2-ylamino)methyl)phenyl)piperazin-1-yl)-1-oxopropan-2-yl)propionamide (DCPMP) (Rene et al., 2010). The K_is of ML00253764 (Vos et al., 2004) and DCPMP (Rene et al., 2010) at the MC4R were 0.16 mM and 0.024 mM, respectively. Ligands with higher affinity might have better rescuing effects, similar to what has been observed for AVPR2 (Mouillac and Mendre, 2014) and GnRHR (Conn and Ulloa-Aguirre, 2011).

Two mutants, S58C and G98R, were rescued to the cell surface but were not functional in cAMP production in response to NDP-MSH stimulation (Table 4.1). G98R had no detectable signaling after ML00253764 treatment, indicating that G98R was also defective in ligand binding and/or signaling. Though poorly expressed at the cell surface, S58C still responded to ligand stimulation with an increased EC_{50} (Lubrano-Berthelier et al., 2003; Tao and Segaloff, 2003), reflecting the presence of spare receptor (Tao, 2005). Its signaling efficacy was not increased by ML00253764 in our study (Figure 4.5) but was previously reported to be increased by DCPMP (Rene et al., 2010), suggesting that different pharmacoperones maintain the mutant receptors in distinct conformations.

The cell surface expression levels of I69R, P78L, P260Q and F261S were not increased with ML00253764 treatment. However, using the more sensitive signaling assays, we showed that the signaling efficacies had been significantly increased for P78L and trended to be increased for P260Q (Figure 4.5). I69R could not be rescued by ML00253764. This mutation

might cause a more severe folding defect that it is unable to bind or to be stabilized by ML00253764.

ML00253764 treatment increased the cell surface expression of the WT MC4R (Figures 4.2 – 4.4). This is not the first time to observe that the WT MC4R is not efficiently expressed and that pharmacoperones can help WT MC4R folding and trafficking (Fan and Tao, 2009; Granell et al., 2010; Rene et al., 2010). Many other WT GPCRs have also been reported to be expressed inefficiently, such as MC2R (Chan et al., 2009; Metherell et al., 2005), δ opioid receptor (Petäjä-Repo et al., 2002; Petaja-Repo et al., 2000), GnRHR (Conn and Ulloa-Aguirre, 2011; Conn et al., 2007), odorant receptors (Saito et al., 2004), and α_{1D}-adrenoceptor (Uberti et al., 2005) (see (Tao and Conn, 2014) for a comprehensive review). Pharmacoperones such as ML00253764 can potentially be used to treat obese patients without *MC4R* mutations (Fan and Tao, 2009; Rene et al., 2010).

ML00253764 treatment did not alter the signaling of Δ88-92, D90N, I102S, and N274S (Figure 4.6 and 4.7). The four mutants have relatively normal cell surface expression but have defects in ligand binding (Δ88-92) (Donohoue et al., 2003), signaling (D90N and I102S) (Biebermann et al., 2003; Tao and Segaloff, 2005), or no defect (N274S) (Tao and Segaloff, 2003). ML00253764 also did not restore the function of an intracellularly retained mutant of another neural MCR, I335S MC3R. These data suggest, as illustrated in Figure 4.9, that ML00253764 specifically rescued only the intracellularly retained MC4R mutants.

The MC4R is primarily expressed in the central nervous system to achieve its major physiological functions in regulating energy homeostasis (Cone, 2006; Tao, 2010). To make our studies more physiologically relevant, in this study, we further studied the pharmacoperone action of ML00253764 on the cell surface expression and function of MC4R in two neuronal cell

lines, Neuro2a and N1E-115. Neuro2a cells have already been used in many MC4R studies (Granell et al., 2010; Granell et al., 2013; Mohammad et al., 2007; Overton and Leibel, 2011). Although Neuro2a (Adan et al., 1996) and N1E-115 (Roth et al., 2002) cells were previously detected to express MC4R mRNA, neither of them responded to NDP-MSH stimulation even at very high doses (10^{-5} M) (data not shown) and our signaling data were corrected with cAMP produced by cells transfected with the empty vector to eliminate the potential effect of endogenous MC4R. In this study, we used transient transfection for Neuro2a and N1E-115 cells due to failure in generating stable cells. Therefore, our data obtained from Neuro2a and N1E-115 cells were consistent with those obtained from HEK293 cells (Table 4.1) with the major exception of Y157S. The discrepancy is probably attributed to cell differences or to the fact that the rescuing effect of ML00253764 being too weak to be observed in neuronal cells.

In summary, our study demonstrated that ML00253764 could act as a MC4R pharmacoperone, increasing the cell surface expression and function of intracellularly retained MC4R mutants with different efficacies. These data will be useful in research towards personalized medicine for obese patients carrying *MC4R* mutations.

Table 4.1 Summary of the effect of ML00253764 on the cell surface expression and function of WT and mutant MC4Rs.

	HEK293 cells		Neuronal cells	
Mutants	**Expression**	**Function**	**Expression**	**Function**
WT	↑	↓	–	–
S58C	↑	–	/	/
N62S	↑	↑	↑	↑
I69R	–	–	–	–
P78L	–	↑	–	–
C84R	↑	↑	↑	↑
G98R	↑	–	–	–
Y157S	↑	↑	–	–
W174C	↑	↑	↑	↑
P260Q	–	–	–	–
F261S	–	/	–	–
C271Y	↑	↑	–	↑

"↑", increasing; "↓", decreasing; "–", no significant effect; "*I*", not studied herein.

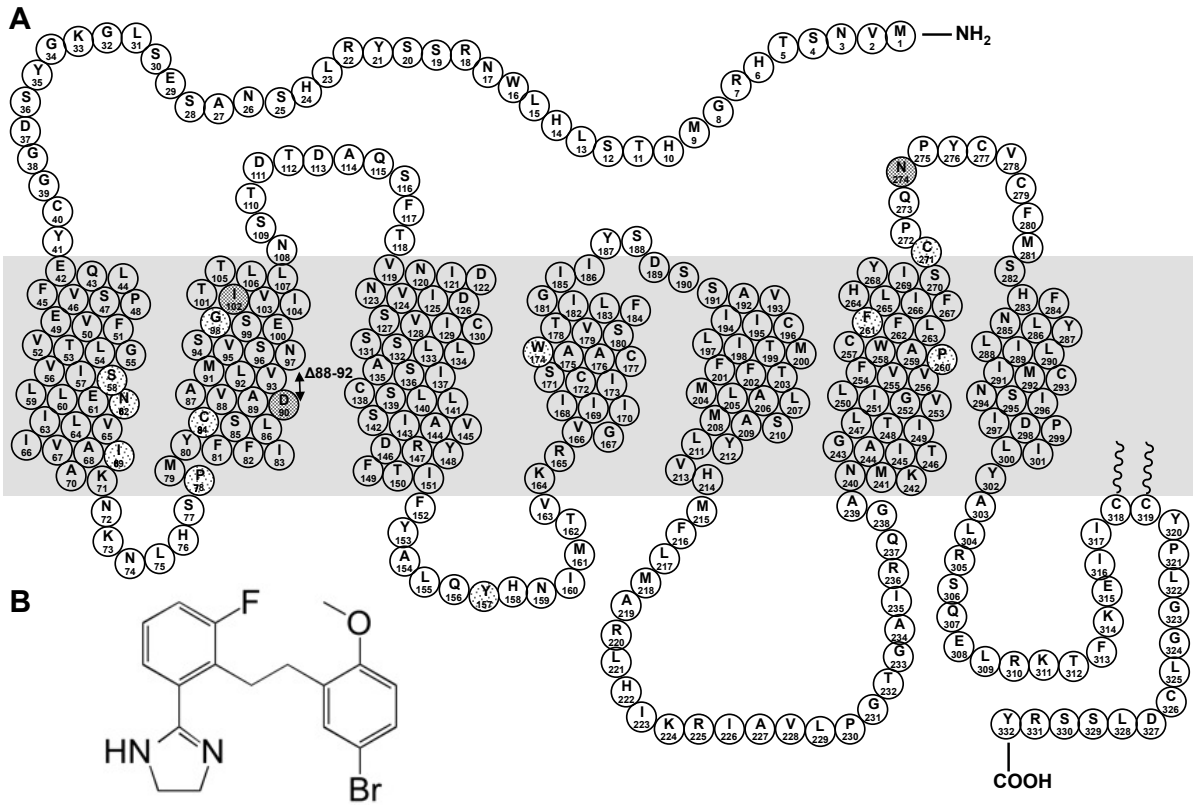

Figure 4.1 Schematic representation of the MC4R (A) and structure of ML0023764 (B).

Class II *MC4R* mutations are highlighted with dotted background whereas other mutations (Class III, IV, and V) are highlighted with cross-line background.

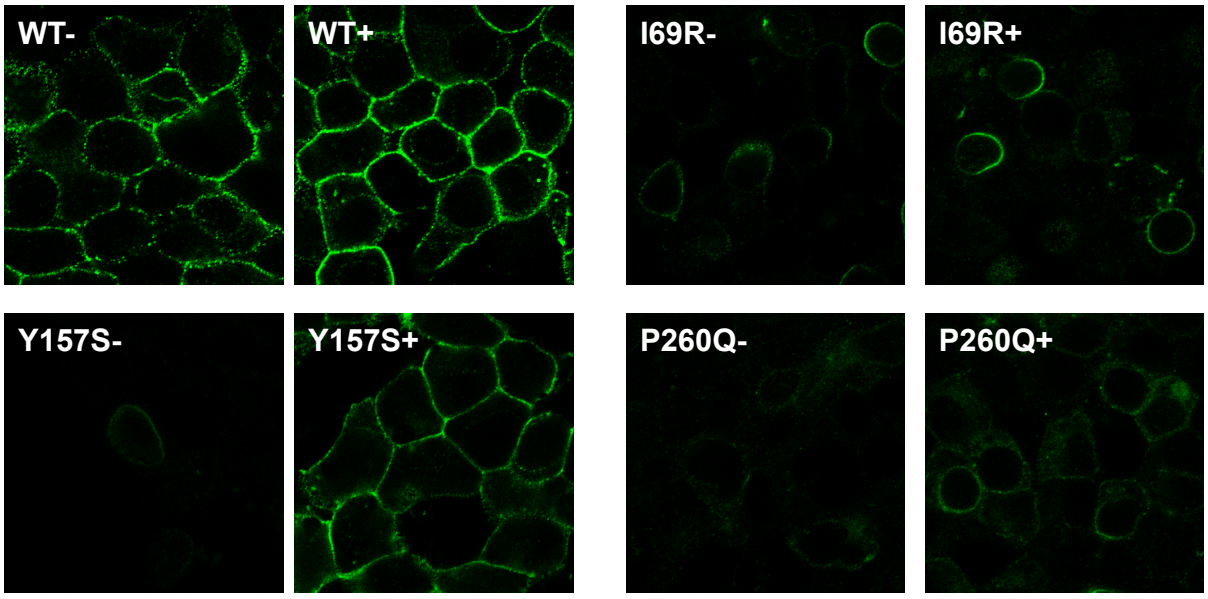

Figure 4.2 Cell surface expression of mutant MC4Rs with or without ML00253764 treatment in HEK293 cells as visualized by confocal microscopy.

The WT or mutant myc-MC4Rs stably expressed in HEK293 cells were treated with 10^{-5} M ML00253764 for 24 h. Cells were stained as described in Materials and Methods and imaged using a Nikon A1 confocal microscope. Experiments were performed at least twice with similar results.

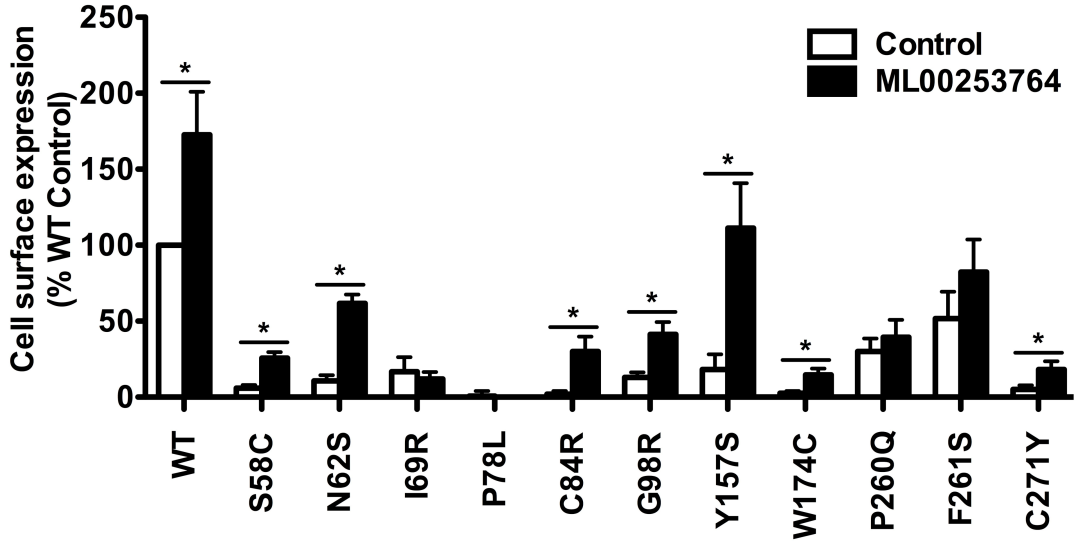

Figure 4.3 Cell surface expression of mutant MC4Rs with or without ML00253764 treatment in HEK293 cells as quantitated by flow cytometry.

The WT or mutant myc-MC4Rs stably expressed in HEK293 cells were treated with 10^{-5} M ML00253764 for 24 h and the cell surface expression levels were measured using a C6 Accuri Cytometer. The results are expressed as percentage of cell surface expression levels of WT MC4R after correction of the nonspecific staining of cells stably transfected with the empty vector. Data are mean ± S.E.M. of at least three independent experiments. *Significantly different from the untreated control group, $p < 0.05$.

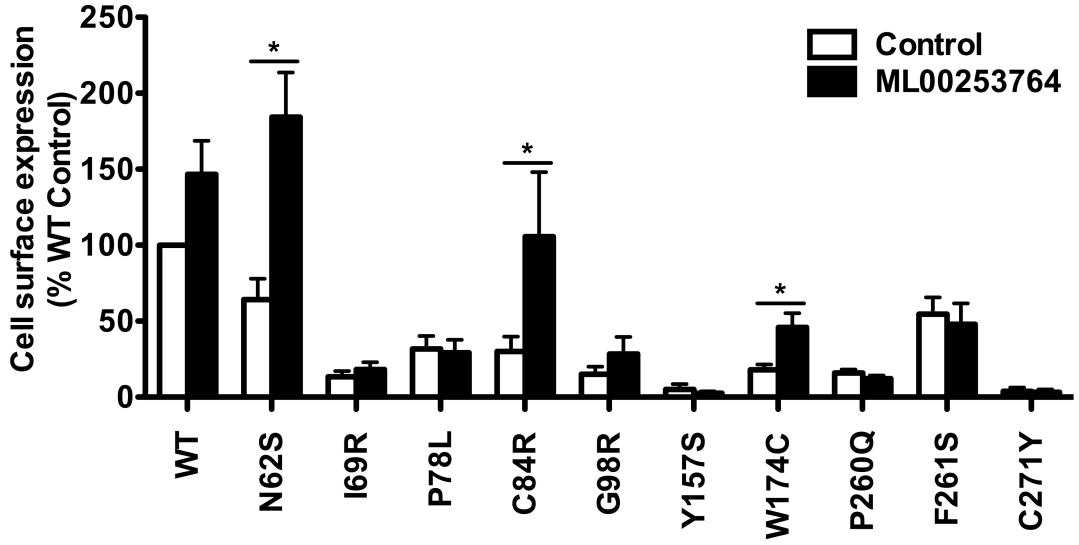

Figure 4.4 Cell surface expression of mutant MC4Rs with or without ML00253764 treatment in Neuro2a cells.

Neuro2a cells were transiently transfected with WT or mutant MC4Rs. Data are mean ± S.E.M. of at least three independent experiments. *Significantly different from the control group treated with DMSO, $p < 0.05$. See the legend to Figure 4.3 for details.

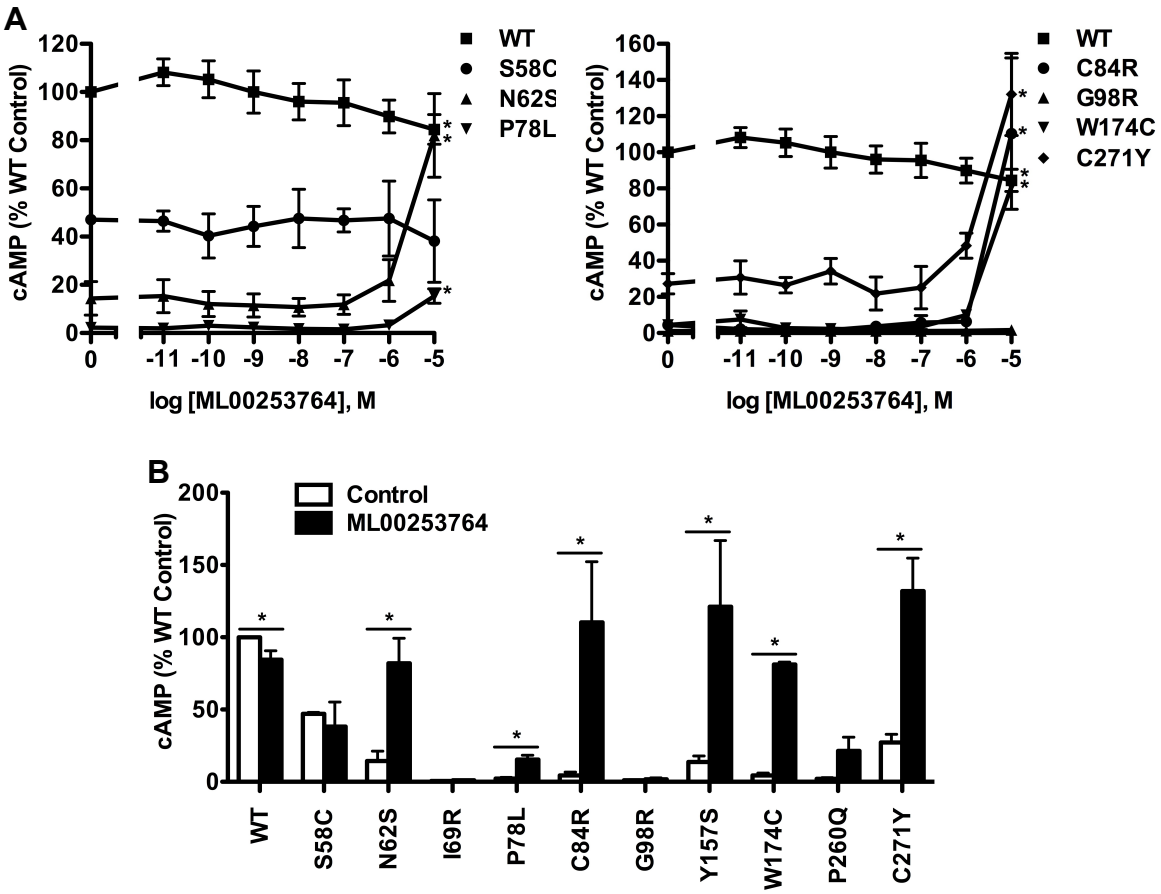

Figure 4.5 Signaling efficacies of mutant MC4Rs with or without ML00253764 treatment in HEK293 cells.

HEK293 cells stably transfected with the WT or mutant MC4Rs were treated with different concentrations of ML00253764 (A) or 10^{-5} M ML00253764 (B) for 24 h and then were washed twice. Intracellular cAMP accumulation in response to 10^{-6} M NDP-MSH stimulation for 1 h was measured using RIA. The results were expressed as percentage of the cAMP produced by untreated WT MC4R. Data are mean ± S.E.M. of at least two or three independent experiments. *Significantly different from the control group treated with DMSO, $p < 0.05$.

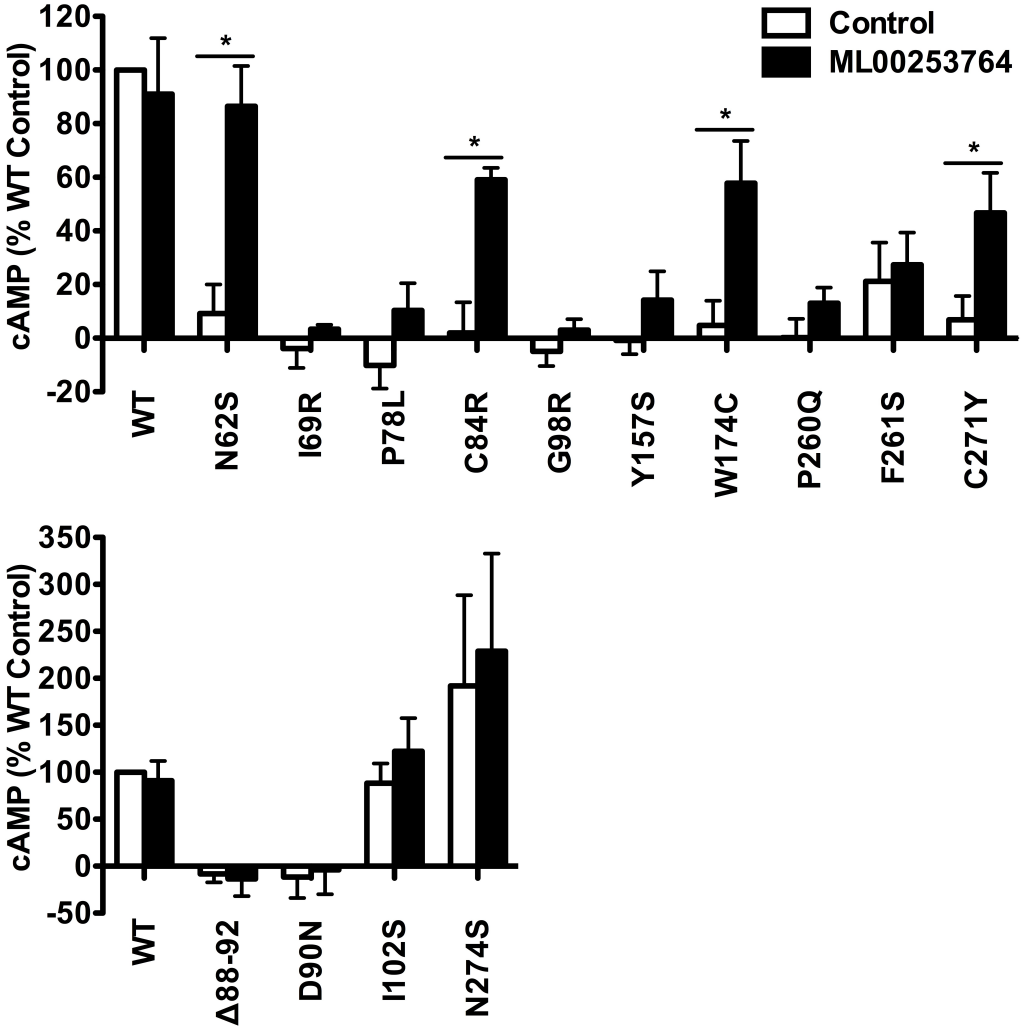

Figure 4.6 Signaling efficacies of mutant MC4Rs with or without ML00253764 treatment in Neuro2a cells.

Neuro2a cells transiently expressing WT or mutant MC4Rs were treated with 10^{-5} M ML00253764 for 24 h and then stimulated with 10^{-6} M NDP-MSH for 1 h. Intracellular cAMP levels were measured with RIA. The results are expressed as percentage of WT untreated cAMP after correction of the cAMP production in cells expressing the empty vector. Data are mean ± S.E.M. of at least three independent experiments. *Significantly different from the control group treated with DMSO, $p < 0.05$. See the legend to Figure 4.5 for details.

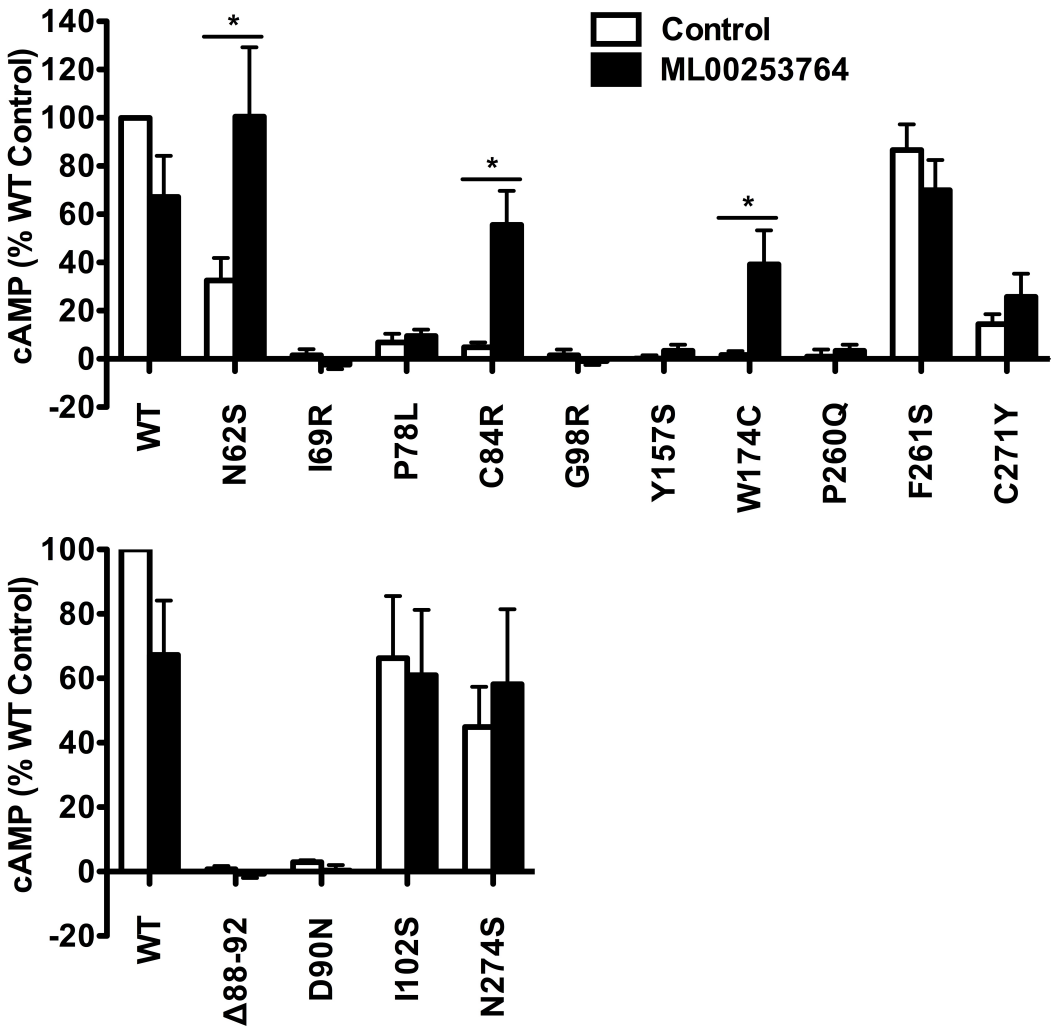

Figure 4.7 Signaling efficacies of mutant MC4Rs with or without ML00253764 treatment in N1E-115 cells.

N1E-115 cells transiently expressing WT or mutant MC4Rs were treated with 10^{-5} M ML00253764 for 24 h and then stimulated with 10^{-6} M NDP-MSH for 1 h. Intracellular cAMP levels were measured with RIA. Data are as mean ± S.E.M. of at least three independent experiments. *Significantly different from the untreated control group, $p<0.05$. See the legend to Figure 4.5 for details.

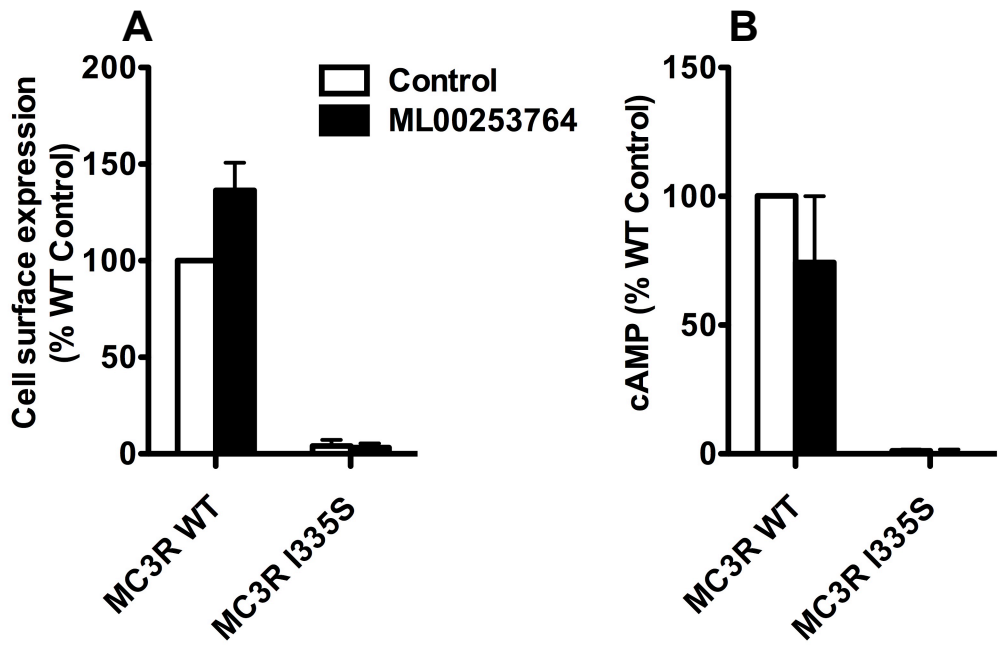

Figure 4.8 ML00253764 did not affect the cell surface expression or function of intracellularly retained MC3R mutant.

Neuro2a cells transiently expressing WT or I335S MC3R were treated with 10^{-5} M ML00253764 for 24 h. The cell surface expression and intracellular cAMP accumulation were measured, respectively. Data are as mean ± S.E.M. of at least three independent experiments.

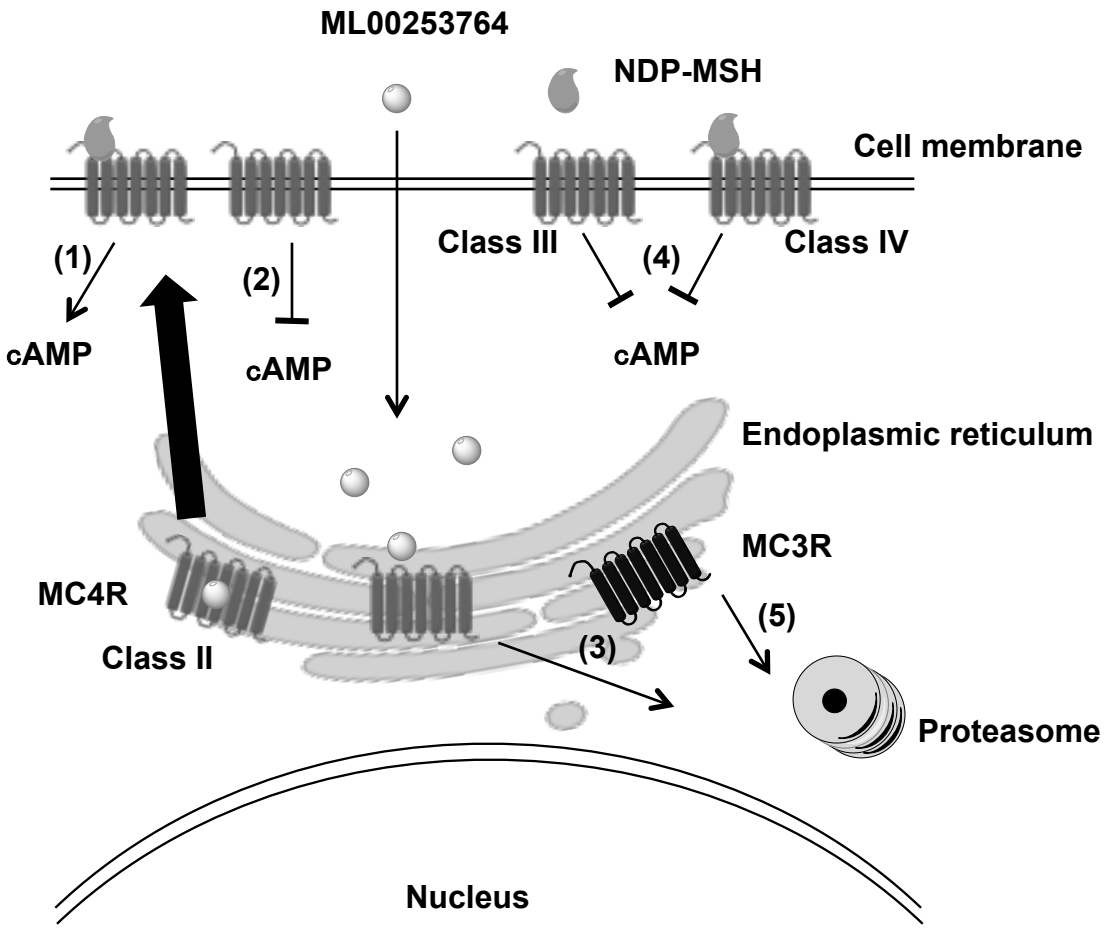

Figure 4.9 Overview of the mechanism of ML00253764 specifically rescuing intracellularly retained MC4R mutants.

ML00253764 rescued the intracellularly retained MC4R mutants (Class II) to the cell surface and some mutants were functional (1) and some were not (2) in cAMP production. (3) ML00253764 could not rescue certain MC4R Class II mutants. (4) ML00253764 did not restore the function of MC4R mutants defective in ligand binding (Class III) or signaling (Class IV). (5) ML00253764 did not rescue a Class II MC3R mutant.

Chapter 5 Ipsen 5i is a novel potent pharmacoperone for intracellularly retained melanocortin-4 receptor mutants

5.1 Introduction

The melanocortin-4 receptor (MC4R) is a G protein-coupled receptor (GPCR) that is widely expressed in the central nervous system including the cortex, thalamus, hypothalamus, hippocampus, brainstem, and spinal cord (Gantz et al., 1993; Mountjoy et al., 1994). The MC4R plays a vital role in the leptin-melanocortin pathway in regulating energy homeostasis, affecting both energy intake and expenditure (Cone, 2005; Huszar et al., 1997). Tissue-specific knockout studies revealed that the MC4R expressed in the paraventricular nucleus and/or amygdala neurons regulates food intake (Balthasar et al., 2005) whereas the MC4R expressed in the cholinergic neurons regulates energy expenditure and hepatic glucose production (Rossi et al., 2011). Inactivating mutations of the *MC4R* cause early-onset severe obesity (Hinney et al., 1999; Vaisse et al., 1998; Yeo et al., 1998), which is the most common cause of monogenic form of obesity in humans (Farooqi et al., 2003).

Most of the loss-of-function MC4R mutants are misfolded and trapped intracellularly by the stringent endoplasmic reticulum (ER) quality control system (Hinney et al., 2013; Hohenadel et al., 2014; Tao, 2010). These mutant MC4Rs may only have minor folding defect but retain pharmacological function. If they are escorted onto the cell surface, they can potentially bind the ligand and initiate signaling. Several studies have attempted to promote the anterograde

trafficking of these mutant MC4Rs, using molecular chaperone (Meimaridou et al., 2011), chemical chaperone (Granell et al., 2010), or pharmacological chaperone (or pharmacoperone) (Fan and Tao, 2009; Rene et al., 2010; Tao, 2010; Ward et al., 2012).

The therapeutic potential of molecular and chemical chaperones is limited due to disruption of proteostasis or significant side effects whereas pharmacoperone is a promising approach. It has been tested in numerous human diseases caused by misfolded proteins, including neurodegenerative diseases, cystic fibrosis, lysosomal storage diseases, and cancer, with several promising clinical trials underway (reviewed in (Lester et al., 2012; Loo and Clarke, 2007; Tao and Conn, 2014)). Misfolding is also the most common defect in diseases caused by mutations in GPCR genes (Tao, 2006). Pharmacoperones have also been identified for several GPCRs, including rhodopsin, V2 arginine vasopressin receptor, gonadotropin-releasing hormone receptor, calcium-sensing receptor, and others (reviewed in (Tao and Conn, 2014)). In the MC4R, we and others reported a few molecules that act as pharmacoperones (Fan and Tao, 2009; Rene et al., 2010; Tao, 2010; Ward et al., 2012). These compounds have low affinities for the MC4R therefore usually need high concentrations (10^{-6} M and higher) to achieve any rescue.

Ipsen 5i was synthesized and identified as a high affinity antagonist and partial inverse agonist of MC4R competing with [Nle^4,D-Phe^7]-α-MSH (NDP-MSH) for binding to the MC4R (Huang and Tao, 2012; Poitout et al., 2007; Tao et al., 2010). We reported recently that although it decreases basal signaling at the classical Gs-cAMP pathway, it acts as an agonist in the mitogen-activated protein kinase pathway (Mo and Tao, 2013). In this study, we investigated whether Ipsen 5i could act as a pharmacoperone promoting the proper folding and trafficking of intracellularly retained mutant MC4Rs using multiple cell lines. A total of fifteen mutants were studied, including eleven (S58C, N62S, I69R, P78L, C84R, G98R, Y157S, W174C, P260Q,

F261S, and C271Y) that are retained intracellularly and four (Δ88-92, D90N, I102S, and N274S) that are expressed relatively normally at the cell surface with other or no defects.

5.2 Materials and methods

5.2.1 Materials and plasmids

NDP-MSH was purchased from Peptides International (Louisville, KY), α-MSH from Pi Proteomics (Huntsville, AL), SHU9119 from Tocris Bioscience (Ellisville, MO), and naltrexone hydrochloride from Alfa Aesar (Ward Hill, MA). Ipsen 5i was custom synthesized by Enzo Life Science (Plymouth Meeting, PA). [^{125}I]-cAMP was iodinated with chloramine T method (Tao et al., 2010). Wild type (WT) and mutant human MC4R with N-terminal c-myc tag and human MC3R with N-terminal 3×HA tag were previously constructed and sequenced (Fan and Tao, 2009; Tao, 2007; Tao and Segaloff, 2003; Tao and Segaloff, 2005; Wang and Tao, 2011).

5.2.2 Cell culture and transfection

Human embryonic kidney (HEK) 293, Neuro2a, and N1E-115 cells were purchased from American Type Culture Collection (Manassas, VA) and cultured in Dulbecco's modified Eagle's medium supplemented with 10% newborn calf serum (HEK293 cells) or 10% fetal bovine serum (Neuro2a and N1E-115 cells) at 37 ^{o}C. HEK293 cells were stably transfected using calcium phosphate precipitation method for transfection and 0.2 mg/ml G418 for selection. Neuro2a and N1E-115 cells were transiently transfected using jetPRIME transfection reagent (Polyplus-transfection, New York, NY) and approximately 24 h later were used for ligand treatment. Cells were treated with indicated concentrations of ligands or 0.1% dimethyl sulfoxide (DMSO) as control for 24 h at 37 ^{o}C. All cell culture plates were pretreated with 0.1% gelatin before cell

plating unless noted otherwise.

5.2.3 Confocal microscopy

HEK293 stable cells seeded into poly-D-lysine-coated 8-well slides (Biocoat cellware from Falcon, BD Systems, Franklin Lakes, NJ) were treated with 0.1% DMSO or 10^{-6} M Ipsen 5i for 24 h. On the day of experiment, cells were washed with phosphate buffered saline for immunohistochemistry (PBS-IH, 137 mM NaCl, 2.7 mM KCl, 1.4 mM KH_2PO_4, 4.3 mM Na_2HPO_4, pH 7.4) and fixed with 4% paraformaldehyde for 15 min. After blocking with 5% bovine serum albumin (BSA) in PBS-IH for 1 h, cells were incubated with mouse anti-myc 9E10 monoclonal antibody (Developmental Studies Hybridoma Bank, The University of Iowa, Iowa City, IA) 1:40 diluted in PBS-IH containing 0.5% BSA for 1 h. Cells were then washed and incubated with Alexa Fluor 488-labeled goat anti-mouse antibody (Invitrogen, Grand Island, NY) 1:2000 diluted in PBS-IH containing 0.5% BSA for 1 h. Cells were washed, covered with Vectashield mounting media (Vector Laboratories, Burlingame, CA) and a glass coverslip, and dried overnight at 4 ^{o}C. Images were taken using a Nikon A1 confocal microscope. All the steps were performed at room temperature unless mentioned otherwise.

5.2.4 Flow cytometry

HEK293 stable cells and Neuro2a transiently transfected cells were treated with 0.1% DMSO, 10^{-6} or 10^{-5} M Ipsen 5i for 24 h at 37 ^{o}C. On the day of experiment, cells were washed with ice-cold PBS-IH, detached, and precipitated by centrifugation at 500 × g for 5 min. Cells were then incubated with antibodies the same way as described above for confocal microscopy. For immunostaining of MC3R, cells were incubated with HA.11 antibody (Covance, Princeton,

NJ) at 1:100 dilution and then stained with secondary antibody as described above. Cells were analyzed using a C6 Accuri Cytometer (Accuri Cytometers, Ann Arbor, MI). Fluorescence of cells expressing the DMSO-treated empty vector was used for background staining. The expression of the mutants was calculated as percentage of DMSO-treated WT receptor expression using the following formula: [(mutant - pcDNA3.1) / (WT - pcDNA3.1) × 100%] (Wang et al., 2008).

5.2.5 Intracellular cAMP accumulation assay

HEK293 stable cells and Neuro2A and N1E-115 transiently transfected cells were treated with 0.1% DMSO or different concentrations of Ipsen 5i for 24 h at 37 ^{o}C. On the day of experiment, cells were washed twice with warm Waymouth's MB752/1 media (Sigma-Aldrich, St. Louis, MO) containing 1 mg/ml BSA (Waymouth's/BSA) and incubated with Waymouth's/BSA containing 0.5 mM isobutylmethylxanthine (Sigma-Aldrich) for 15 min. Cells were then stimulated with 10^{-6} M NDP-MSH for 1h at 37 ^{o}C. Intracellular cAMP were extracted by adding 0.5 M percholoric acid containing 180 μg/ml theophylline (Sigma-Aldrich) and neutralized with 0.72 M KOH/0.6 M $KHCO_3$. The cAMP concentration was determined by RIA (Tao et al., 2010). The intracellular cAMP accumulation of the mutants was calculated as percentage of DMSO-treated WT receptor using the formula [mutant / WT × 100%] for HEK293 cells or the formula [(mutant - pcDNA3.1) / (WT - pcDNA3.1) × 100%] for Neuro2a and N1E-115 cells.

5.2.6 Data analysis

Data were analyzed using GraphPad Prism 4.0 software (San Diego, CA). The statistical

significance of the differences between DMSO and Ipsen 5i treated cells were assessed by Student's t-test.

5.3 Results

5.3.1 Ipsen 5i rescued the cell surface expression of mutant MC4Rs

To investigate whether Ipsen 5i acted as a pharmacoperone rescuing the cell surface expression of mutant MC4Rs, we studied eleven mutants (S58C, N62S, I69R, P78L, C84R, G98R, Y157S, W174C, P260Q, F261S, and C271Y) that have reduced or absent cell surface expression (Fan and Tao, 2009; Tao and Segaloff, 2003; Wang and Tao, 2011) (Figure 5.1). We first visualized the cell surface expression of the eleven mutants stably expressed in HEK293 cells treated with 10^{-6} M Ipsen 5i using a confocal microscope. As shown in Figure 5.2, with 10^{-6} M Ipsen 5i treatment for 24 h, the immunostaining of ten mutants (S58C, N62S, P78L, C84R, G98R, Y157S, W174C, P260Q, F261S, and C271Y) were dramatically enhanced compared with that of the DMSO-treated control cells whereas that of one mutant (I69R) was not obviously changed.

To quantitate the rescuing effect of Ipsen 5i on the cell surface expression of mutant MC4Rs, flow cytometry studies were performed using HEK293 and Neuro2a cells. HEK293 cells stably expressing WT or mutant MC4Rs were treated with 10^{-5} M (Figure 5.3A) or 10^{-6} M (Figure 5.3B) Ipsen 5i for 24 h. Consistent with confocal microscopy results, the cell surface expression of ten mutants (S58C, N62S, P78L, C84R, G98R, Y157S, W174C, P260Q, F261S, and C271Y) was significantly increased with Ipsen 5i treatment to a level similar to or even higher than that of the DMSO-treated WT receptor. I69R was not rescued by Ipsen 5i.

Neuro2a cells transiently expressing WT or mutant MC4Rs were treated with 10^{-6} M

Ipsen 5i for 24 h and then were used for flow cytometry studies. S58C was not further studied in neuronal cells because as described later its function was not rescued by Ipsen 5i. As shown in Figure 5.4, the cell surface expression of eight mutants (N62S, I69R, P78L, C84R, G98R, W174C, P260Q, and C271Y) was increased with Ipsen 5i treatment compared with the DMSO-treated control group. The cell surface expression of I69R was slightly (although significantly) increased in Neuro2a cells whereas it was not increased in HEK293 cells. The increase of cell surface expression of F261S was not statistically significant in Neuro2a cells. One mutant (Y157S) that was rescued by Ipsen 5i in HEK293 cells was not rescued in Neuro2a cells.

5.3.2 The majority of the mutant MC4Rs rescued with Ipsen 5i could signal in response to agonist stimulation

We next investigated whether Ipsen 5i-rescued mutant MC4Rs were functional in generating cAMP at the cell surface. HEK293 cells stably expressing WT or mutant MC4Rs were incubated with different concentrations of Ipsen 5i for 24 h. The intracellular cAMP concentration in response to 10^{-6} M NDP-MSH stimulation was measured. As shown in Figure 5.5, the cAMP accumulation of WT MC4R was decreased by approximately 30% with 10^{-6} Ipsen 5i treatment and by 80% with 10^{-5} M Ipsen 5i treatment. We observed an increase in cAMP accumulation at 10^{-9} M Ipsen 5i for C84R and W174C and a maximal increase at a concentration between 10^{-8} M and 10^{-6} M for N62S, P78L, C84R, Y15YS, W174C, P260Q, and C271Y. Unlike most of the mutants that decreased cAMP accumulation at 10^{-5} M Ipsen 5i, I69R had a maximal cAMP accumulation at that concentration. The signaling of S58C and G98R was not increased by Ipsen 5i.

In Neuro2a cells transiently expressing MC4Rs, we also observed an increase in cAMP

accumulation at 10^{-9} M Ipsen 5i and a maximal increase at 10^{-6} M Ipsen 5i (or at 10^{-5} M Ipsen 5i for I69R) in Neuro2a cells (Figure 5.6A). As shown in Figure 5.6B, with 10^{-6} M Ipsen 5i treatment in Neuro2a cells, seven mutants (N62S, I69R, P78L, C84R, W174C, P260Q, and C271Y) had significantly increased cAMP accumulation whereas signaling of three mutants (G98R, Y157S, and F261S) was not increased by Ipsen 5i. High concentration of Ipsen 5i did not decrease the cAMP accumulation of WT or mutant MC4Rs as dramatically as seen in HEK293 cells (Figure 5.6A). Our results obtained from N1E-115 cells were similar with those obtained from Neuro2a cells (Figure 5.7).

5.3.3 Ipsen 5i did not affect mutant MC4Rs that are expressed normally at the cell surface

To investigate whether Ipsen 5i rescued the function of mutant MC4Rs that are expressed at the cell surface but have other defects, we studied four mutants that are defective in ligand binding ((Δ88-92) (Donohoue et al., 2003) (Class III according the classification proposed by Tao (Tao and Segaloff, 2005)), signaling (D90N and I102S) (Biebermann et al., 2003; Tao and Segaloff, 2005) (Class IV), or with no obvious defect (N274S) (Tao and Segaloff, 2003) (Class V). As shown in Figure 5.6B and Figure 5.7B, 10^{-6} Ipsen 5i had no effect on the signaling of these four mutants.

5.3.4 Specificity of the MC4R mutant rescue

To investigate whether cell impermeable peptide ligands of the MC4R or cell permeable ligands of other receptors could rescue mutant MC4Rs, we studied the effect of two MC4R peptide agonists (NDP-MSH and α-MSH), one MC4R peptide antagonist (SHU9119), and one pharmacoperone of δ opioid receptor (naltrexone) (Petäjä-Repo et al., 2002) (Figure 5.8A) on

C84R MC4R. As shown in Figure 5.8B, NDP-MSH and α-MSH decreased the signaling of WT MC4R by approximately 50%. However, none of the four ligands rescued the signaling of C84R MC4R.

To investigate whether Ipsen 5i specifically rescues mutant MC4Rs, we studied the effect of Ipsen 5i on one of intracellularly retained mutant MC3Rs (I335S) (Mencarelli et al., 2011; Tao, 2007). As shown in Figure 5.8C, Ipsen 5i had no effect on the cell surface expression or signaling of I335S MC3R.

5.4 Discussion

Most of the inactivating mutations in GPCRs causing human diseases result from protein misfolding and subsequent retention and degradation by the ER quality control system (Tao, 2006). Misrouted receptors may retain intrinsic function and become functional when correctly located (Conn and Ulloa-Aguirre, 2011). Pharmacoperones that can permeate plasma membrane specifically stabilize the conformation and correct the trafficking of misfolded receptors, thus rescuing the receptor and curing human diseases (Conn et al., 2007; Huang and Breitwieser, 2007; Maya-Nunez et al., 2012; Newton et al., 2011). In the current study, we identified Ipsen 5i, an antagonist of the MC4R, as a potent pharmacoperone specifically rescuing the cell surface expression and function of intracellularly retained mutant MC4Rs.

Our results showed that all eleven intracellularly retained mutants studied herein could be rescued to the cell surface by Ipsen 5i in at least one cell line (Table 5.1). Y157S could be significantly rescued in HEK293 cells but not in neuronal cells whereas I69R was partially rescued in neuronal cells but not in HEK293 cells. The effects of Ipsen 5i on eight mutants were similar between HEK293 and neuronal cell lines. The cell surface expression of most mutants

treated with Ipsen 5i was increased to at least 50% of or even similar to that of the DMSO-treated WT receptor. The rescuing efficacies of Ipsen 5i were different for different mutations. I69R was the most difficult to rescue because it could only be maximally rescued with the highest concentration of Ipsen 5i (10^{-5} M) and could not be rescued with another pharmacoperone of the MC4R, ML00253764 (unpublished observations). This suggests that I69R induces a large change in the receptor conformation that is difficult to be stabilized.

Eight of the eleven mutants rescued to the cell surface were functional in cAMP production (N62S, I69R, P78L, C84R, Y157S, W174C, P260Q, and C271Y) in HEK293 cells and seven mutants, with the exception of Y157S, in neuronal cells (Table 5.1). These results suggest that these mutants, although misfolded and retained intracellularly, retain the ability to bind to agonist and initiate downstream signaling. Ipsen 5i treatment did not significantly increase F261S signaling. G98R, although rescued to the cell surface, did not respond to NDP-MSH stimulation with increased cAMP generation, suggesting that this mutant is also defective in ligand binding and/or signaling. Despite low cell surface expression, S58C has significant signaling (Tao and Segaloff, 2003), likely due to the presence of spare receptor (Tao, 2005). Ipsen 5i treatment significantly increased cell surface expression of S58C (Figures 5.2 and 5.3). However, its signaling was not increased and tended to decrease.

The signaling of WT MC4R was dramatically decreased when treated with 10^{-5} M Ipsen 5i in HEK293 cells (Figure 5.5). The residual Ipsen 5i that had not been washed away presumably still occupied the binding site of the MC4R and therefore antagonized the stimulation of NDP-MSH. Although Ipsen 5i has a high affinity with the MC4R (K_i, 2 nM), it has relatively low functional antagonist potency (77 nM) (Poitout et al., 2007), minimizing its antagonizing effect on NDP-MSH. Indeed, in our study, 10^{-6} M and 10^{-7} M Ipsen 5i, which

already had significant pharmacoperone rescuing ability, only decreased the signaling of WT MC4R by approximately 30% or 20% in HEK293 cells, respectively (Figure 5.5). Interestingly, we had not observed such dramatic decrease in WT MC4R signaling in neuronal cells (Figure 5.6 and 5.7), suggesting that it might be easier for Ipsen 5i to dissociate from the MC4R expressed in neuronal cells.

Ipsen 5i has low affinity for the MC3R (K_i, 400 nM) and therefore we investigated whether Ipsen 5i could rescue MC3R misrouted mutant I335S. We found that Ipsen 5i did not increase the cell surface expression or function of I335S MC3R, suggesting that Ipsen 5i was a pharmacoperone specific for the MC4R. Although Ipsen 5i was a potent pharmacoperone of the MC4R, it had no effect on mutant MC4Rs defective in ligand binding or signaling, suggesting that Ipsen 5i could only rescue the function of the intracellularly retained mutant MC4Rs. As expected, cell impermeable peptide ligands of the MC4R did not rescue the function of misrouted mutant MC4R C84R whereas cell permeable Ipsen 5i did. Consistent with previous reports on several other proteins (Bernier et al., 2004b; Janovick et al., 2002; Morello et al., 2000; Petäjä-Repo et al., 2002), this observation suggests that only cell permeable small compound could act as a pharmacoperone and the rescuing action occured intracellularly. Peptide ligands decreased the signaling of WT MC4R probably by inducing internalization and down-regulation (NDP-MSH and α-MSH) or by antagonizing NDP-MSH (SHU9119). Naltrexone, a pharmacoperone of δ opioid receptor (Petäjä-Repo et al., 2002), also did not correct the function of C84R MC4R, suggesting that only ligands for the MC4R could act as MC4R pharmacoperones. In Figure 5.9, we schematically presented the actions of Ipsen 5i.

In summary, Ipsen 5i increased the cell surface expression of all eleven intracellularly retained mutant MC4Rs (100%) studied herein and eight of the eleven mutants (73%) were

functional at the cell surface in at least one cell line. Ipsen 5i could rescue mutant MC4Rs at a concentration as low as 10^{-9} M. To our knowledge, it was the most potent pharmacoperone of the MC4R identified so far.

Table 5.1 Summary of the effect of Ipsen 5i on the cell surface expression and function of WT and mutant MC4Rs.

	HEK293 cells		Neuronal cells	
Mutants	**Expression**	**Function**	**Expression**	**Function**
WT	↑	↓	–	–
S58C	↑	–	/	/
N62S	↑	↑	↑	↑
I69R	–	↑	↑	↑
P78L	↑	↑	↑	↑
C84R	↑	↑	↑	↑
G98R	↑	–	↑	–
Y157S	↑	↑	–	–
W174C	↑	↑	↑	↑
P260Q	↑	↑	↑	↑
F261S	↑	/	–	–
C271Y	↑	↑	↑	↑

"↑", increase; "↓", decrease; "–", no significant effect; "*/*", not studied herein.

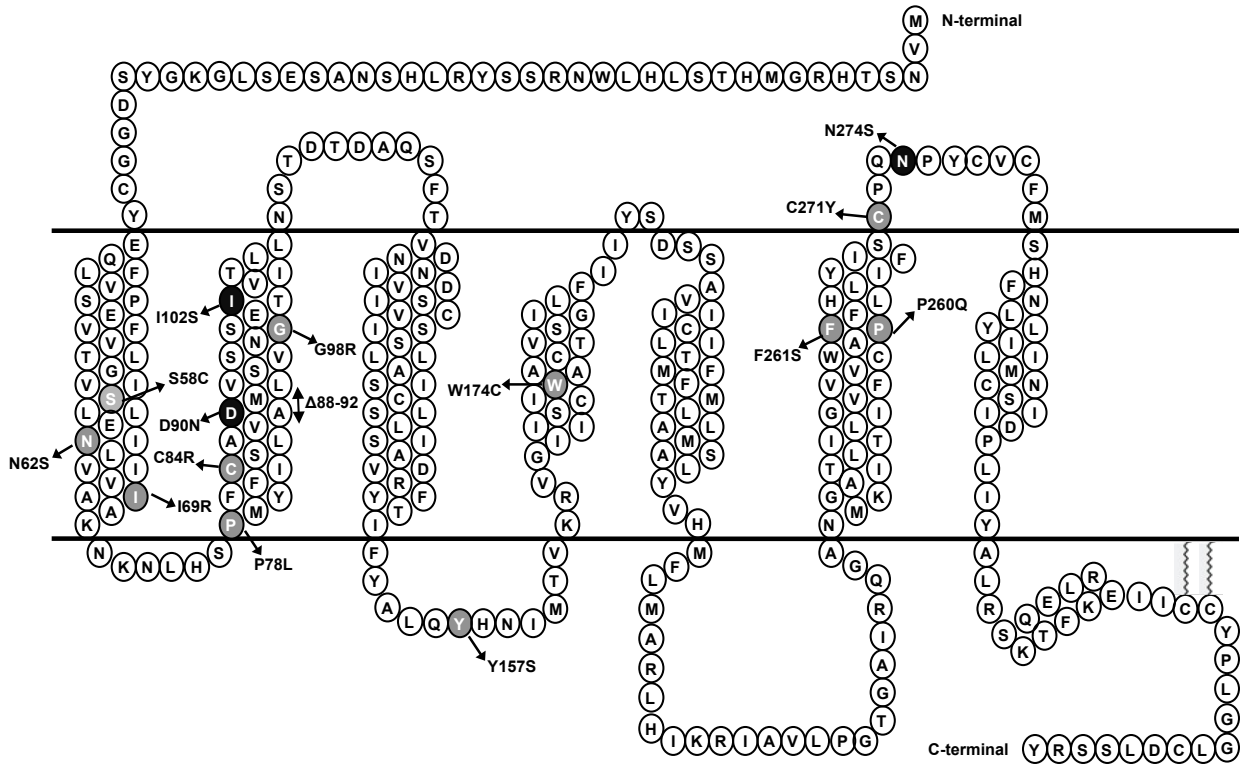

Figure 5.1 Schematic representation of MC4R.

Naturally occurring mutations of the *MC4R* characterized in this study are highlighted; mutations that result in intracellularly retention of the MC4R are highlighted in gray whereas mutations that do not interfere with the cell surface expression of the MC4R are highlighted in dark.

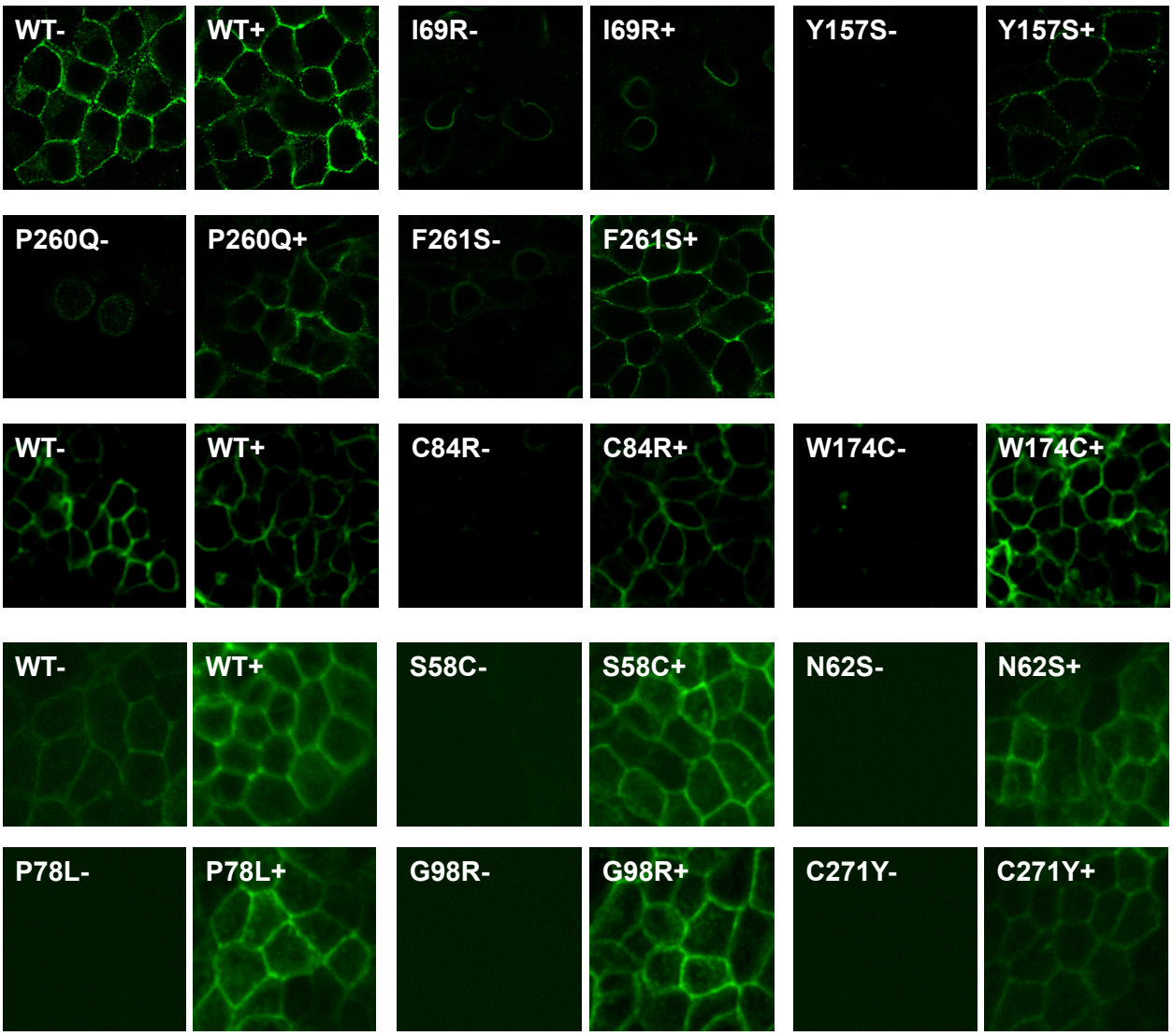

Figure 5.2 Ipsen 5i rescued the cell surface expression of intracellularly retained mutant MC4Rs in HEK293 cells as visualized by confocal microscopy.

HEK293 cells stably expressing WT or mutant MC4Rs were treated with 10^{-6} M Ipsen 5i for 24 h and then stained with Alexa Fluor 488-conjugated antibody. Cells were visualized using a Nikon A1 confocal microscope. Results are representative of at least two independent experiments.

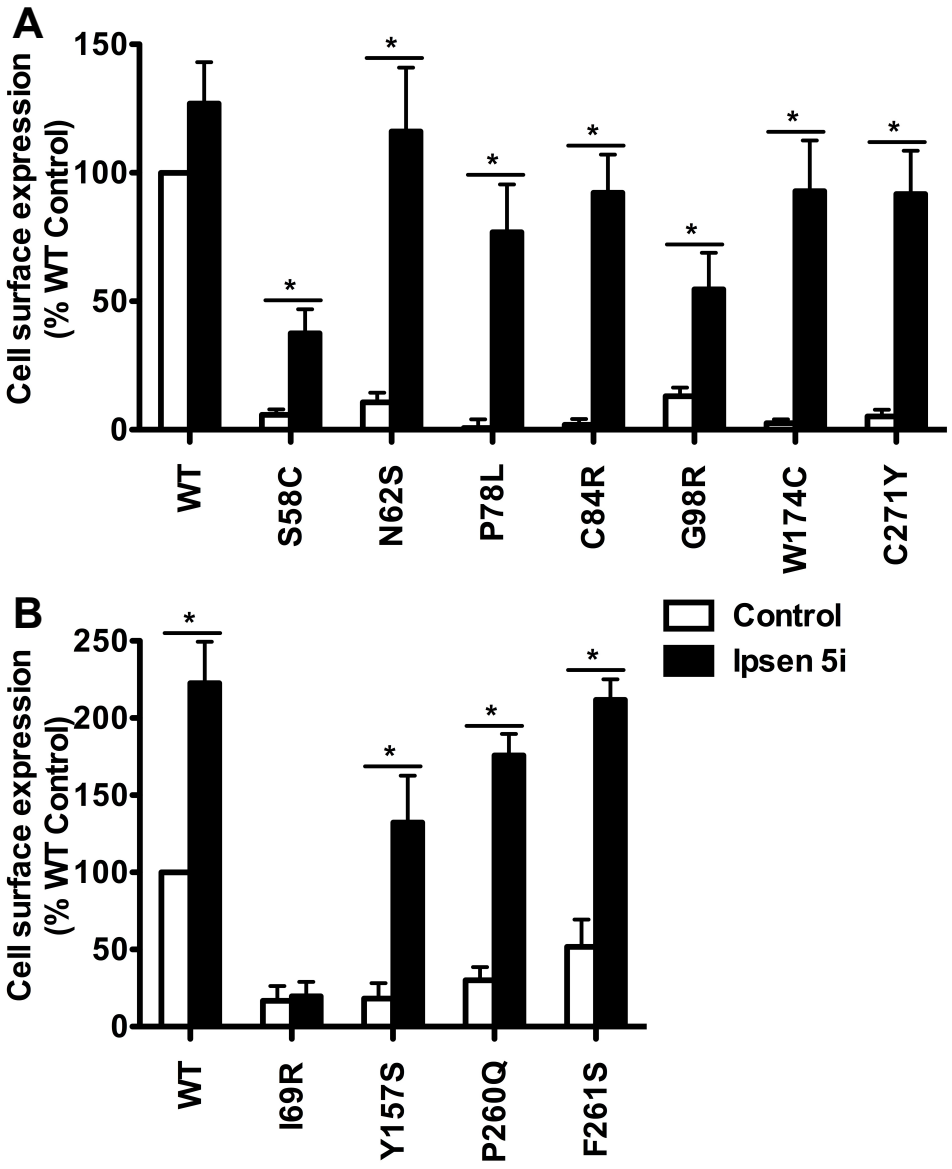

Figure 5.3 Ipsen 5i rescued the cell surface expression of intracellularly retained mutant MC4Rs in HEK293 cells as quantitated by flow cytometry.

HEK293 cells stably expressing WT or mutant MC4Rs were treated with 10^{-5} (A) or 10^{-6} (B) M Ipsen 5i for 24 h and then stained with Alexa Fluor 488-conjugated antibody. The immunostaining was measured using a C6 Accuri Cytometer. The results are expressed as % DMSO-treated WT cell surface expression level after correction of the nonspecific staining in

cells expressing the empty vector. Results are shown as mean ± S.E.M. of at least three independent experiments. *Significantly different from the DMSO-treated control group, $p < 0.05$.

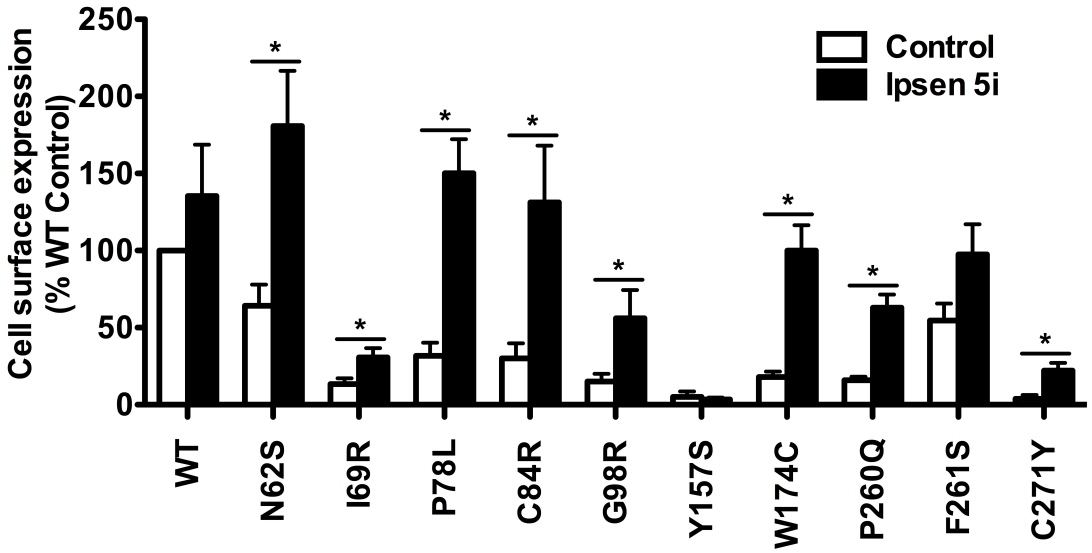

Figure 5.4 Ipsen 5i rescued the cell surface expression of intracellularly retained mutant MC4Rs in Neuro2a cells.

Neuro2a cells transiently expressing WT or mutant MC4Rs were treated with 10^{-6} M Ipsen 5i. Results are shown as mean ± S.E.M. of at least three independent experiments. See the legend to Figure 5.3 for details.

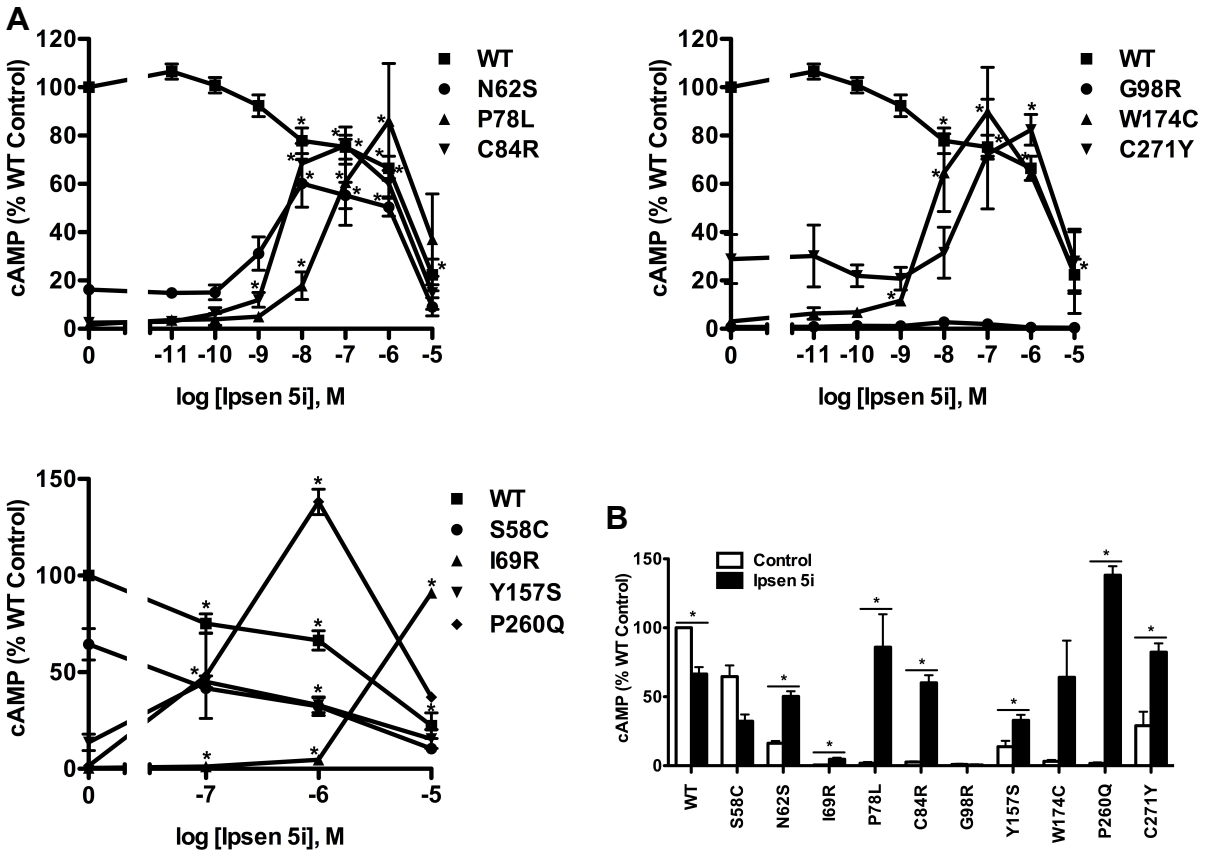

Figure 5.5 Ipsen 5i rescued the function of intracellularly retained mutant MC4Rs in HEK293 cells.

HEK293 cells stably expressing WT or mutant MC4Rs were treated with different concentrations of Ipsen 5i (A) or 10^{-6} M Ipsen 5i (B) for 24 h. Cells were washed twice and stimulated with 10^{-6} M NDP-MSH for 1h. Intracellular cAMP samples were collected and cAMP concentrations were measured using RIA. The results are expressed as % DMSO-treated WT cAMP production. Data points are shown as mean ± S.E.M. of at least two or three independent experiments. *Significantly different from the DMSO-treated control group, $p < 0.05$.

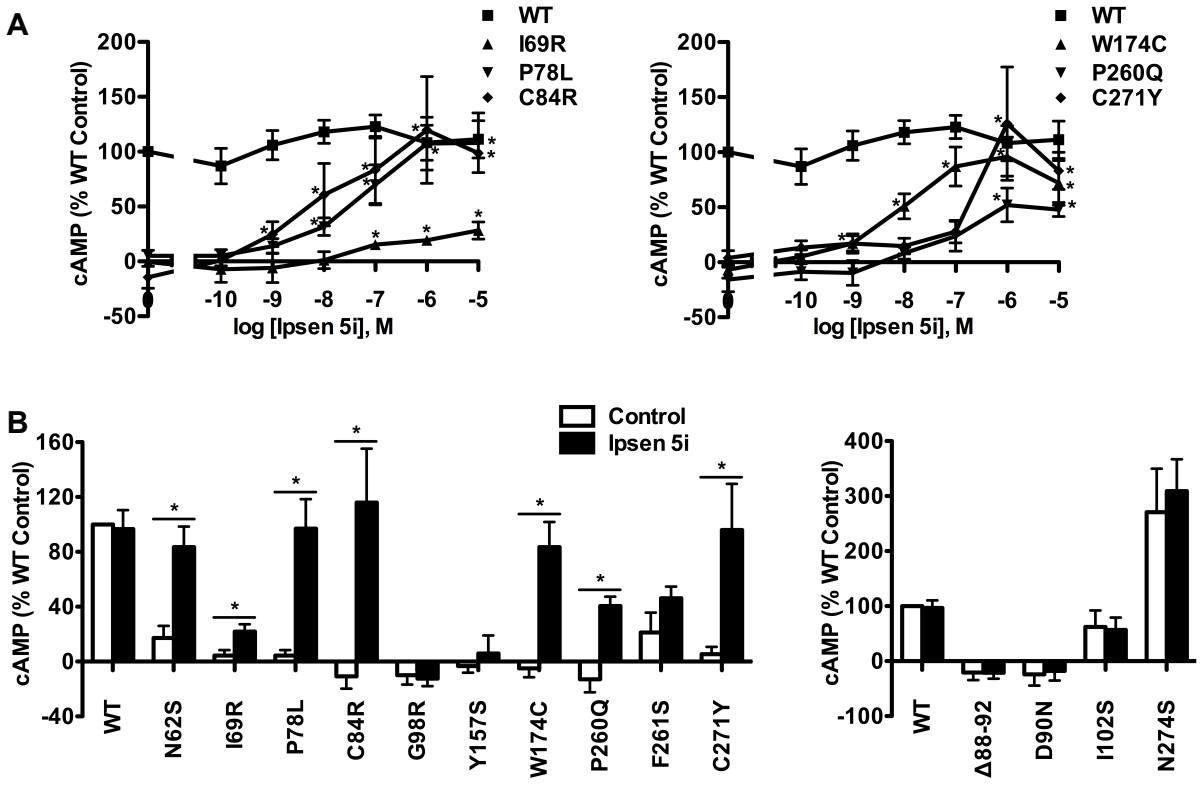

Figure 5.6 Ipsen 5i rescued the function of intracellularly retained mutant MC4Rs in Neuro2a cells.

Neuro2a cells transiently expressing WT or mutant MC4Rs were treated with different concentrations of Ipsen 5i (A) or 10^{-6} M Ipsen 5i (B). The results are expressed as % DMSO-treated WT cAMP production after correction of the cAMP production in cells expressing the empty vector. Data points are mean ± S.E.M. of at least three independent experiments. See the legend to Figure 5.5 for other details.

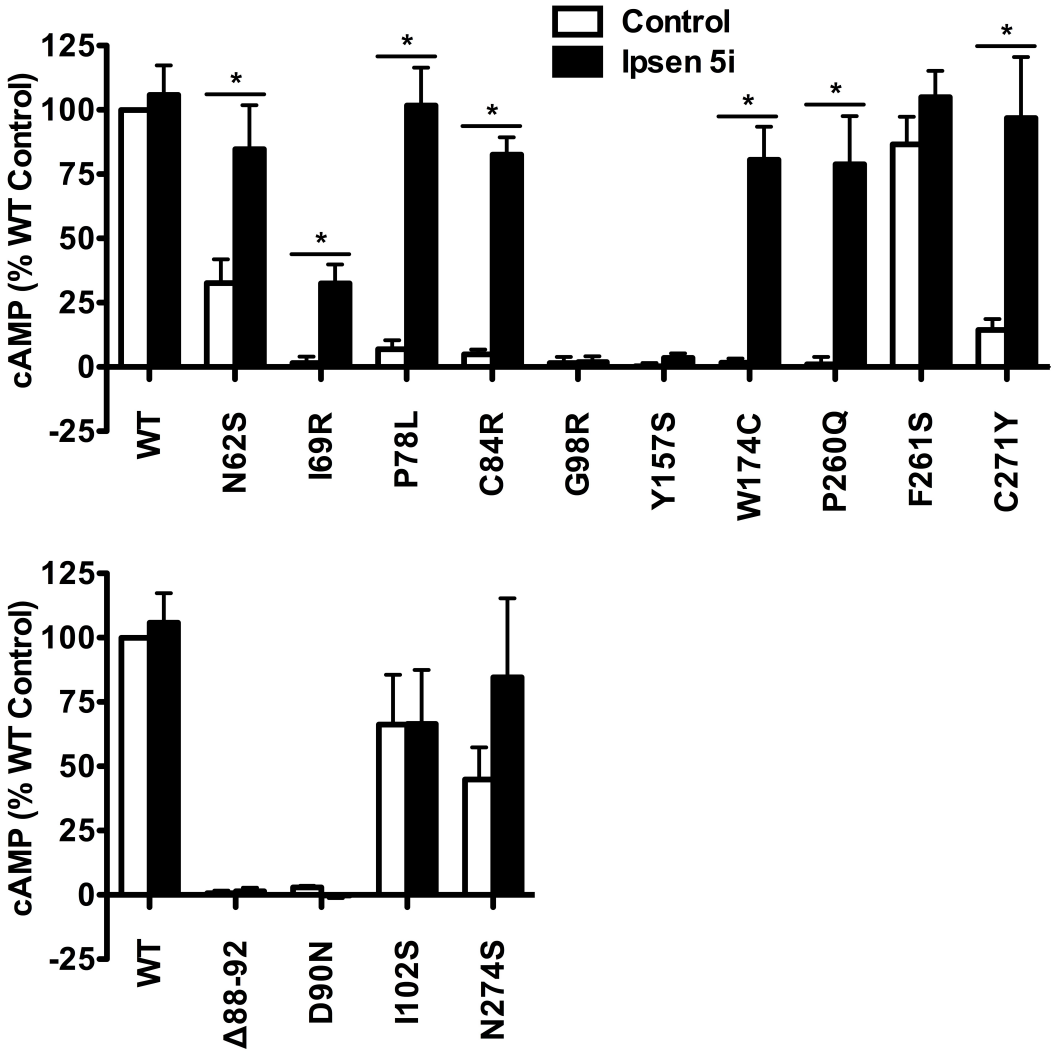

Figure 5.7 Ipsen 5i rescued the function of intracellularly retained mutant MC4Rs in N1E-115 cells.

N1E-115 cells transiently expressing WT or mutant MC4Rs were treated with 10^{-6} M Ipsen 5i. The results are expressed as % DMSO-treated WT cAMP production after correction of the cAMP production in cells expressing the empty vector. Results are shown as mean ± S.E.M. of at least three independent experiments. See the legend to Figure 5.5 for details.

A

a. NDP-MSH

Ac-Ser-Tyr-Ser-Nle-Glu-His-D-Phe-Arg-Trp-Gly-Lys-Pro-Val-NH2

b. α-MSH

Ac-Ser-Tyr-Ser-Met-Glu-His-Phe-Arg-Trp-Gly-Lys-Pro-Val-NH_2

c. SHU9119

Ac-Nle-cyclo(-Asp-His-D-2-Nal-Arg-Trp-Lys)-NH2

d. Naltrexone

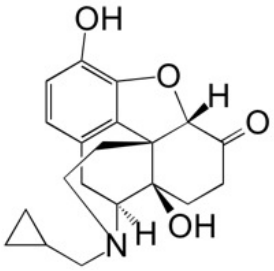

e. Ipsen 5i

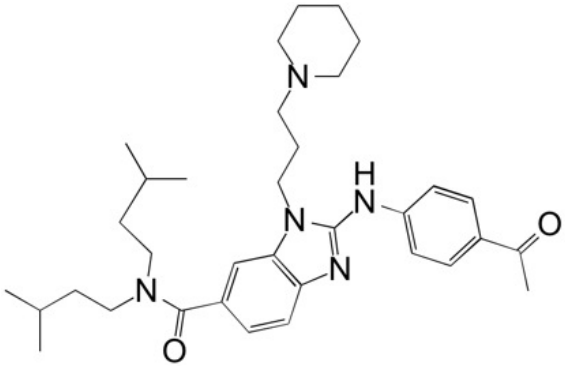

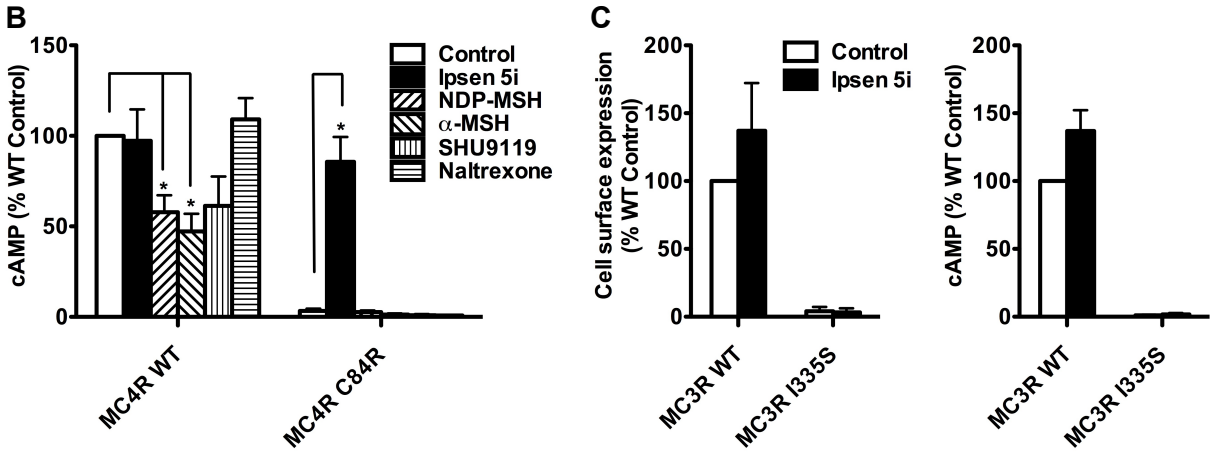

Figure 5.8 Ipsen 5i specifically rescued mutant MC4Rs and the rescue action occurred intracellularly.

(A) Structures of the ligands studied. The peptide ligands NDP-MSH and α-MSH are agonists of

MC4R whereas SHU9119 is an MC4R antagonist. Naltrexone is a small molecule antagonist of opioid receptor. Ipsen 5i is a small molecule antagonist of MC4R. (B) Neuro2a cells transiently expressing WT or C84R MC4R were treated with different ligands for 24 h (10^{-5} M NDP-MSH, α-MSH, SHU9119 or naltrexone or 10^{-6} M Ipsen 5i). Cells were washed twice and then stimulated with 10^{-6} M NDP-MSH for 1 h and intracellular cAMP concentrations were measured. (C) Neuro2a cells transiently expressing WT or I335S MC3Rs were treated with 10^{-6} M Ipsen 5i for 24 h. Then the cell surface expression and intracellular cAMP production of MC3Rs were measured. Results are shown as mean ± S.E.M. of at least three independent experiments. *Significantly different from the DMSO-treated control group, $p < 0.05$.

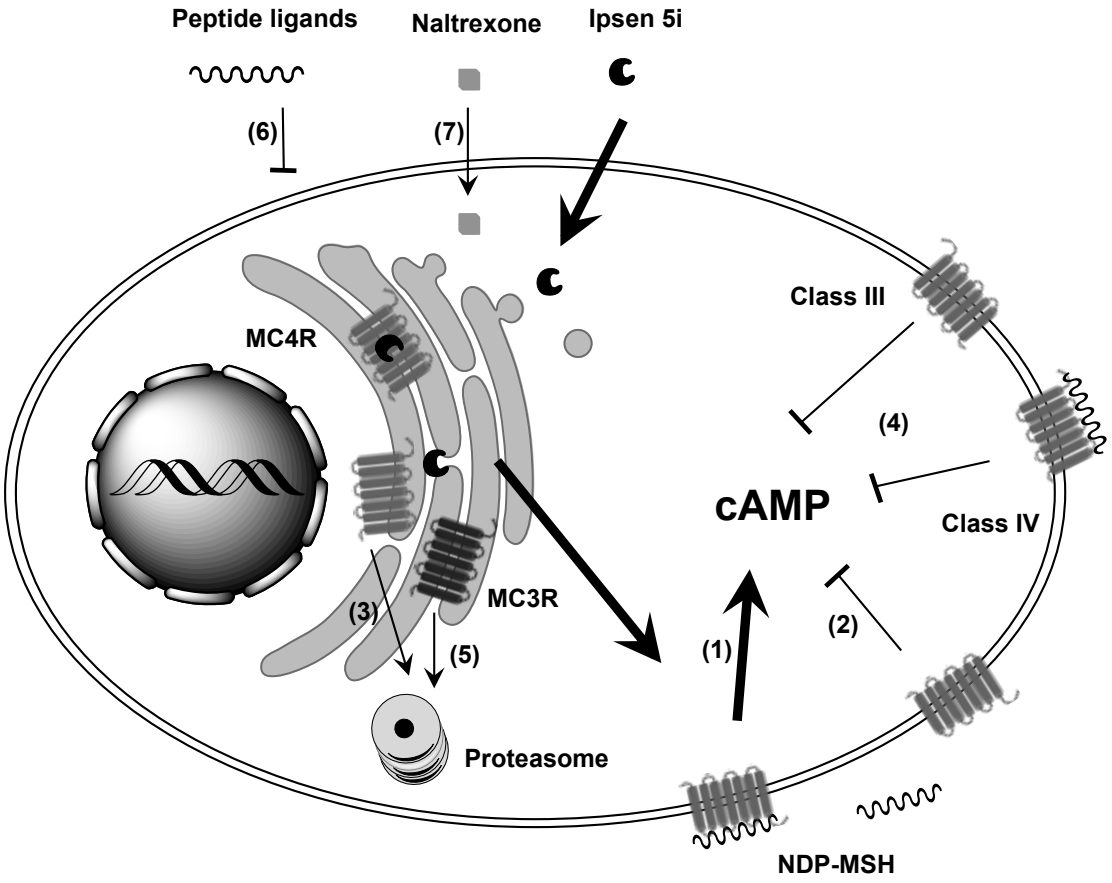

Figure 5.9 Overview of the mechanism of Ipsen 5i specifically rescuing intracellularly retained mutant MC4Rs.

Intracellularly retained mutant MC4Rs were stabilized by Ipsen 5i to pass the scrutiny of the ER quality control system and to be targeted to the cell surface. Most of the rescued mutants were functional (1) whereas some were not (2). Ipsen 5i could not rescue certain intracellularly retained mutant MC4Rs (3). Ipsen 5i did not rescue mutant MC4Rs with ligand binding or signaling defects (4) or an intracellularly retained MC3R mutant (5). Cell impermeable peptide ligands of MC4R (6) or cell permeable ligand of δ opioid receptor (7) could not rescue intracellularly retained C84R MC4R.

Chapter 6 The effect of THIQ on the cell surface expression and function of intracellularly retained melanocortin-4 receptor mutants

6.1 Introduction

The melanocortin-4 receptor (MC4R) predominantly expressed in the CNS plays a crucial role in regulating food intake and energy expenditure (Gantz et al., 1993; Huszar et al., 1997). The MC4R is activated by α/β-melanocyte-stimulating hormone (MSH) from pro-opiomelanocortin neurons and inhibited by agouti-related peptide from agouti-related peptide neurons in the hypothalamic arcuate nucleus. Activation of the MC4R activates heterotrimeric stimulatory G protein, which subsequently activates adenylyl cyclase to produce cAMP.

Extensive functional studies of MC4R mutants identified from obese patients suggest that most of the dysfunctional mutants are misfolded and retained intracellularly by the cellular quality control system rather than being transported to the cell surface (Hinney et al., 2013; Tao, 2005). These mutants are dysfunctional mainly due to mislocalization. Several studies have been performed to correct the localization of misfolded MC4Rs using heat shock cognate protein 70 (Meimaridou et al., 2011), 4-phenyl butyric acid (Granell et al., 2010), and several nonpeptide MC4R antagonists as pharmacological chaperones (pharmacoperones) (Fan and Tao, 2009; Rene et al., 2010; Tao, 2010; Ward et al., 2012). A most recent study using co-expression of endoplasmic reticulum-targeted α-MSH with I316S MC4R also promoted the cell surface expression of this mutant (Granell et al., 2013). In these studies, most of the intracellularly

retained MC4Rs became functional when corrected to the cell surface.

Pharmacoperones have been considered as an alternative to gene therapy and a potential treatment for G protein-coupled receptor (GPCR) misfolded diseases. A number of antagonists and/or some agonists have been developed as pharmacoperones for many GPCRs, such as antagonists and agonists for adenosine A_1 receptor, V2 arginine vasopressin receptor (AVPR2), δ-, κ-, and μ-opioid receptor, antagonists for glucagon receptor, gonadotropin releasing hormone receptor, and rhodopsin, and allosteric ligands for calcium-sensing receptor and luteinizing hormone receptor (reviewed in (Conn and Ulloa-Aguirre, 2011; Conn et al., 2007; Janovick et al., 2013; Tao and Conn, 2014)). Further studies on pharmacoperones have been successfully extended from in vitro using cell lines to in vivo using animals (Janovick et al., 2013) or in a clinical trial (Bernier et al., 2006).

THIQ is the first selective small molecule (MW, 589) agonist of the MC4R with high affinity (IC_{50}, 1.2 nM) and potency (EC_{50}, 2.1 nM) reported (Sebhat et al., 2002). Several structur-function relationship studies show that THIQ competing with [Nle^4,D-Phe^7]-α-MSH (NDP-MSH) for binding to the MC4R shares common interaction determinants with the endogenous ligands and also possesses several specific interaction determinants (Hogan et al., 2006; Pogozheva et al., 2005; Yang et al., 2009). In the present study, we investigated the effect of THIQ on the cell surface expression and signaling of ten misrouted MC4R mutants (N62S, I69R, P78L, C84R, G98R, Y157S, W174C, P260Q, F261S, and C271Y) and on the signaling of four correctly routed MC4R mutants (Δ88-92, D90N, I102S, and N274S).

6.2 Materials and methods

6.2.1 Materials and plasmids

NDP-MSH was purchased from Peptides International (Louisville, KY). THIQ (N-[(3R)-1,2,3,4-Tetrahydroisoquinolinium-3-ylcarbonyl]-(1R)-1-(4-chlorobenzyl)-2-[4-cyclohexyl-4-(1H-1,2,4-triazol-1-ylmethyl)piperidin-1-yl]-2-oxoethylamine) was purchased from Tocris Bioscience (Ellisville, MO). Dulbecco's modified Eagle's medium, newborn calf serum, fetal bovine serum, and antibiotics were purchased from Invitrogen (Carlsbad, CA). Cell culture plastic wares were purchased from Corning (Corning, NY). Radiolabeled cAMP was iodinated with chloramine T method (Tao et al., 2010). The N-terminal c-myc-tagged WT and mutant human MC4Rs and 3×HA-tagged human MC3Rs subcloned into pcDNA3.1 were previously generated and sequenced (Fan and Tao, 2009; Tao, 2007; Tao and Segaloff, 2003; Tao and Segaloff, 2005; Wang and Tao, 2011).

6.2.3 Cell culture and transfection

Human embryonic kidney (HEK) 293, Neuro2a, and N1E-115 cells (American Type Culture Collection, Manassas, VA) were maintained in DMEM containing 10% newborn calf serum (HEK293 cells) or 10% fetal bovine serum (Neuro2a and N1E-115 cells) in a 5% CO_2-humidified atmosphere at 37 ^{o}C. Approximately 24 h after seeding into 0.1% gelatin-coated dishes, HEK293 cells were transfected using calcium phosphate precipitation method and were then selected using 0.2 mg/ml G418 for stable transfection (Tao and Segaloff, 2003). Neuro2a and N1E-115 cells were transiently transfected using jetPRIME transfection reagent (Polyplus-transfection, New York, NY). Approximately 24 h after plating (HEK293 cells) or transfection (Neuro2a and N1E-115 cells), cells were cultured for an additional 24 h in the presence of 0.1% dimethyl sulphoxide (DMSO) or different concentrations of THIQ at 37 ^{o}C. Cells were then rinsed and used for confocal microscopy, flow cytometry, or cAMP assays.

6.2.4 Confocal microscopy

HEK293 cells stably expressing WT or mutant receptors were plated into poly-D-lysine-coated eight well slides (Biocoat cellware from Falcon, BD Systems, Franklin Lakes, NJ) for 24 h and incubated for another 24 h in the presence of 0.1% DMSO or 10^{-5} M THIQ. On the day of experiment, cells were processed for confocal imaging as previously described (Huang and Tao, 2012). Briefly, cells were rinsed with ice-cold phosphate buffered saline for immunohistochemistry (PBS-IH, 137 mM NaCl, 2.7 mM KCl, 1.4 mM KH_2PO_4, 4.3 mM Na_2HPO_4, pH 7.4) and fixed with 4% paraformaldehyde for 15 min. Nonspecific sites were blocked with 5% bovine serum albumin (BSA) in PBS-IH for 1 h. Cells were incubated with mouse anti-myc 9E10 antibody (Developmental Studies Hybridoma Bank, The University of Iowa, Iowa City, IA) 1:40 diluted in PBS-IH with 0.5% BSA for 1 h. Cells were then extensively rinsed and incubated with goat anti-mouse Alexa Fluor 488-labeled antibody (Invitrogen) 1:2000 diluted in PBS-IH with 0.5% BSA for 1 in the dark. After extensive rinsing, microscope slides were mounted with coverslips using Vectashield mounting media (Vector Laboratories, Burlingame, CA) and dried overnight at 4 ^{o}C. Cells were viewed using a Nikon A1 confocal microscope. All procedures were performed at room temperature unless noted otherwise.

6.2.5 Flow cytometry

HEK293 cells stably or Neuro2A cells transiently expressing WT or mutant receptors were incubated for 24 h in the presence of 0.1% DMSO or different concentrations of THIQ. On the day of experiment, cells were processed for flow cytometry study as previously described (Fan and Tao, 2009). Briefly, cells seeded into six well plates were plated on ice and rinsed once

with ice-cold PBS-IH. Cells were then detached and centrifuged at 500 × g for 5 min. Antibodies used and antibody dilutions were the same as described above for confocal microscopy with the exception that for the study of MC3R expression, cells were incubated with the primary antibody mouse anti-HA.11 (Covance, Princeton, NJ) 1:100 diluted in PBS-IH with 0.5% BSA. Cells were rinsed and analyzed using a C6 Accuri Cytometer (Accuri Cytometers, Ann Arbor, MI). Immunostaining of cells expressing empty vector was taken as the background staining. The cell surface expression level of the mutants was calculated using the following formula: [(mutant - empty vector) / (WT - empty vector) × 100%]. All the procedures were performed at room temperature unless noted otherwise.

6.2.6 cAMP assay

HEK293 cells stably or Neuro2A and N1E-115 cells transiently expressing WT or mutant receptors were incubated for 24 h in the presence of 0.1% DMSO or different concentrations of THIQ. On the day of experiment, cells were processed for intracellular cAMP detection as previously described (Tao and Segaloff, 2003). Briefly, cells were rinsed twice with warm Waymouth's MB752/1 media (Sigma-Aldrich) containing 1 mg/ml BSA (Waymouth/BSA). Cells were pretreated with 0.5 mM isobutylmethylxanthine (Sigma-Aldrich) in Waymouth/BSA for 15 min and then stimulated with 10^{-6} M NDP-MSH for 1 h at 37 ^{o}C in the presence of isobutylmethylxanthine. Intracellular cAMP was extracted by adding 0.5 M percholoric acid containing 180 μg/ml theophylline (Sigma-Aldrich) and measured by RIA. The cAMP concentration of the mutants was calculated using the following formula: [mutant / WT × 100%] (HEK293 cells) or [(mutant - empty vector) / (WT - empty vector) × 100%] (Neuro2a and N1E-115 cells).

6.2.8 Data analysis

Data were calculated as percentage of the DMSO-treated WT receptor and analyzed using Student's t-test performed by GraphPad Prism 4.0 software (San Diego, CA).

6.3 Results

6.3.1 The effect of THIQ on the cell surface expression of intracellularly retained MC4R mutants

To investigate the effect of THIQ on the cell surface expression of intracellularly retained MC4R mutants, we studied ten misrouted MC4R mutants with decreased cell surface expression (N62S, I69R, P78L, C84R, G98R, Y157S, W174C, P260Q, F261S, and C271Y) (Fan and Tao, 2009; Tao and Segaloff, 2003; Wang and Tao, 2011). HEK293 cells stably transfected with WT or mutant MC4Rs were treated with 10^{-5} M THIQ for 24 h and then immunostained at non-permeabilized status for confocal microscopy (Figure 6.1A) and flow cytometry study (Figure 6.1B). Our results showed that THIQ treatment obviously decreased the signal intensity of WT MC4R by approximately 50% whereas increased that of three mutants (N62S, C84R, and C271Y) in HEK293 cells. THIQ had no obvious effect on the signal intensity of other mutants.

Considering that the MC4R is mainly distributed in the CNS, we further quantitated the effect of THIQ on the cell surface expression of WT and mutant MC4Rs using a neuronal cell line, Neuro2a. Neuro2a cells transiently transfected with the WT or mutant MC4Rs were treated with 10^{-5} M THIQ for 24 h. Unexpectedly, as shown in Figure 6.2, THIQ did not decrease the cell surface expression of WT MC4R in Neuro2a cells. THIQ significantly increased the cell surface expression of seven mutants, including three that of which were also increased in

HEK293 cells (N62S, C84R, and C271Y) and four that of which were not (I69R, P78L, W174C, and P260Q).

6.3.2 The effect of THIQ on the signaling of intracellularly retained MC4R mutants

To investigate the effect of THIQ on the signaling of intracellularly retained MC4R mutants, different cell lines (HEK293, Neuro2a, and N1E-115 cells) were used. HEK293 cells stably transfected with the WT or mutant MC4Rs were treated with 10^{-5} M THIQ for 24 h. Cells were washed twice and stimulated by 10^{-6} M NDP-MSH for 1 h and then the intracellular cAMP concentration was measured. As shown in Figure 6.3, THIQ decreased the cAMP production of WT MC4R by approximately 30%. THIQ significantly increased the cell surface expression of four mutants (N62S, P78L, C84R, and P260Q) and decreased that of one mutant (F261S) in HEK293 cells.

In Neuro2a cells transiently transfected with the WT or mutant MC4Rs, THIQ began to significantly decrease the cAMP production of WT MC4R at 10^{-8} M and decreased that by approximately 50% at 10^{-5} M (Figure 6.4A). THIQ dose-dependently increased the cAMP production of the mutants with different potencies for different mutants. At 10^{-5} M, THIQ significantly increased the cAMP production of six mutants (N62S, P78L, C84R, W174C, P260Q, and C271Y) (Figure 6.4B). In N1E-115 cells, 10^{-5} M THIQ significantly increased the signaling of the six mutants that were also rescued in Neuro2a cells and one more mutant (I69R) that had a trend to increase but not statistically significant in cAMP production in Neuro2a cells (Figure 6.4C).

6.3.3 The effect of THIQ on the signaling of MC4R mutants with other defects and on one intracellularly retained MC3R mutant

We also studied the effect of THIQ on four correctly routed MC4R mutants with ligand binding, signaling, or no defects (Δ88-92, D90N, I102S, and N274S) (Biebermann et al., 2003; Donohoue et al., 2003; Tao and Segaloff, 2003; Tao and Segaloff, 2005). As shown in Figure 6.4B and Figure 6.4C in Neuro2a or N1E-115 cells, respectively, 10^{-5} M THIQ did not increase the signaling of the four mutants.

To investigate whether THIQ also rescued misrouted MC3R mutants, we studied one intracellularly retained MC3R mutant, I335S. 10^{-5} M THIQ did not increase the cell surface expression (Figure 6.5A) or signaling (Figure 6.5B) of I335S MC3R whereas decreased the signaling of WT MC3R by approximately 50%.

6.4 Discussion

Although mutations in the *MC4R* are the most common cause of monogenic form of obesity (Farooqi et al., 2003), we still have no effective therapeutics specific for obese patients harboring these mutations. One approach is to develop MC4R pharmacoperones. Several antagonists have been identified as pharmacoperones for the MC4R and, to our knowledge, no agonist has been reported acting as a pharmacoperone for the MC4R (Fan and Tao, 2009; Rene et al., 2010; Tao, 2010; Ward et al., 2012). In the present study, we investigated the effect of a small molecule agonist of the MC4R, THIQ, on the cell surface expression and signaling of ten misrouted MC4R mutants (N62S, I69R, P78L, C84R, G98R, Y157S, W174C, P260Q, F261S, and C271Y) using different cell lines.

THIQ significantly decreased the cell surface expression and signaling of WT MC4R in

HEK293 cells. Several studies reported that agonists dose-dependently induced MC4R internalization and that nonpeptide agonists induced less internalization than peptide agonists did (Gao et al., 2003; Nickolls et al., 2005; Shinyama et al., 2003). However, other studies suggested that the MC4R underwent constitutive internalization and that α-MSH reduced the cell surface expression of the MC4R by blocking the recycling of internalized receptor rather than by increasing its endocytosis rate (McDaniel et al., 2012; Mohammad et al., 2007). THIQ-mediated desensitization, internalization, or inhibited recycling of the MC4R probably accounted for the reduced cell surface expression and signaling of WT MC4R.

THIQ significantly increased the cell surface expression of three mutants (N62S, C84R, and C271Y) and increased the signaling of two of them (N62S and C84R) in HEK293 cells (Table 6.1). The increased amount of the MC4R was a result of the dynamic equilibrium with mutants being stabilized and chaperoned to the plasma membrane and internalized to the cytoplasm. The result suggests that, as illustrated in Figure 6.5C, THIQ acted as a pharmacoperone of the MC4R stabilizing the conformation of intracellularly retained mutants and increasing the plasma membrane targeting and/or signaling of these mutants.

THIQ did not significantly increase the cell surface expression of the other seven mutants (I69R, P78L, G98R, Y157S, W174C, P260Q, and F261S) but increased the signaling of two of them (P78L and P260Q) in HEK293 cells (Table 6.1). The increase of the signaling of P78L and P260Q was probably due to signal amplification that a small increase in the cell surface expression induced a large increase in the signaling or due to improved signaling efficacy of the mutants at the cell surface as observed in calcium-sensing receptor (Rus et al., 2008). It was also possible that residual THIQ induced intracellular signaling. Recently, in addition to the canonical signaling at the plasma membrane, intracellular signaling in the endoplasmic reticulum, Golgi

apparatus, or the endosome has also been observed in several GPCRs, such as the β_2-adrenoceptor (Irannejad et al., 2013). Similar observation on the AVPR2 was also reported that three nonpeptide AVPR2 agonists activated AVPR2 mutants intracellularly and such activation did not induce degradation (Robben et al., 2009). Further studies need to be performed to determine the mechanism of THIQ activating MC4R mutants without increasing their cell surface expression.

Interestingly, THIQ did not decrease the cell surface expression of WT MC4R but decreased its signaling in neuronal cells (Table 6.1). For all the experiments, cells were treated with THIQ for 24 h and therefore it was less possible that THIQ only induced desensitization but not internalization of the MC4R in neuronal cells. It was more possible that the forward trafficking rate of the MC4R chaperoned with THIQ (pharmacoperone effect) was more efficient than THIQ-induced internalization or THIQ-blocked recycling (agonist effect), resulting a non-changed receptor amount at the plasma membrane in neuronal cells. Although the total receptor amount was not decreased, the receptor became desensitized upon prolonged agonist exposure, resulting in reduced signaling. However, we have not observed such a different rescuing efficiency of antagonists as pharmacoperones of the MC4R in HEK293 and neuronal cells (data unpublished).

THIQ rescued the cell surface expression and signaling of seven mutants (N62S, I69R, P78L, C84R, W174C, P260Q, and C271Y) in neuronal cells (Table 6.1), which also demonstrated a more efficient pharmacoperone action of THIQ in neuronal cells than in HEK293 cells. The rescuing efficacy of THIQ was varied for different mutants studied herein. Interestingly, G98R, the expression of which was rescued by two MC4R antagonists ((Tao, 2010) and data unpublished), was not rescued by THIQ.

THIQ did not restore the signaling of MC4R mutants with ligand binding or signaling defects. THIQ, sharing the binding pocket with MC4R endogenous ligands, is an orthosteric ligand of the MC4R. To rescue mutants defective in ligand binding or signaling, allosteric ligands are better candidates. THIQ has low affinity with the MC3R (IC_{50}, 634-fold over that of the MC4R) (Sebhat et al., 2002). In out study, THIQ treatment decreased the signaling of WT MC3R by approximately 50%. Although THIQ did not correct the cell surface expression or signaling of I335S MC3R, it could not be excluded that THIQ might be able to rescue other misrouted MC3R mutants.

In summary, our results demonstrated that THIQ was a pharmacoperone of the MC4R rescuing the cell surface expression and signaling of intracellularly retained MC4Rs. THIQ also increased the signaling of two mutants (P78L and P260Q) without increasing their cell surface expression, implying that THIQ might activate the MC4R intracellularly. To our knowledge, THIQ was the first agonist identified as a pharmacoperone of the MC4R.

Table 6.1 Summary of the effect of THIQ on the cell surface expression and signaling of WT and mutant MC4Rs.

	HEK293 cells		Neuronal cells	
Mutants	**Expression**	**Function**	**Expression**	**Function**
WT	↓	↓	–	↓
N62S	↑	↑	↑	↑
I69R	–	–	↑	↑
P78L	–	↑	↑	↑
C84R	↑	↑	↑	↑
G98R	–	–	–	–
Y157S	–	–	–	–
W174C	–	–	↑	↑
P260Q	–	↑	↑	↑
F261S	–	↓	–	–
C271Y	↑	–	↑	↑

"↑", increasing; "↓", decreasing; "–", no significant effect.

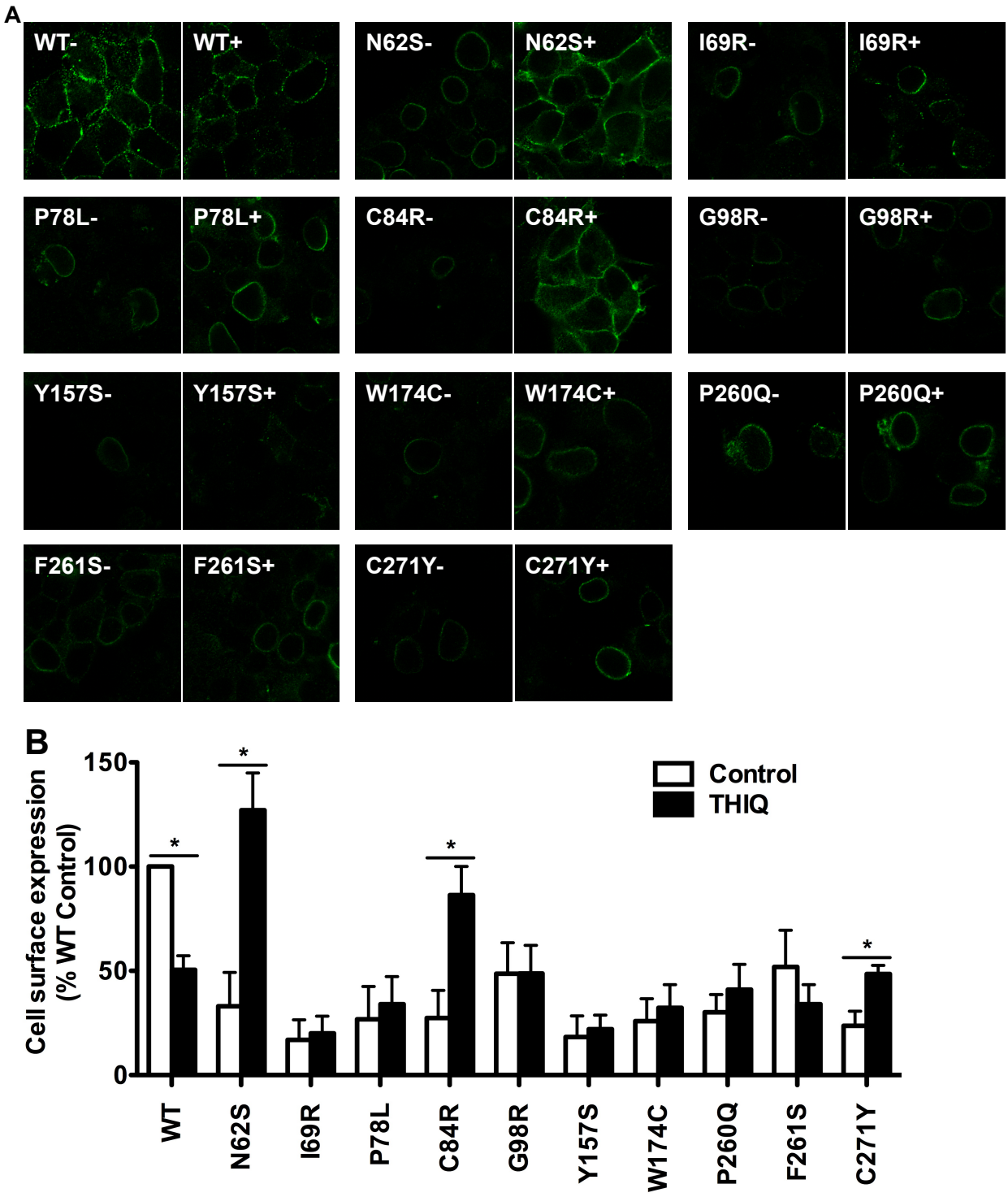

Figure 6.1 Effect of THIQ on the cell surface expression of MC4R mutants in HEK293 cells.

HEK293 cells stably transfected with WT or mutant MC4Rs were incubated with 10^{-5} M THIQ

for 24 h. Cells were then processed for cell surface immunofluorescent detection of myc-MC4R using a Nikon A1 confocal microscope (A) or a C6 Accuri Cytometer (B). (A) Experiments were done at least twice. (B) Data are shown as percentage of DMSO-treated WT MC4R after correcting the background staining from cells transfected with the empty vector. Quantification was done from at least three independent experiments and shown as mean ± S.E.M.. *Significantly different from the DMSO-treated control group, $p < 0.05$.

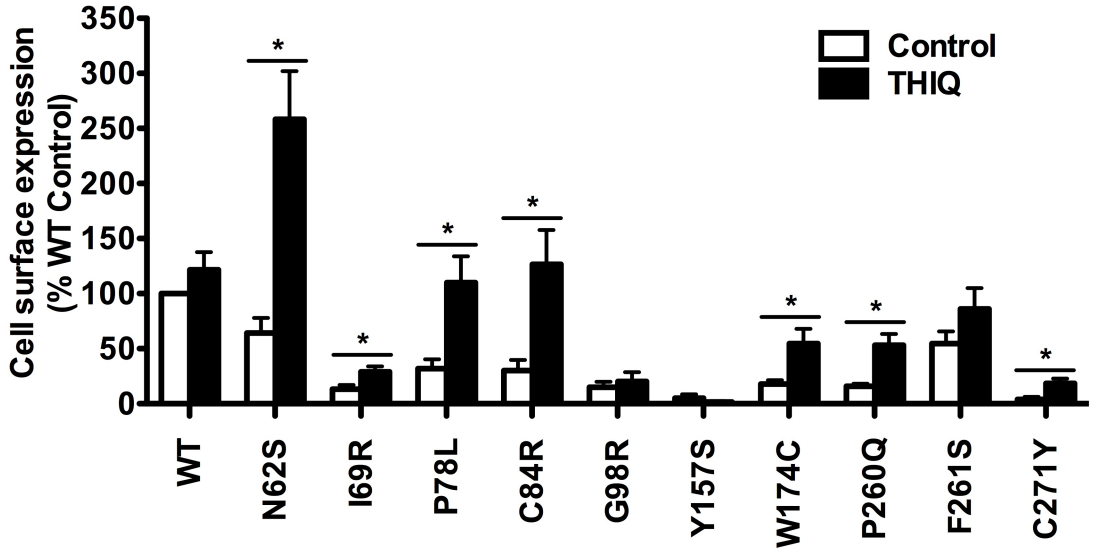

Figure 6.2 Effect of THIQ on the cell surface expression of MC4R mutants in Neuro2a cells.

Neuro2a cells transiently transfected with WT or mutant MC4Rs were incubated with 10^{-5} M THIQ for 24 h. Quantification was done from at least three independent experiments and shown as mean ± S.E.M.. See the legend to Figure 6.1 for details.

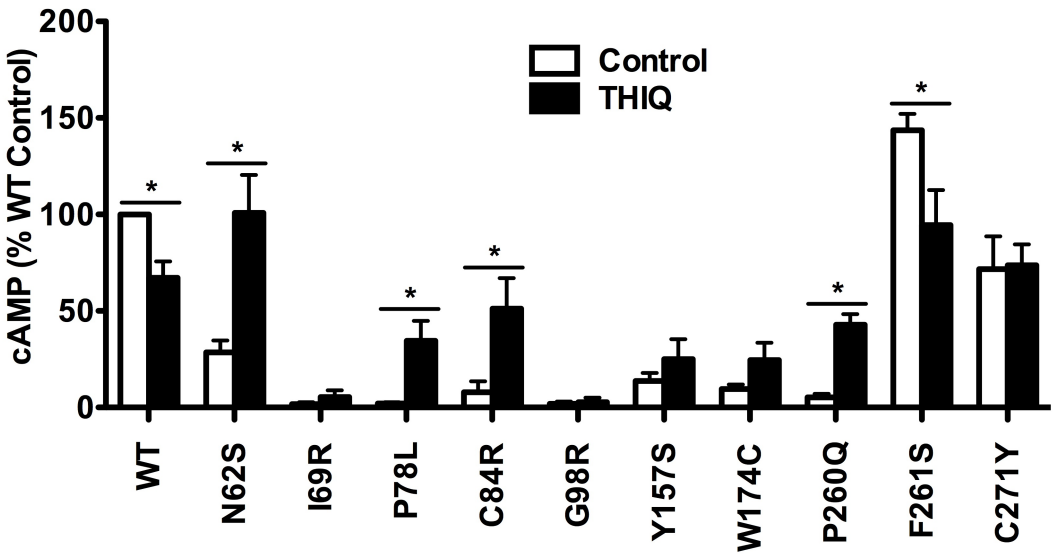

Figure 6.3 Effect of THIQ on the signaling of MC4R mutants in HEK293 cells.

HEK293 cells stably transfected with WT or mutant MC4Rs were incubated with 10^{-5} M THIQ for 24 h. Cells were rinsed twice before stimulated by 10^{-6} M NDP-MSH for 1 h. Intracellular cAMP concentrations were measured by RIA. Data are shown as percentage of DMSO-treated WT MC4R. Quantification was done from at least three independent experiments and shown as mean ± S.E.M.. *Significantly different from the DMSO-treated control group, $p < 0.05$.

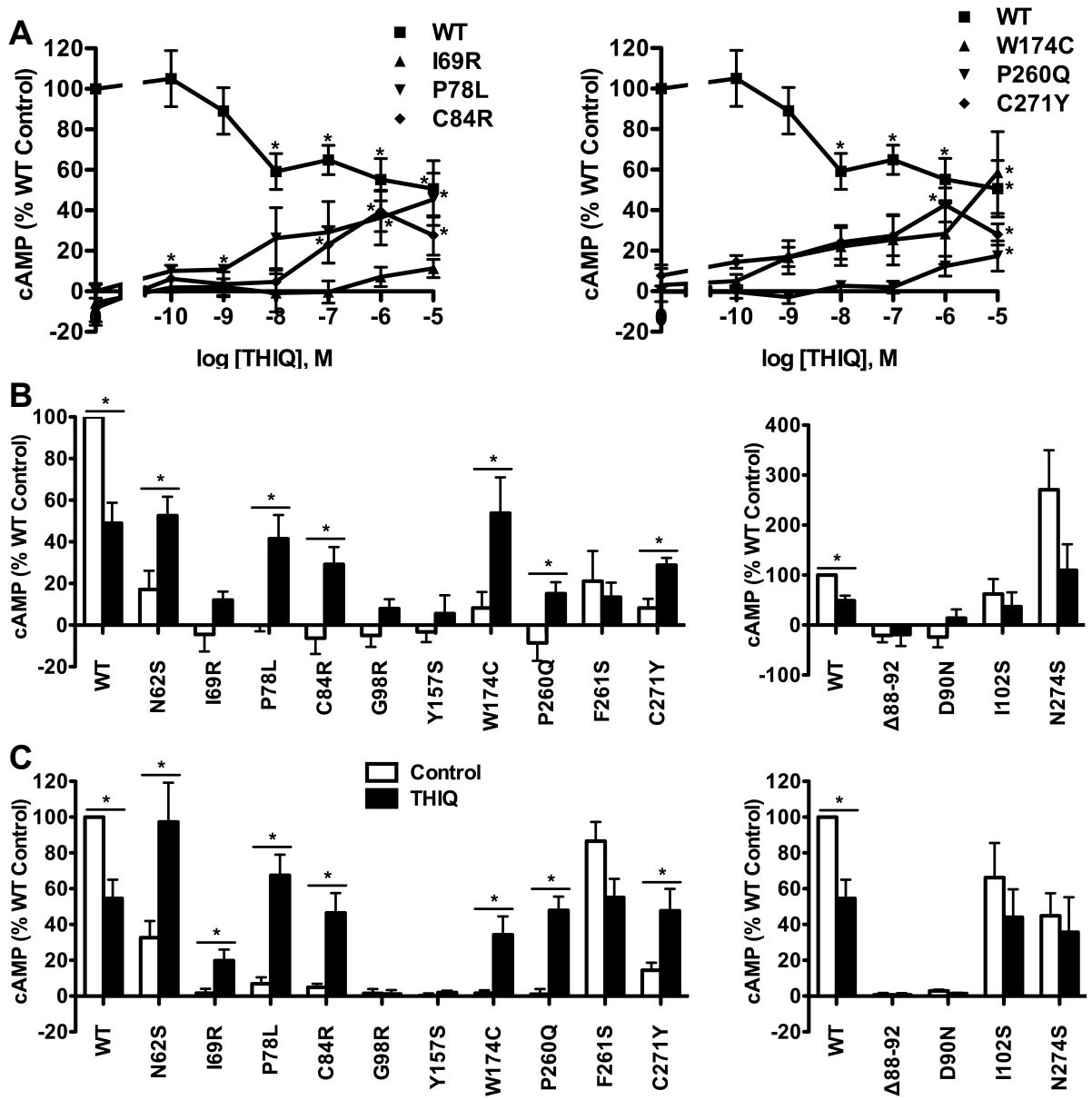

Figure 6.4 Effect of THIQ on the signaling of MC4R mutants in neuronal cells.

Neuro2a cells (A and B) and N1E-115 cells (C) transiently transfected with WT or mutant MC4Rs were incubated with different concentrations of (A) or 10^{-5} M THIQ (B and C) for 24 h. Data are shown as percentage of DMSO-treated WT MC4R after correcting the cAMP production from cells transfected with the empty vector. Quantification was done from at least

three independent experiments and shown as mean ± S.E.M.. See the legend to Figure 6.3 for details.

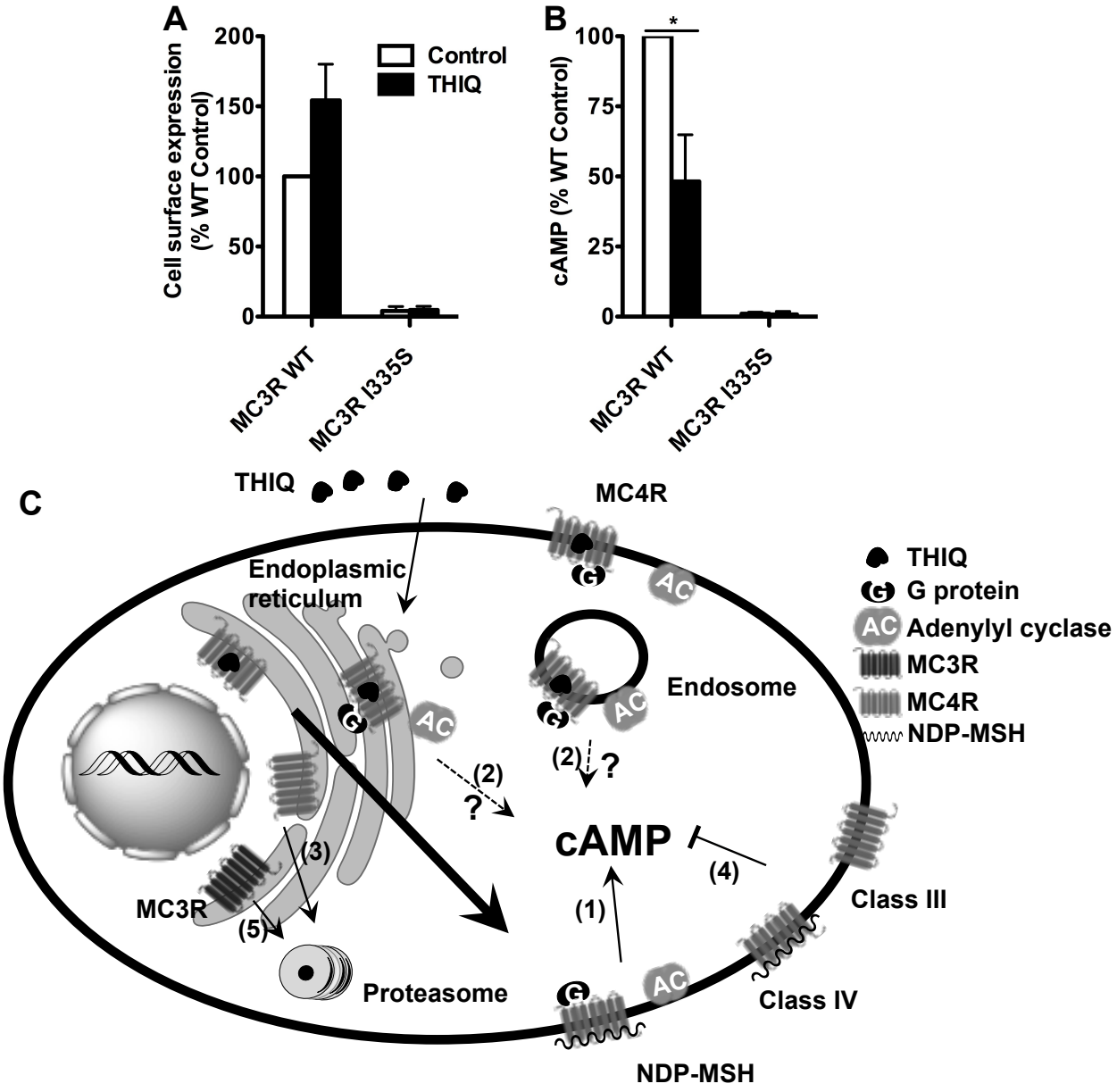

Figure 6.5 Effect of THIQ on the cell surface expression and signaling of the MC3R (A) and model of the effect of THIQ on the MC4R and the MC3R (B).

(A) Neuro2a cells transiently transfected with WT or I335S MC3Rs were treated with 10^{-5} M THIQ for 24 h. The cell surface immunofluorescence of 3×HA-MC3R and intracellular cAMP production were measured. Data are shown as percentage of DMSO-treated WT MC3R after

correcting the background staining or the cAMP production from cells transfected with the empty vector. Quantification was done from at least three independent experiments and shown as mean ± S.E.M.. *Significantly different from the DMSO-treated control group, $p < 0.05$. (B) Model of the effect of THIQ on the MC4R and the MC3R. THIQ stabilized the conformation of intracellularly retained MC4R mutants and coaxed them to the cell surface. The rescued mutants were functional in cAMP production (1). THIQ rescued the function of some mutants without increasing their cell surface expression in HEK293 cells possibly by increasing their cell surface expression that was not detected (1) or inducing intracellular signaling by residue THIQ that was not washed away (2). THIQ did not rescue some MC4R mutants (3). THIQ did not rescue the signaling of MC4R mutants defective in ligand binding (Class III) or signaling (Class IV) (4). THIQ did not rescue one MC3R intracellularly retained mutant (5).

Conclusions

In conclusion, firstly, we have performed comprehensive functional study of the TM6 of the MC4R. We showed that two residues (L250 and P260) were important for the MC4R cell surface expression, five residues (F254, F261, H264, L265, and Y268) were required for α- and β-MSH binding, and six residues (T246, L247, I251, G252, W258, and F262) were important for the cAMP signaling. Nine mutants were defective in basal cAMP signaling. Seven mutants were constitutively active in the cAMP signaling that could be partially inhibited by two MC4R inverse agonists, Ipsen 5i and ML00253764. Five mutants were also constitutively active in the MAP kinase signaling with enhanced basal ERK1/2 phosphorylation.

Secondly, we have performed detailed functional studies on nine MC4R mutants (G55V, R165G, R165W, R165Q, C172R, F202L, M208V, I269N, and A303P) that were identified from Pima Indian heritage and Hispanic heritage. We showed that six mutants (R165G, R165W, R165Q, C172R, I269N, and A303P) were completely or partially loss of cell surface expression, two mutants (G55V and M208V) were defective in ligand binding and signaling, and one mutant (F202L) was functioning normally. Three mutants (G55V, C172R, and M208V) were impaired in basal cAMP signaling whereas one mutant (A303P) was constitutively active with increased basal cAMP signaling.

Finally, we investigated whether three small molecule ligands of the MC4R, including two antagonists (Ipsen 5i and ML00253764) and one agonist (THIQ), could act as

pharmacoperones, rescuing the cell surface expression and signaling of intracellularly retained MC4R mutants. We studied eleven intracellularly retained MC4R mutants (S58C, N62S, I69R, P78L, C84R, G98R, Y157S, W174C, P260Q, F261S, and C271Y) using different cell lines. We showed that ML00253764 rescued the cell surface expression and function of five mutants (N62S, C84R, Y157S, W174C, and C271Y) in HEK293 cells. Two mutants (S58C and G98R) were rescued to the cell surface but did not respond to NDP-MSH stimulation. The other four mutants were not rescued by ML00253764. We obtained similar results from neuronal cells with the exception of Y157S, which could not be rescued in neuronal cells.

When using Ipsen 5i to treat cells, we showed that Ipsen 5i rescued the cell surface expression of all the eleven mutants studied herein and seven (N62S, I69R, P78L, C84R, W174C, P260Q, and C271Y) were functional in cAMP production. Three mutants (S58C, G98R, and F261S) had increased cell surface expression but not signaling. Y157S was rescued in HEK293 cells but not in neuronal cells whereas results obtained for other mutants were consistent between different cell lines.

When using THIQ to treat cells, we showed that THIQ increased the cell surface expression of three mutants (N62S, C84R, and C271Y) and two of them (N62S and C84R) had increased signaling in HEK293 cells. Interestingly, THIQ increased the signaling of two other mutants (P78L and P260Q) without increasing their cell surface expression in HEK293 cells. In neuronal cells, THIQ exhibited a more potent effect, correcting the cell surface expression and signaling of seven mutants (N62S, I69R, P78L, C84R, W174C, P260Q, and C271Y). Other mutants were not rescued by THIQ.

We also showed that the three small molecule ligands had no effect on the signaling of MC4R mutants defective in ligand binding or signaling or with no obvious defect (Δ88-92,

D90N, I102S, and N274S) or on one of intracellularly retained MC3R mutants (I335S).

References

Abbott, C.R., M. Rossi, M. Kim, S.H. AlAhmed, G.M. Taylor, M.A. Ghatei, D.M. Smith, and S.R. Bloom. 2000. Investigation of the melanocyte stimulating hormones on food intake. Lack of evidence to support a role for the melanocortin-3-receptor. *Brain Res*. 869:203-210.

Abell, A.N., and D.L. Segaloff. 1997. Evidence for the direct involvement of transmembrane region six of the lutropin/choriogonadotropin receptor in activating G_s. *J Biol Chem*. 272:14586-14591.

Adan, R.A., M. van der Kraan, R.P. Doornbos, P.R. Bar, J.P. Burbach, and W.H. Gispen. 1996. Melanocortin receptors mediate α-MSH-induced stimulation of neurite outgrowth in neuro 2A cells. *Mol Brain Res*. 36:37-44.

Akingbemi, B.T. 2013. Adiponectin receptors in energy homeostasis and obesity pathogenesis. *Prog Mol Biol Transl Sci*. 114:317-342.

Angelova, K., F. Fanelli, and D. Puett. 2002. A model for constitutive lutropin receptor activation based on molecular simulation and engineered mutations in transmembrane helices 6 and 7. *J Biol Chem*. 277:32202-32213.

Antal-Zimanyi, I., and X. Khawaja. 2009. The role of melanin-concentrating hormone in energy homeostasis and mood disorders. *J Mol Neurosci*. 39:86-98.

Arakawa, T., D. Ejima, Y. Kita, and K. Tsumoto. 2006. Small molecule pharmacological chaperones: from thermodynamic stabilization to pharmaceutical drugs. *Biochim Biophys Acta*. 1764:1677-1687.

Babcock, J.J., and M. Li. 2013. Inside job: ligand-receptor pharmacology beneath the plasma membrane. *Acta Pharmacol Sin*. 34:859-869.

Ballesteros, J.A., A.D. Jensen, G. Liapakis, S.G. Rasmussen, L. Shi, U. Gether, and J.A. Javitch. 2001. Activation of the β_2-adrenergic receptor involves disruption of an ionic lock between the cytoplasmic ends of transmembrane segments 3 and 6. *J Biol Chem*. 276:29171-29177.

Ballesteros, J.A., and H. Weinstein. 1995. Integrated methods for the construction of three-dimensional models and computational probing of structure-function relations in G protein-coupled receptors. *Method Neurosci*. 25:366-428.

Balthasar, N., L.T. Dalgaard, C.E. Lee, J. Yu, H. Funahashi, T. Williams, M. Ferreira, V. Tang, R.A. McGovern, C.D. Kenny, L.M. Christiansen, E. Edelstein, B. Choi, O. Boss, C. Aschkenasi, C.Y. Zhang, K. Mountjoy, T. Kishi, J.K. Elmquist, and B.B. Lowell. 2005. Divergence of melanocortin pathways in the control of food intake and energy expenditure. *Cell*. 123:493-505.

Benned-Jensen, T., J. Mokrosinski, and M.M. Rosenkilde. 2011. The E92K melanocortin 1 receptor mutant induces cAMP production and arrestin recruitment but not ERK activity indicating biased constitutive signaling. *PLoS One*. 6:e24644.

Bernier, V., D.G. Bichet, and M. Bouvier. 2004a. Pharmacological chaperone action on G-protein-coupled receptors. *Curr Opin Pharmacol*. 4:528-533.

Bernier, V., M. Lagace, M. Lonergan, M.F. Arthus, D.G. Bichet, and M. Bouvier. 2004b. Functional rescue of the constitutively internalized V2 vasopressin receptor mutant R137H by the pharmacological chaperone action of SR49059. *Mol Endocrinol*. 18:2074-2084.

Bernier, V., J.P. Morello, A. Zarruk, N. Debrand, A. Salahpour, M. Lonergan, M.F. Arthus, A. Laperriere, R. Brouard, M. Bouvier, and D.G. Bichet. 2006. Pharmacologic chaperones as a potential treatment for X-linked nephrogenic diabetes insipidus. *J Am Soc Nephrol*. 17:232-243.

Biebermann, H., H. Krude, A. Elsner, V. Chubanov, T. Gudermann, and A. Gruters. 2003. Autosomal-dominant mode of inheritance of a melanocortin-4 receptor mutation in a patient with severe early-onset obesity is due to a dominant-negative effect caused by receptor dimerization. *Diabetes*. 52:2984-2988.

Bjarnadottir, T.K., D.E. Gloriam, S.H. Hellstrand, H. Kristiansson, R. Fredriksson, and H.B. Schioth. 2006. Comprehensive repertoire and phylogenetic analysis of the G protein-coupled receptors in human and mouse. *Genomics*. 88:263-273.

Bloemer, J., S. Bhattacharya, R. Amin, and V. Suppiramaniam. 2014. Impaired insulin signaling and mechanisms of memory loss. *Prog Mol Biol Transl Sci*. 121:413-449.

Bockaert, J., and J.P. Pin. 1999. Molecular tinkering of G protein-coupled receptors: an evolutionary success. *EMBO J*. 18:1723-1729.

Breit, A., T.R. Buch, I. Boekhoff, H.J. Solinski, E. Damm, and T. Gudermann. 2011. Alternative G protein coupling and biased agonism: new insights into melanocortin-4 receptor signalling. *Mol Cell Endocrinol*. 331:232-240.

Broom, D.C., E.M. Jutkiewicz, K.C. Rice, J.R. Traynor, and J.H. Woods. 2002. Behavioral effects of δ-opioid receptor agonists: potential antidepressants? *Jpn J Pharmacol*. 90:1-6.

Buch, T.R., D. Heling, E. Damm, T. Gudermann, and A. Breit. 2009. Pertussis toxin-sensitive signaling of melanocortin-4 receptors in hypothalamic GT1-7 cells defines agouti-related protein as a biased agonist. *J Biol Chem*. 284:26411-26420.

Bykov, V.J., N. Issaeva, A. Shilov, M. Hultcrantz, E. Pugacheva, P. Chumakov, J. Bergman, K.G. Wiman, and G. Selivanova. 2002. Restoration of the tumor suppressor function to mutant p53 by a low-molecular-weight compound. *Nat Med*. 8:282-288.

Calebiro, D., V.O. Nikolaev, M.C. Gagliani, T. de Filippis, C. Dees, C. Tacchetti, L. Persani, and M.J. Lohse. 2009. Persistent cAMP-signals triggered by internalized G-protein-coupled receptors. *PLoS Biol*. 7:e1000172.

Calebiro, D., V.O. Nikolaev, and M.J. Lohse. 2010. Imaging of persistent cAMP signaling by internalized G protein-coupled receptors. *J Mol Endocrinol*. 45:1-8.

Chai, B., J.Y. Li, W. Zhang, E. Newman, J. Ammori, and M.W. Mulholland. 2006. Melanocortin-4 receptor-mediated inhibition of apoptosis in immortalized hypothalamic neurons via mitogen-activated protein kinase. *Peptides*. 27:2846-2857.

Chan, L.F., T.R. Webb, T.T. Chung, E. Meimaridou, S.N. Cooray, L. Guasti, J.P. Chapple, M. Egertová, M.R. Elphick, M.E. Cheetham, L.A. Metherell, and A.J.L. Clark. 2009. MRAP and MRAP2 are bidirectional regulators of the melanocortin receptor family. *Proc Natl Acad Sci U S A*. 106:6146-6151.

Chaudhuri, T.K., and S. Paul. 2006. Protein-misfolding diseases and chaperone-based therapeutic approaches. *FEBS J*. 273:1331-1349.

Chen, C., W. Jiang, F. Tucci, J.A. Tran, B.A. Fleck, S.R. Hoare, M. Joppa, S. Markison, J. Wen, Y. Sai, M. Johns, A. Madan, T. Chen, C.W. Chen, D. Marinkovic, M. Arellano, J. Saunders, and A.C. Foster. 2007a. Discovery of 1-[2-[(1S)-(3-dimethylaminopropionyl)amino-2-methylpropyl]-4-methylphenyl] -4-[(2R)-methyl-3-(4-chlorophenyl)-propionyl]piperazine as an orally active antagonist of the melanocortin-4 receptor for the potential treatment of cachexia. *J Med Chem*. 50:5249-5252.

Chen, M., M. Cai, C.J. Aprahamian, K.E. Georgeson, V. Hruby, C.M. Harmon, and Y. Yang. 2007b. Contribution of the conserved amino acids of the melanocortin-4 receptor in D-[Nle^4,Phe^7]-α-melanocyte-stimulating hormone binding and signaling. *J Biol Chem*. 282:21712-21719.

Chen, M., M. Cai, D. McPherson, V. Hruby, C.M. Harmon, and Y. Yang. 2009. Contribution of the transmembrane domain 6 of melanocortin-4 receptor to peptide [Pro^5, DNal (2')^8]-γ-MSH selectivity. *Biochem Pharmacol*. 77:114-124.

Cherezov, V., D.M. Rosenbaum, M.A. Hanson, S.G. Rasmussen, F.S. Thian, T.S. Kobilka, H.J. Choi, P. Kuhn, W.I. Weis, B.K. Kobilka, and R.C. Stevens. 2007. High-resolution crystal structure of an engineered human β_2-adrenergic G protein-coupled receptor. *Science*. 318:1258-1265.

Chien, E.Y., W. Liu, Q. Zhao, V. Katritch, G.W. Han, M.A. Hanson, L. Shi, A.H. Newman, J.A. Javitch, V. Cherezov, and R.C. Stevens. 2010. Structure of the human dopamine D3 receptor in complex with a D2/D3 selective antagonist. *Science*. 330:1091-1095.

Clarke, J.T., D.J. Mahuran, S. Sathe, E.H. Kolodny, B.A. Rigat, J.A. Raiman, and M.B. Tropak. 2011. An open-label Phase I/II clinical trial of pyrimethamine for the treatment of

patients affected with chronic GM2 gangliosidosis (Tay-Sachs or Sandhoff variants). *Mol Genet Metab*. 102:6-12.

Cone, R.D. 2005. Anatomy and regulation of the central melanocortin system. *Nat Neurosci*. 8:571-578.

Cone, R.D. 2006. Studies on the physiological functions of the melanocortin system. *Endocr Rev*. 27:736-749.

Conn, P.J., A. Christopoulos, and C.W. Lindsley. 2009. Allosteric modulators of GPCRs: a novel approach for the treatment of CNS disorders. *Nat Rev Drug Discov*. 8:41-54.

Conn, P.M., and A. Ulloa-Aguirre. 2011. Pharmacological chaperones for misfolded gonadotropin-releasing hormone receptors. *Adv Pharmacol*. 62:109-141.

Conn, P.M., A. Ulloa-Aguirre, J. Ito, and J.A. Janovick. 2007. G protein-coupled receptor trafficking in health and disease: lessons learned to prepare for therapeutic mutant rescue in vivo. *Pharmacol Rev*. 59:225-250.

Czyzyk, T.A., M.A. Sikorski, L. Yang, and G.S. McKnight. 2008. Disruption of the RIIbeta subunit of PKA reverses the obesity syndrome of Agouti lethal yellow mice. *Proc Natl Acad Sci U S A*. 105:276-281.

Davenport, A.P., S.P.H. Alexander, J.L. Sharman, A.J. Pawson, H.E. Benson, A.E. Monaghan, W.C. Liew, C.P. Mpamhanga, T.I. Bonner, R.R. Neubig, J.P. Pin, M. Spedding, and A.J. Harmar. 2013. International Union of Basic and Clinical Pharmacology. LXXXVIII. G protein-coupled receptor List: recommendations for new pairings with cognate ligands. *Pharmacol Rev*. 65:967-986.

DeMaria, E.J. 2007. Bariatric surgery for morbid obesity. *N Engl J Med*. 356:2176-2183.

Donohoue, P.A., Y.X. Tao, M. Collins, G.S.H. Yeo, S. O'Rahilly, and D.L. Segaloff. 2003. Deletion of codons 88-92 of the melanocortin-4 receptor gene: a novel deleterious mutation in an obese female. *J Clin Endocrinol Metab*. 88:5841-5845.

Fan, W., B.A. Boston, R.A. Kesterson, V.J. Hruby, and R.D. Cone. 1997. Role of melanocortinergic neurons in feeding and the agouti obesity syndrome. *Nature*. 385:165-168.

Fan, Z.C., and Y.X. Tao. 2009. Functional characterization and pharmacological rescue of melanocortin-4 receptor mutations identified from obese patients. *J Cell Mol Med*. 13:3268-3282.

Farmakis, D., G. Filippatos, D.T. Kremastinos, and M. Gheorghiade. 2008. Vasopressin and vasopressin antagonists in heart failure and hyponatremia. *Curr Heart Fail Rep*. 5:91-96.

Farooqi, I.S., J.M. Keogh, G.S. Yeo, E.J. Lank, T. Cheetham, and S. O'Rahilly. 2003. Clinical spectrum of obesity and mutations in the melanocortin 4 receptor gene. *N Engl J Med*. 348:1085-1095.

Farooqi, I.S., G.S. Yeo, J.M. Keogh, S. Aminian, S.A. Jebb, G. Butler, T. Cheetham, and S. O'Rahilly. 2000. Dominant and recessive inheritance of morbid obesity associated with melanocortin 4 receptor deficiency. *J Clin Invest*. 106:271-279.

Feinstein, T.N., V.L. Wehbi, J.A. Ardura, D.S. Wheeler, S. Ferrandon, T.J. Gardella, and J.P. Vilardaga. 2011. Retromer terminates the generation of cAMP by internalized PTH receptors. *Nat Chem Biol*. 7:278-284.

Ferrandon, S., T.N. Feinstein, M. Castro, B. Wang, R. Bouley, J.T. Potts, T.J. Gardella, and J.P. Vilardaga. 2009. Sustained cyclic AMP production by parathyroid hormone receptor endocytosis. *Nat Chem Biol*. 5:734-742.

Fleck, B.A., N. Ling, and C. Chen. 2007. Substituted NDP-MSH peptides paired with mutant melanocortin-4 receptors demonstrate the role of transmembrane 6 in receptor activation. *Biochemistry*. 46:10473-10483.

Flegal, K.M., M.D. Carroll, C.L. Ogden, and L.R. Curtin. 2010. Prevalence and trends in obesity among US adults, 1999-2008. *J Am Med Assoc*. 303:235-241.

Foord, S.M., T.I. Bonner, R.R. Neubig, E.M. Rosser, J.P. Pin, A.P. Davenport, M. Spedding, and A.J. Harmar. 2005. International Union of Pharmacology. XLVI. G protein-coupled receptor list. *Pharmacol Rev*. 57:279-288.

Foster, B.A., H.A. Coffey, M.J. Morin, and F. Rastinejad. 1999. Pharmacological rescue of mutant p53 conformation and function. *Science*. 286:2507-2510.

Fredriksson, R., M.C. Lagerstrom, L.G. Lundin, and H.B. Schioth. 2003. The G-protein-coupled receptors in the human genome form five main families. Phylogenetic analysis, paralogon groups, and fingerprints. *Mol Pharmacol*. 63:1256-1272.

Frustaci, A., C. Chimenti, R. Ricci, L. Natale, M.A. Russo, M. Pieroni, C.M. Eng, and R.J. Desnick. 2001. Improvement in cardiac function in the cardiac variant of Fabry's disease with galactose-infusion therapy. *N Engl J Med*. 345:25-32.

Gantz, I., H. Miwa, Y. Konda, Y. Shimoto, T. Tashiro, S.J. Watson, J. DelValle, and T. Yamada. 1993. Molecular cloning, expression, and gene localization of a fourth melanocortin receptor. *J Biol Chem*. 268:15174-15179.

Gao, Z., D. Lei, J. Welch, K. Le, J. Lin, S. Leng, and D. Duhl. 2003. Agonist-dependent internalization of the human melanocortin-4 receptors in human embryonic kidney 293 cells. *J Pharmacol Exp Ther*. 307:870-877.

Germain, D.P., R. Giugliani, D.A. Hughes, A. Mehta, K. Nicholls, L. Barisoni, C.J. Jennette, A. Bragat, J. Castelli, S. Sitaraman, D.J. Lockhart, and P.F. Boudes. 2012. Safety and pharmacodynamic effects of a pharmacological chaperone on α-galactosidase A activity and globotriaosylceramide clearance in Fabry disease: report from two phase 2 clinical studies. *Orphanet J Rare Dis*. 7:91.

Giugliani, R., S. Waldek, D.P. Germain, K. Nicholls, D.G. Bichet, J.K. Simosky, A.C. Bragat, J.P. Castelli, E.R. Benjamin, and P.F. Boudes. 2013. A Phase 2 study of migalastat hydrochloride in females with Fabry disease: selection of population, safety and pharmacodynamic effects. *Mol Genet Metab*. 109:86-92.

Graham, M., J.R. Shutter, U. Sarmiento, I. Sarosi, and K.L. Stark. 1997. Overexpression of Agrt leads to obesity in transgenic mice. *Nat Genet*. 17:273-274.

Granell, S., S. Mohammad, R. Ramanagoudr-Bhojappa, and G. Baldini. 2010. Obesity-linked variants of melanocortin-4 receptor are misfolded in the endoplasmic reticulum and can be rescued to the cell surface by a chemical chaperone. *Mol Endocrinol*. 24:1805-1821.

Granell, S., B.M. Molden, and G. Baldini. 2013. Exposure of MC4R to agonist in the endoplasmic reticulum stabilizes an active conformation of the receptor that does not desensitize. *Proc Natl Acad Sci U S A*. 110:E4733-E4742.

Gregory, K.J., N.E. Hall, A.B. Tobin, P.M. Sexton, and A. Christopoulos. 2010. Identification of orthosteric and allosteric site mutations in M2 muscarinic acetylcholine receptors that contribute to ligand-selective signaling bias. *J Biol Chem*. 285:7459-7474.

Guh, D.P., W. Zhang, N. Bansback, Z. Amarsi, C.L. Birmingham, and A.H. Anis. 2009. The incidence of co-morbidities related to obesity and overweight: a systematic review and meta-analysis. *BMC Public Health*. 9:88.

Hanson, M.A., C.B. Roth, E. Jo, M.T. Griffith, F.L. Scott, G. Reinhart, H. Desale, B. Clemons, S.M. Cahalan, S.C. Schuerer, M.G. Sanna, G.W. Han, P. Kuhn, H. Rosen, and R.C. Stevens. 2012. Crystal structure of a lipid G protein-coupled receptor. *Science*. 335:851-855.

Haskell-Luevano, C., R.D. Cone, E.K. Monck, and Y.P. Wan. 2001. Structure activity studies of the melanocortin-4 receptor by in vitro mutagenesis: identification of agouti-related protein (AGRP), melanocortin agonist and synthetic peptide antagonist interaction determinants. *Biochemistry*. 40:6164-6179.

Haskell-Luevano, C., and E.K. Monck. 2001. Agouti-related protein functions as an inverse agonist at a constitutively active brain melanocortin-4 receptor. *Regul Pept*. 99:1-7.

Hinney, A., A. Schmidt, K. Nottebom, O. Heibult, I. Becker, A. Ziegler, G. Gerber, M. Sina, T. Gorg, H. Mayer, W. Siegfried, M. Fichter, H. Remschmidt, and J. Hebebrand. 1999. Several mutations in the melanocortin-4 receptor gene including a nonsense and a frameshift mutation associated with dominantly inherited obesity in humans. *J Clin Endocrinol Metab*. 84:1483-1486.

Hinney, A., A.L. Volckmar, and N. Knoll. 2013. Melanocortin-4 receptor in energy homeostasis and obesity pathogenesis. *Prog Mol Biol Transl Sci*. 114:147-191.

Hogan, K., S. Peluso, S. Gould, I. Parsons, D. Ryan, L.J. Wu, and I. Visiers. 2006. Mapping the binding site of melanocortin 4 receptor agonists: a hydrophobic pocket formed by I3.28(125), I3.32(129), and I7.42(291) is critical for receptor activation. *J Med Chem*. 49:911-922.

Hohenadel, M.G., M.S. Thearle, B.A. Grice, H. Huang, M.H. Dai, Y.X. Tao, L.A. Hunter, G.I. Palaguachi, Z. Mou, R.C. Kim, M.M. Tsang, K. Haack, V.S. Voruganti, S.A. Cole, N.F.

Butte, A.G. Comuzzie, Y.L. Muller, L.J. Baier, J. Krakoff, W.C. Knowler, J.A. Yanovski, and J.C. Han. 2014. Brain-derived neurotrophic factor in human subjects with function-altering melanocortin-4 receptor variants. *Int J Obes*. DOI: 10.1038/ijo.2013.221.

Huang, H., M.H. Dai, and Y.X. Tao. 2014. Physiology and therapeutics of the free fatty acid receptor GPR40. *Prog Mol Biol Transl Sci*. 121:67-94.

Huang, H., and Y.X. Tao. 2012. Pleiotropic functions of the transmembrane domain 6 of human melanocortin-4 receptor. *J Mol Endocrinol*. 49:237-248.

Huang, Y., and G.E. Breitwieser. 2007. Rescue of calcium-sensing receptor mutants by allosteric modulators reveals a conformational checkpoint in receptor biogenesis. *J Biol Chem*. 282:9517-9525.

Huszar, D., C.A. Lynch, V. Fairchild-Huntress, J.H. Dunmore, Q. Fang, L.R. Berkemeier, W. Gu, R.A. Kesterson, B.A. Boston, R.D. Cone, F.J. Smith, L.A. Campfield, P. Burn, and F. Lee. 1997. Targeted disruption of the melanocortin-4 receptor results in obesity in mice. *Cell*. 88:131-141.

Irannejad, R., J.C. Tomshine, J.R. Tomshine, M. Chevalier, J.P. Mahoney, J. Steyaert, S.G. Rasmussen, R.K. Sunahara, H. El-Samad, B. Huang, and M. von Zastrow. 2013. Conformational biosensors reveal GPCR signalling from endosomes. *Nature*. 495:534-538.

Jaakola, V.P., M.T. Griffith, M.A. Hanson, V. Cherezov, E.Y. Chien, J.R. Lane, A.P. Ijzerman, and R.C. Stevens. 2008. The 2.6 angstrom crystal structure of a human A_{2A} adenosine receptor bound to an antagonist. *Science*. 322:1211-1217.

Janovick, J.A., G. Maya-Nunez, and P.M. Conn. 2002. Rescue of hypogonadotropic hypogonadism-causing and manufactured GnRH receptor mutants by a specific protein-

folding template: misrouted proteins as a novel disease etiology and therapeutic target. *J Clin Endocrinol Metab*. 87:3255-3262.

Janovick, J.A., G. Maya-Nunez, A. Ulloa-Aguirre, I.T. Huhtaniemi, J.A. Dias, P. Verbost, and P.M. Conn. 2009. Increased plasma membrane expression of human follicle-stimulating hormone receptor by a small molecule thienopyr(im)idine. *Mol Cell Endocrinol*. 298:84-88.

Janovick, J.A., M.D. Stewart, D. Jacob, L.D. Martin, J.M. Deng, C.A. Stewart, Y. Wang, A. Cornea, L. Chavali, S. Lopez, S. Mitalipov, E. Kang, H.S. Lee, P.R. Manna, D.M. Stocco, R.R. Behringer, and P.M. Conn. 2013. Restoration of testis function in hypogonadotropic hypogonadal mice harboring a misfolded GnRHR mutant by pharmacoperone drug therapy. *Proc Natl Acad Sci U S A*. 110:21030-21035.

Jaquette, J., and D.L. Segaloff. 1997. Temperature sensitivity of some mutants of the lutropin/choriogonadotropin receptor. *Endocrinology*. 138:85-91.

Jeyaraj, S.C., M.A. Chotani, S. Mitra, H.E. Gregg, N.A. Flavahan, and K.J. Morrison. 2001. Cooling evokes redistribution of α_{2c}-adrenoceptors from golgi to plasma membrane in transfected human embryonic kidney 293 cells. *Mol Pharmacol*. 60:1195-1200.

Jones, B.J., T. Tan, and S.R. Bloom. 2012. Minireview: glucagon in stress and energy homeostasis. *Endocrinology*. 153:1049-1054.

Jong, Y.J., V. Kumar, and K.L. O'Malley. 2009. Intracellular metabotropic glutamate receptor 5 (mGluR5) activates signaling cascades distinct from cell surface counterparts. *J Biol Chem*. 284:35827-35838.

Kelly, T., W. Yang, C.S. Chen, K. Reynolds, and J. He. 2008. Global burden of obesity in 2005 and projections to 2030. *Int J Obes*. 32:1431-1437.

Khanna, R., E.R. Benjamin, L. Pellegrino, A. Schilling, B.A. Rigat, R. Soska, H. Nafar, B.E. Ranes, J. Feng, Y. Lun, A.C. Powe, D.J. Palling, B.A. Wustman, R. Schiffmann, D.J. Mahuran, D.J. Lockhart, and K.J. Valenzano. 2010. The pharmacological chaperone isofagomine increases the activity of the Gaucher disease L444P mutant form of β-glucosidase. *FEBS J*. 277:1618-1638.

Kotowski, S.J., F.W. Hopf, T. Seif, A. Bonci, and M. von Zastrow. 2011. Endocytosis promotes rapid dopaminergic signaling. *Neuron*. 71:278-290.

Kraschnewski, J.L., J. Boan, J. Esposito, N.E. Sherwood, E.B. Lehman, D.K. Kephart, and C.N. Sciamanna. 2010. Long-term weight loss maintenance in the United States. *Int J Obes*. 34:1644-1654.

Krude, H., H. Biebermann, W. Luck, R. Horn, G. Brabant, and A. Gruters. 1998. Severe early-onset obesity, adrenal insufficiency and red hair pigmentation caused by POMC mutations in humans. *Nat Genet*. 19:155-157.

Kumar, V., P.G. Fahey, Y.J. Jong, N. Ramanan, and K.L. O'Malley. 2012. Activation of intracellular metabotropic glutamate receptor 5 in striatal neurons leads to up-regulation of genes associated with sustained synaptic transmission including Arc/Arg3.1 protein. *J Biol Chem*. 287:5412-5425.

Leanos-Miranda, A., A. Ulloa-Aguirre, J.A. Janovick, and P.M. Conn. 2005. In vitro coexpression and pharmacological rescue of mutant gonadotropin-releasing hormone receptors causing hypogonadotropic hypogonadism in humans expressing compound heterozygous alleles. *J Clin Endocrinol Metab*. 90:3001-3008.

Lebon, G., T. Warne, P.C. Edwards, K. Bennett, C.J. Langmead, A.G. Leslie, and C.G. Tate. 2011. Agonist-bound adenosine A_{2A} receptor structures reveal common features of GPCR activation. *Nature*. 474:521-525.

Lefkowitz, R.J. 2013. A brief history of G-protein coupled receptors (Nobel Lecture). *Angew Chem Int Ed Engl*. 52:6366-6378.

Lemmens, V.E., A. Oenema, K.I. Klepp, H.B. Henriksen, and J. Brug. 2008. A systematic review of the evidence regarding efficacy of obesity prevention interventions among adults. *Obes Rev*. 9:446-455.

Lester, H.A., J.M. Miwa, and R. Srinivasan. 2012. Psychiatric drugs bind to classical targets within early exocytotic pathways: therapeutic effects. *Biol Psychiat*. 72:907-915.

Li, Z., Y. Li, and W. Zhang. 2013. Ghrelin receptor in energy homeostasis and obesity pathogenesis. *Prog Mol Biol Transl Sci*. 114:45-87.

Lieberman, R.L., B.A. Wustman, P. Huertas, A.C. Powe, Jr., C.W. Pine, R. Khanna, M.G. Schlossmacher, D. Ringe, and G.A. Petsko. 2007. Structure of acid β-glucosidase with pharmacological chaperone provides insight into Gaucher disease. *Nat Chem Biol*. 3:101-107.

Lohse, M.J., and D. Calebiro. 2013. Cell biology: receptor signals come in waves. *Nature*. 495:457-458.

Loo, T.W., and D.M. Clarke. 1997. Correction of defective protein kinesis of human P-glycoprotein mutants by substrates and modulators. *J Biol Chem*. 272:709-712.

Loo, T.W., and D.M. Clarke. 2007. Chemical and pharmacological chaperones as new therapeutic agents. *Expert Rev Mol Med*. 9:1-18.

Los, E.L., P.M.T. Deen, and J.H. Robben. 2010. Potential of nonpeptide (Ant)agonists to rescue vasopressin V2 receptor mutants for the treatment of X-linked nephrogenic diabetes insipidus. *J Neuroendocrinol*. 22:393-399.

Lubrano-Berthelier, C., E. Durand, B. Dubern, A. Shapiro, P. Dazin, J. Weill, C. Ferron, P. Froguel, and C. Vaisse. 2003. Intracellular retention is a common characteristic of childhood obesity-associated MC4R mutations. *Hum Mol Genet*. 12:145-153.

Málaga-Diéguez, L., Q. Yang, J. Bauer, H. Pankevych, M. Freissmuth, and C. Nanoff. 2010. Pharmacochaperoning of the A1 adenosine receptor is contingent on the endoplasmic reticulum. *Mol Pharmacol*. 77:940-952.

Mansour, M. 2014. The roles of peroxisome proliferator-activated receptors in the metabolic syndrome. *Prog Mol Biol Transl Sci*. 121:217-266.

Masters, R.K., E.N. Reither, D.A. Powers, Y.C. Yang, A.E. Burger, and B.G. Link. 2013. The impact of obesity on US mortality levels: the importance of age and cohort factors in population estimates. *Am J Public Health*:e1-e7.

Maya-Nunez, G., A. Ulloa-Aguirre, J.A. Janovick, and P.M. Conn. 2012. Pharmacological chaperones correct misfolded GPCRs and rescue function: protein trafficking as a therapeutic target. *Subcell Biochem*. 63:263-289.

McDaniel, F.K., B.M. Molden, S. Mohammad, G. Baldini, L. McPike, P. Narducci, S. Granell, and G. Baldini. 2012. Constitutive cholesterol-dependent endocytosis of melanocortin-4 receptor (MC4R) is essential to maintain receptor responsiveness to α-melanocyte-stimulating hormone (α-MSH). *J Biol Chem*. 287:21873-21890.

McLatchie, L.M., N.J. Fraser, M.J. Main, A. Wise, J. Brown, N. Thompson, R. Solari, M.G. Lee, and S.M. Foord. 1998. RAMPs regulate the transport and ligand specificity of the calcitonin-receptor-like receptor. *Nature*. 393:333-339.

Meimaridou, E., S.B. Gooljar, N. Ramnarace, L. Anthonypillai, A.J. Clark, and J.P. Chapple. 2011. The cytosolic chaperone Hsc70 promotes traffic to the cell surface of intracellular retained melanocortin-4 receptor mutants. *Mol Endocrinol*. 25:1650-1660.

Mencarelli, M., B. Dubern, R. Alili, S. Maestrini, L. Benajiba, M. Tagliaferri, P. Galan, M. Rinaldi, C. Simon, P. Tounian, S. Hercberg, A. Liuzzi, A.M. Di Blasio, and K. Clement. 2011. Rare melanocortin-3 receptor mutations with in vitro functional consequences are associated with human obesity. *Hum Mol Genet*. 20:392-399.

Mencarelli, M., G.E. Walker, S. Maestrini, L. Alberti, B. Verti, A. Brunani, M.L. Petroni, M. Tagliaferri, A. Liuzzi, and A.M. Di Blasio. 2008. Sporadic mutations in melanocortin receptor 3 in morbid obese individuals. *Eur J Hum Genet*. 16:581-586.

Metherell, L.A., J.P. Chapple, S. Cooray, A. David, C. Becker, F. Ruschendorf, D. Naville, M. Begeot, B. Khoo, P. Nurnberg, A. Huebner, M.E. Cheetham, and A.J.L. Clark. 2005. Mutations in MRAP, encoding a new interacting partner of the ACTH receptor, cause familial glucocorticoid deficiency type 2. *Nat Genet*. 37:166-170.

Mirshahi, U.L., C.D. Still, K.K. Masker, G.S. Gerhard, D.J. Carey, and T. Mirshahi. 2011. The MC4R(I251L) allele is associated with better metabolic status and more weight loss after gastric bypass surgery. *J Clin Endocrinol Metab*. 96:E2088-E2096.

Mo, X.L., and Y.X. Tao. 2013. Activation of MAPK by inverse agonists in six naturally occurring constitutively active mutant human melanocortin-4 receptors. *Biochim Biophys Acta*. 1832:1939-1948.

Mo, X.L., R. Yang, and Y.X. Tao. 2012. Functions of transmembrane domain 3 of human melanocortin-4 receptor. *J Mol Endocrinol*. 49:221-235.

Mo, X.L., Z. Yang, and Y.X. Tao. 2014. Targeting GPR119 for the potential treatment of type 2 diabetes mellitus. *Prog Mol Biol Transl Sci*. 121:95-131.

Mohammad, S., G. Baldini, S. Granell, P. Narducci, A.M. Martelli, and G. Baldini. 2007. Constitutive traffic of melanocortin-4 receptor in Neuro2A cells and immortalized hypothalamic neurons. *J Biol Chem*. 282:4963-4974.

Montague, C.T., I.S. Farooqi, J.P. Whitehead, M.A. Soos, H. Rau, N.J. Wareham, C.P. Sewter, J.E. Digby, S.N. Mohammed, J.A. Hurst, C.H. Cheetham, A.R. Earley, A.H. Barnett, J.B. Prins, and S. O'Rahilly. 1997. Congenital leptin deficiency is associated with severe early-onset obesity in humans. *Nature*. 387:903-908.

Morello, J.P., A. Salahpour, A. Laperriere, V. Bernier, M.F. Arthus, M. Lonergan, U. Petaja-Repo, S. Angers, D. Morin, D.G. Bichet, and M. Bouvier. 2000. Pharmacological chaperones rescue cell-surface expression and function of misfolded V2 vasopressin receptor mutants. *J Clin Invest*. 105:887-895.

Mouillac, B., and C. Mendre. 2014. Vasopressin receptors and pharmacological chaperones: from functional rescue to promising therapeutic strategies. *Pharmacol Res*. 83:74-78.

Mountjoy, K.G., C.S. Jenny Wu, L.M. Dumont, and J.M. Wild. 2003. Melanocortin-4 receptor messenger ribonucleic acid expression in rat cardiorespiratory, musculoskeletal, and integumentary systems. *Endocrinology*. 144:5488-5496.

Mountjoy, K.G., M.T. Mortrud, M.J. Low, R.B. Simerly, and R.D. Cone. 1994. Localization of the melanocortin-4 receptor (MC4-R) in neuroendocrine and autonomic control circuits in the brain. *Mol Endocrinol*. 8:1298-1308.

Mullershausen, F., F. Zecri, C. Cetin, A. Billich, D. Guerini, and K. Seuwen. 2009. Persistent signaling induced by FTY720-phosphate is mediated by internalized S1P1 receptors. *Nat Chem Biol*. 5:428-434.

Murakami, M., and T. Kouyama. 2008. Crystal structure of squid rhodopsin. *Nature*. 453:363-367.

Nakamura, A., T. Hotsubo, K. Kobayashi, H. Mochizuki, K. Ishizu, and T. Tajima. 2013. Loss-of-function and gain-of-function mutations of calcium-sensing receptor: functional analysis and the effect of allosteric modulators NPS R-568 and NPS 2143. *J Clin Endocrinol Metab*. 98:E1692-E1701.

Nanoff, C., and M. Freissmuth. 2012. ER-bound steps in the biosynthesis of G protein-coupled receptors. *Subcell Biochem*. 63:1-21.

Newman, E.A., B.X. Chai, W. Zhang, J.Y. Li, J.B. Ammori, and M.W. Mulholland. 2006. Activation of the melanocortin-4 receptor mobilizes intracellular free calcium in immortalized hypothalamic neurons. *J Surg Res*. 132:201-207.

Newton, C.L., A.M. Whay, C.A. McArdle, M. Zhang, C.J. van Koppen, R. van de Lagemaat, D.L. Segaloff, and R.P. Millar. 2011. Rescue of expression and signaling of human luteinizing hormone G protein-coupled receptor mutants with an allosterically binding small-molecule agonist. *Proc Natl Acad Sci U S A*. 108:7172-7176.

Nicholson, J.R., G. Kohler, F. Schaerer, C. Senn, P. Weyermann, and K.G. Hofbauer. 2006. Peripheral administration of a melanocortin 4-receptor inverse agonist prevents loss of lean body mass in tumor-bearing mice. *J Pharmacol Exp Ther*. 317:771-777.

Nickolls, S.A., B. Fleck, S.R. Hoare, and R.A. Maki. 2005. Functional selectivity of melanocortin 4 receptor peptide and nonpeptide agonists: evidence for ligand-specific conformational states. *J Pharmacol Exp Ther*. 313:1281-1288.

Nijenhuis, W.A.J., J. Oosterom, and R.A.H. Adan. 2001. AgRP(83-132) acts as an inverse agonist on the human-melanocortin-4 receptor. *Mol Endocrinol*. 15:164-171.

Noorwez, S.M., V. Kuksa, Y. Imanishi, L. Zhu, S. Filipek, K. Palczewski, and S. Kaushal. 2003. Pharmacological chaperone-mediated in vivo folding and stabilization of the P23H-opsin mutant associated with autosomal dominant retinitis pigmentosa. *J Biol Chem*. 278:14442-14450.

O'Rahilly, S., I.S. Farooqi, G.S. Yeo, and B.G. Challis. 2003. Minireview: human obesity-lessons from monogenic disorders. *Endocrinology*. 144:3757-3764.

Ogden, C.L., M.D. Carroll, B.K. Kit, and K.M. Flegal. 2012a. Prevalence of obesity and trends in body mass index among US children and adolescents, 1999-2010. *J Am Med Assoc*. 307:483-490.

Ogden, C.L., M.D. Carroll, B.K. Kit, and K.M. Flegal. 2012b. Prevalence of obesity in the United States, 2009-2010. *NCHS Data Brief*:1-8.

Overton, J.D., and R.L. Leibel. 2011. Mahoganoid and mahogany mutations rectify the obesity of the yellow mouse by effects on endosomal traffic of MC4R protein. *J Biol Chem*. 286:18914-18929.

Palczewski, K., T. Kumasaka, T. Hori, C.A. Behnke, H. Motoshima, B.A. Fox, I. Le Trong, D.C. Teller, T. Okada, R.E. Stenkamp, M. Yamamoto, and M. Miyano. 2000. Crystal structure of rhodopsin: a G protein-coupled receptor. *Science*. 289:739-745.

Pan, Y., A. Metzenberg, S. Das, B. Jing, and J. Gitschier. 1992. Mutations in the V2 vasopressin receptor gene are associated with X-linked nephrogenic diabetes insipidus. *Nat Genet*. 2:103-106.

Park, J.H., P. Scheerer, K.P. Hofmann, H.W. Choe, and O.P. Ernst. 2008. Crystal structure of the ligand-free G-protein-coupled receptor opsin. *Nature*. 454:183-187.

Persani, L., A. Lania, L. Alberti, R. Romoli, G. Mantovani, S. Filetti, A. Spada, and M. Conti. 2000. Induction of specific phosphodiesterase isoforms by constitutive activation of the cAMP pathway in autonomous thyroid adenomas. *J Clin Endocrinol Metab*. 85:2872-2878.

Petäjä-Repo, U.E., M. Hogue, S. Bhalla, A. Laperrière, J.-P. Morello, and M. Bouvier. 2002. Ligands act as pharmacological chaperones and increase the efficiency of δ opioid receptor maturation. *EMBO J*. 21:1628-1637.

Petaja-Repo, U.E., M. Hogue, A. Laperriere, P. Walker, and M. Bouvier. 2000. Export from the endoplasmic reticulum represents the limiting step in the maturation and cell surface expression of the human δ opioid receptor. *J Biol Chem*. 275:13727-13736.

Pogozheva, I.D., B.X. Chai, A.L. Lomize, T.M. Fong, D.H. Weinberg, R.P. Nargund, M.W. Mulholland, I. Gantz, and H.I. Mosberg. 2005. Interactions of human melanocortin 4 receptor with nonpeptide and peptide agonists. *Biochemistry*. 44:11329-11341.

Poitout, L., V. Brault, C. Sackur, S. Bernetiere, J. Camara, P. Plas, and P. Roubert. 2007. Identification of a novel series of benzimidazoles as potent and selective antagonists of the human melanocortin-4 receptor. *Bioorg Med Chem Lett*. 17:4464-4470.

Proneth, B., Z. Xiang, I.D. Pogozheva, S.A. Litherland, O.S. Gorbatyuk, A.M. Shaw, W.J. Millard, H.I. Mosberg, and C. Haskell-Luevano. 2006. Molecular mechanism of the

constitutive activation of the L250Q human melanocortin-4 receptor polymorphism. *Chem Biol Drug Des*. 67:215-229.

Ramachandrappa, S., and I.S. Farooqi. 2011. Genetic approaches to understanding human obesity. *J Clin Invest*. 121:2080-2086.

Ramon, E., A. Cordomi, L. Bosch, E.Y. Zernii, Senin, II, J. Manyosa, P.P. Philippov, J.J. Perez, and P. Garriga. 2007. Critical role of electrostatic interactions of amino acids at the cytoplasmic region of helices 3 and 6 in rhodopsin conformational properties and activation. *J Biol Chem*. 282:14272-14282.

Rasmussen, S.G., H.J. Choi, J.J. Fung, E. Pardon, P. Casarosa, P.S. Chae, B.T. Devree, D.M. Rosenbaum, F.S. Thian, T.S. Kobilka, A. Schnapp, I. Konetzki, R.K. Sunahara, S.H. Gellman, A. Pautsch, J. Steyaert, W.I. Weis, and B.K. Kobilka. 2011. Structure of a nanobody-stabilized active state of the β_2 adrenoceptor. *Nature*. 469:175-180.

Rasmussen, S.G., H.J. Choi, D.M. Rosenbaum, T.S. Kobilka, F.S. Thian, P.C. Edwards, M. Burghammer, V.R. Ratnala, R. Sanishvili, R.F. Fischetti, G.F. Schertler, W.I. Weis, and B.K. Kobilka. 2007. Crystal structure of the human β_2 adrenergic G-protein-coupled receptor. *Nature*. 450:383-387.

Reinehr, T., J. Hebebrand, S. Friedel, A.M. Toschke, H. Brumm, H. Biebermann, and A. Hinney. 2009. Lifestyle intervention in obese children with variations in the melanocortin 4 receptor gene. *Obesity*. 17:382-389.

Reiter, E., S. Ahn, A.K. Shukla, and R.J. Lefkowitz. 2012. Molecular mechanism of β-arrestin-biased agonism at seven-transmembrane receptors. *Annu Rev Pharmacol Toxicol*. 52:179-197.

Rene, P., C. Le Gouill, I.D. Pogozheva, G. Lee, H.I. Mosberg, I.S. Farooqi, K.J. Valenzano, and M. Bouvier. 2010. Pharmacological chaperones restore function to MC4R mutants responsible for severe early-onset obesity. *J Pharmacol Exp Ther*. 335:520-532.

Revankar, C.M., D.F. Cimino, L.A. Sklar, J.B. Arterburn, and E.R. Prossnitz. 2005. A transmembrane intracellular estrogen receptor mediates rapid cell signaling. *Science*. 307:1625-1630.

Ringe, D., and G. Petsko. 2009. Q&A: What are pharmacological chaperones and why are they interesting? *J Biol*. 8:80.

Robben, J.H., M.L.A. Kortenoeven, M. Sze, C. Yae, G. Milligan, V.M. Oorschot, J. Klumperman, N.V.A.M. Knoers, and P.M.T. Deen. 2009. Intracellular activation of vasopressin V2 receptor mutants in nephrogenic diabetes insipidus by nonpeptide agonists. *Proc Natl Acad Sci U S A*. 106:12195-12200.

Rosenbaum, D.M., V. Cherezov, M.A. Hanson, S.G. Rasmussen, F.S. Thian, T.S. Kobilka, H.J. Choi, X.J. Yao, W.I. Weis, R.C. Stevens, and B.K. Kobilka. 2007. GPCR engineering yields high-resolution structural insights into β_2-adrenergic receptor function. *Science*. 318:1266-1273.

Rossi, J., N. Balthasar, D. Olson, M. Scott, E. Berglund, C.E. Lee, M.J. Choi, D. Lauzon, B.B. Lowell, and J.K. Elmquist. 2011. Melanocortin-4 receptors expressed by cholinergic neurons regulate energy balance and glucose homeostasis. *Cell Metab*. 13:195-204.

Roth, J.D., D.K. Yee, L.R. Kisley, and S.J. Fluharty. 2002. Modeling the pathways of energy balance using the N1E-115 murine neuroblastoma cell line. *Mol Brain Res*. 103:146-150.

Rucker, D., R. Padwal, S.K. Li, C. Curioni, and D.C. Lau. 2007. Long term pharmacotherapy for obesity and overweight: updated meta-analysis. *BMJ*. 335:1194-1199.

Rus, R., C. Haag, C. Bumke-Vogt, V. Bahr, B. Mayr, M. Mohlig, E. Schulze, K. Frank-Raue, F. Raue, and C. Schofl. 2008. Novel inactivating mutations of the calcium-sensing receptor: the calcimimetic NPS R-568 improves signal transduction of mutant receptors. *J Clin Endocrinol Metab*. 93:4797-4803.

Saito, H., M. Kubota, R.W. Roberts, Q.Y. Chi, and H. Matsunami. 2004. RTP family members induce functional expression of mammalian odorant receptors. *Cell*. 119:679-691.

Sampson, H.M., R. Robert, J. Liao, E. Matthes, G.W. Carlile, J.W. Hanrahan, and D.Y. Thomas. 2011. Identification of a NBD1-binding pharmacological chaperone that corrects the trafficking defect of F508del-CFTR. *Chem Biol*. 18:231-242.

Sayegh, A.I. 2013. The role of bombesin and bombesin-related peptides in the short-term control of food intake. *Prog Mol Biol Transl Sci*. 114:343-370.

Scheerer, P., J.H. Park, P.W. Hildebrand, Y.J. Kim, N. Krauss, H.W. Choe, K.P. Hofmann, and O.P. Ernst. 2008. Crystal structure of opsin in its G-protein-interacting conformation. *Nature*. 455:497-502.

Schneider, E.H., D. Schnell, A. Strasser, S. Dove, and R. Seifert. 2010. Impact of the DRY motif and the missing "ionic lock" on constitutive activity and G-protein coupling of the human histamine H_4 receptor. *J Pharmacol Exp Ther*. 333:382-392.

Schrier, R.W., P. Gross, M. Gheorghiade, T. Berl, J.G. Verbalis, F.S. Czerwiec, and C. Orlandi. 2006. Tolvaptan, a selective oral vasopressin V-2-receptor antagonist, for hyponatremia. *New Engl J Med*. 355:2099-2112.

Schubert, U., L.C. Anton, J. Gibbs, C.C. Norbury, J.W. Yewdell, and J.R. Bennink. 2000. Rapid degradation of a large fraction of newly synthesized proteins by proteasomes. *Nature*. 404:770-774.

Sebhat, I.K., W.J. Martin, Z.X. Ye, K. Barakat, R.T. Mosley, D.B.R. Johnston, R. Bakshi, B. Palucki, D.H. Weinberg, T. MacNeil, R.N. Kalyani, R. Tang, R.A. Stearns, R.R. Miller, C. Tamvakopoulos, A.M. Strack, E. McGowan, D.E. Cashen, J.E. Drisko, G.J. Hom, A.D. Howard, D.E. MacIntyre, L.H.T. van der Ploeg, A.A. Patchett, and R.P. Nargund. 2002. Design and pharmacology of N-[(3R)-1,2,3,4-tetrahydroisoquinolinium-3-ylcarbonyl]-(1R)-1-(4-chlorobenzyl)2-[4-cyclohexyl-4-(1H-1,2,4-triazol-1-ylmethyl)piperidin-1-yl]-2-oxoethylamine (1), a potent, selective, melanocortin subtype-4 receptor agonist. *J Med Chem*. 45:4589-4593.

Shenoy, S.K., and R.J. Lefkowitz. 2011. β-arrestin-mediated receptor trafficking and signal transduction. *Trends Pharmacol Sci*. 32:521-533.

Shi, H., S.P. Kumar, and X. Liu. 2013. G protein-coupled estrogen receptor in energy homeostasis and obesity pathogenesis. *Prog Mol Biol Transl Sci*. 114:193-250.

Shinozaki, H., V. Butnev, Y.X. Tao, K.L. Ang, M. Conti, and D.L. Segaloff. 2003. Desensitization of Gs-coupled receptor signaling by constitutively active mutants of the human lutropin/choriogonadotropin receptor. *J Clin Endocrinol Metab*. 88:1194-1204.

Shinyama, H., H. Masuzaki, H. Fang, and J.S. Flier. 2003. Regulation of melanocortin-4 receptor signaling: agonist-mediated desensitization and internalization. *Endocrinology*. 144:1301-1314.

Srinivasan, S., C. Lubrano-Berthelier, C. Govaerts, F. Picard, P. Santiago, B.R. Conklin, and C. Vaisse. 2004. Constitutive activity of the melanocortin-4 receptor is maintained by its N-terminal domain and plays a role in energy homeostasis in humans. *J Clin Invest*. 114:1158-1164.

Sturm, R., and A. Hattori. 2013. Morbid obesity rates continue to rise rapidly in the United States. *Int J Obes*. 37:889-891.

Stutzmann, F., K. Tan, V. Vatin, C. Dina, B. Jouret, J. Tichet, B. Balkau, N. Potoczna, F. Horber, S. O'Rahilly, I.S. Farooqi, P. Froguel, and D. Meyre. 2008. Prevalence of melanocortin-4 receptor deficiency in Europeans and their age-dependent penetrance in multigenerational pedigrees. *Diabetes*. 57:2511-2518.

Stutzmann, F., V. Vatin, S. Cauchi, A. Morandi, B. Jouret, O. Landt, P. Tounian, C. Levy-Marchal, R. Buzzetti, L. Pinelli, B. Balkau, F. Horber, P. Bougneres, P. Froguel, and D. Meyre. 2007. Non-synonymous polymorphisms in melanocortin-4 receptor protect against obesity: the two facets of a Janus obesity gene. *Hum Mol Genet*. 16:1837-1844.

Sung, C.H., C.M. Davenport, J.C. Hennessey, I.H. Maumenee, S.G. Jacobson, J.R. Heckenlively, R. Nowakowski, G. Fishman, P. Gouras, and J. Nathans. 1991. Rhodopsin mutations in autosomal dominant retinitis-pigmentosa. *Proc Natl Acad Sci U S A*. 88:6481-6485.

Sutton, G.M., B. Duos, L.M. Patterson, and H.R. Berthoud. 2005. Melanocortinergic modulation of cholecystokinin-induced suppression of feeding through extracellular signal-regulated kinase signaling in rat solitary nucleus. *Endocrinology*. 146:3739-3747.

Tan, K., I.D. Pogozheva, G.S. Yeo, D. Hadaschik, J.M. Keogh, C. Haskell-Leuvano, S. O'Rahilly, H.I. Mosberg, and I.S. Farooqi. 2009. Functional characterization and structural modeling of obesity associated mutations in the melanocortin 4 receptor. *Endocrinology*. 150:114-125.

Tao, Y.X. 2005. Molecular mechanisms of the neural melanocortin receptor dysfunction in severe early onset obesity. *Mol Cell Endocrinol*. 239:1-14.

Tao, Y.X. 2006. Inactivating mutations of G protein-coupled receptors and diseases: structure-function insights and therapeutic implications. *Pharmacol Ther*. 111:949-973.

Tao, Y.X. 2007. Functional characterization of novel melanocortin-3 receptor mutations identified from obese subjects. *Biochim Biophys Acta*. 1772:1167-1174.

Tao, Y.X. 2008. Constitutive activation of G protein-coupled receptors and diseases: insights into mechanism of activation and therapeutics. *Pharmacol Ther*. 120:129-148.

Tao, Y.X. 2009. Mutations in melanocortin-4 receptor and human obesity. *Prog Mol Biol Transl Sci*. 88:173-204.

Tao, Y.X. 2010. The melanocortin-4 receptor: physiology, pharmacology, and pathophysiology. *Endocr Rev*. 31:506-543.

Tao, Y.X., and P.M. Conn. 2014. Chaperoning G protein-coupled receptors: from cell biology to therapeutics. *Endocr Rev*. DOI: http://dx.doi.org/10.1210/er.2013-1121.

Tao, Y.X., H. Huang, Z.Q. Wang, F. Yang, J.N. Williams, and G.V. Nikiforovich. 2010. Constitutive Activity of Neural Melanocortin Receptors. *Method Enzymol*. 484:267-279.

Tao, Y.X., and X.F. Liang. 2014. G protein-coupled receptors as regulators of glucose homeostasis and therapeutic targets for diabetes mellitus. *Prog Mol Biol Transl Sci*. 121:1-21.

Tao, Y.X., D. Mizrachi, and D.L. Segaloff. 2002. Chimeras of the rat and human FSH receptors (FSHRs) identify residues that permit or suppress transmembrane 6 mutation-induced constitutive activation of the FSHR via rearrangements of hydrophobic interactions between helices 6 and 7. *Mol Endocrinol*. 16:1881-1892.

Tao, Y.X., and D.L. Segaloff. 2003. Functional characterization of melanocortin-4 receptor mutations associated with childhood obesity. *Endocrinology*. 144:4544-4551.

Tao, Y.X., and D.L. Segaloff. 2005. Functional analyses of melanocortin-4 receptor mutations identified from patients with binge eating disorder and nonobese or obese subjects. *J Clin Endocrinol Metab*. 90:5632-5638.

Tao, Y.X., Z.H. Yuan, and J. Xie. 2013. G protein-coupled receptors as regulators of energy homeostasis. *Prog Mol Biol Transl Sci*. 114:1-43.

Terranova, L., L. Busetto, A. Vestri, and M.A. Zappa. 2012. Bariatric surgery: cost-effectiveness and budget impact. *Obes Surg*. 22:646-653.

Thearle, M.S., Y.L. Muller, R.L. Hanson, M. Mullins, M. AbdusSamad, J. Tran, W.C. Knowler, C. Bogardus, J. Krakoff, and L.J. Baier. 2012. Greater impact of melanocortin-4 receptor deficiency on rates of growth and risk of type 2 diabetes during childhood compared with adulthood in Pima Indians. *Diabetes*. 61:250-257.

Torregrossa, M.M., E.M. Jutkiewicz, H.I. Mosberg, G. Balboni, S.J. Watson, and J.H. Woods. 2006. Peptidic delta opioid receptor agonists produce antidepressant-like effects in the forced swim test and regulate BDNF mRNA expression in rats. *Brain Res*. 1069:172-181.

Uberti, M.A., C. Hague, H. Oller, K.P. Minneman, and R.A. Hall. 2005. Heterodimerization with β_2-adrenergic receptors promotes surface expression and functional activity of α_{1D}-adrenergic receptors. *J Pharmacol Exp Ther*. 313:16-23.

Vaisse, C., K. Clement, B. Guy-Grand, and P. Froguel. 1998. A frameshift mutation in human MC4R is associated with a dominant form of obesity. *Nat Genet*. 20:113-114.

Varela, L., and T.L. Horvath. 2012. Leptin and insulin pathways in POMC and AgRP neurons that modulate energy balance and glucose homeostasis. *Embo Rep*. 13:1079-1086.

Villanueva, E.C., and M.G. Myers, Jr. 2008. Leptin receptor signaling and the regulation of mammalian physiology. *Int J Obes*. 32 Suppl 7:S8-12.

Violin, J.D., and R.J. Lefkowitz. 2007. β-arrestin-biased ligands at seven-transmembrane receptors. *Trends Pharmacol Sci*. 28:416-422.

Vogt, M.C., and J.C. Bruning. 2013. CNS insulin signaling in the control of energy homeostasis and glucose metabolism - from embryo to old age. *Trends Endocrin Met*. 24:76-84.

Vongs, A., N.M. Lynn, and C.I. Rosenblum. 2004. Activation of MAP kinase by MC4-R through PI3 kinase. *Regul Pept*. 120:113-118.

Vos, T.J., A. Caracoti, J.L. Che, M. Dai, C.A. Farrer, N.E. Forsyth, S.V. Drabic, R.A. Horlick, D. Lamppu, D.L. Yowe, S. Balani, P. Li, H. Zeng, I.B.J.K. Joseph, L.E. Rodriguez, M.P. Maguire, M.A. Patane, and C.F. Claiborne. 2004. Identification of 2-{2-[2-(5-bromo-2-methoxyphenyl)-ethyl]-3-fluoro-phenyl}-4,5-dihydro-1H-imidazole (ML00253764), a small molecule melanocortin 4 receptor antagonist that effectively reduces tumor-induced weight loss in a mouse model. *J Med Chem*. 47:1602-1604.

Wadden, T.A., R.I. Berkowitz, L.G. Womble, D.B. Sarwer, S. Phelan, R.K. Cato, L.A. Hesson, S.Y. Osei, R. Kaplan, and A.J. Stunkard. 2005. Randomized trial of lifestyle modification and pharmacotherapy for obesity. *N Engl J Med*. 353:2111-2120.

Wang, S.X., Z.C. Fan, and Y.X. Tao. 2008. Functions of acidic transmembrane residues in human melanocortin-3 receptor binding and activation. *Biochem Pharmacol*. 76:520-530.

Wang, Z.Q., and Y.X. Tao. 2011. Functional studies on twenty novel naturally occurring melanocortin-4 receptor mutations. *Biochim Biophys Acta*. 1812:1190-1199.

Ward, N.A., S. Hirst, J. Williams, and J.B. Findlay. 2012. Pharmacological chaperones increase the cell-surface expression of intracellularly retained mutants of the melanocortin 4 receptor with unique rescuing efficacy profiles. *Biochem Soc Trans*. 40:717-720.

Warne, T., R. Moukhametzianov, J.G. Baker, R. Nehme, P.C. Edwards, A.G.W. Leslie, G.F.X. Schertler, and C.G. Tate. 2011. The structural basis for agonist and partial agonist action on a β_1-adrenergic receptor. *Nature*. 469:241-244.

Warne, T., M.J. Serrano-Vega, J.G. Baker, R. Moukhametzianov, P.C. Edwards, R. Henderson, A.G. Leslie, C.G. Tate, and G.F. Schertler. 2008. Structure of a β_1-adrenergic G-protein-coupled receptor. *Nature*. 454:486-491.

White, E., J. McKenna, A. Cavanaugh, and G.E. Breitwieser. 2009. Pharmacochaperone-mediated rescue of calcium-sensing receptor loss-of-function mutants. *Mol Endocrinol*. 23:1115-1123.

White, J.H., A. Wise, M.J. Main, A. Green, N.J. Fraser, G.H. Disney, A.A. Barnes, P. Emson, S.M. Foord, and F.H. Marshall. 1998. Heterodimerization is required for the formation of a functional $GABA_B$ receptor. *Nature*. 396:679-682.

Wortley, K.E., K.D. Anderson, J. Yasenchak, A. Murphy, D. Valenzuela, S. Diano, G.D. Yancopoulos, S.J. Wiegand, and M.W. Sleeman. 2005. Agouti-related protein-deficient mice display an age-related lean phenotype. *Cell Metab*. 2:421-427.

Wu, H., D. Wacker, M. Mileni, V. Katritch, G.W. Han, E. Vardy, W. Liu, A.A. Thompson, X.P. Huang, F.I. Carroll, S.W. Mascarella, R.B. Westkaemper, P.D. Mosier, B.L. Roth, V. Cherezov, and R.C. Stevens. 2012. Structure of the human κ-opioid receptor in complex with JDTic. *Nature*. 485:327-332.

Xiang, Z., S.A. Litherland, N.B. Sorensen, B. Proneth, M.S. Wood, A.M. Shaw, W.J. Millard, and C. Haskell-Luevano. 2006. Pharmacological characterization of 40 human melanocortin-4 receptor polymorphisms with the endogenous proopiomelanocortin-

derived agonists and the agouti-related protein (AGRP) antagonist. *Biochemistry*. 45:7277-7288.

Xiang, Z., I.D. Pogozheva, N.B. Sorenson, A.M. Wilczynski, J.R. Holder, S.A. Litherland, W.J. Millard, H.I. Mosberg, and C. Haskell-Luevano. 2007. Peptide and small molecules rescue the functional activity and agonist potency of dysfunctional human melanocortin-4 receptor polymorphisms. *Biochemistry*. 46:8273-8287.

Xiang, Z.M., B. Proneth, M.L. Dirain, S.A. Litherland, and C. Haskell-Luevano. 2010. Pharmacological characterization of 30 human melanocortin-4 receptor polymorphisms with the endogenous proopiomelanocortin-derived agonists, synthetic agonists, and the endogenous agouti-related protein antagonist. *Biochemistry*. 49:4583-4600.

Xu, F., H. Wu, V. Katritch, G.W. Han, K.A. Jacobson, Z.G. Gao, V. Cherezov, and R.C. Stevens. 2011. Structure of an agonist-bound human A_{2A} adenosine receptor. *Science*. 332:322-327.

Yam, G.H., N. Bosshard, C. Zuber, B. Steinmann, and J. Roth. 2006. Pharmacological chaperone corrects lysosomal storage in Fabry disease caused by trafficking-incompetent variants. *Am J Physiol Cell Physiol*. 290:C1076-C1082.

Yang, Y., M. Cai, M. Chen, H. Qu, D. McPherson, V. Hruby, and C.M. Harmon. 2009. Key amino acid residues in the melanocortin-4 receptor for nonpeptide THIQ specific binding and signaling. *Regul Pept*. 155:46-54.

Yang, Y.K., T.M. Fong, C.J. Dickinson, C. Mao, J.Y. Li, M.R. Tota, R. Mosley, L.H. Van Der Ploeg, and I. Gantz. 2000. Molecular determinants of ligand binding to the human melanocortin-4 receptor. *Biochemistry*. 39:14900-14911.

Yeo, G.S.H., I.S. Farooqi, S. Aminian, D.J. Halsall, R.C. Stanhope, and S. O'Rahilly. 1998. A frameshift mutation in MC4R associated with dominantly inherited human obesity. *Nat Genet*. 20:111-112.

Zhang, J.V., L. Li, Q. Huang, and P.G. Ren. 2013. Obestatin receptor in energy homeostasis and obesity pathogenesis. *Prog Mol Biol Transl Sci*. 114:89-107.

Zhang, L., M.S. Bijker, and H. Herzog. 2011. The neuropeptide Y system: pathophysiological and therapeutic implications in obesity and cancer. *Pharmacol Ther*. 131:91-113.

Zhang, Y., R. Proenca, M. Maffei, M. Barone, L. Leopold, and J.M. Friedman. 1994. Positional cloning of the mouse obese gene and its human homologue. *Nature*. 372:425-432.